MODELLING, MATHEMATICAL AND NUMERICAL STUDY OF A SOLUTAL PHASE-FIELD MODEL

THÈSE N^O 2459 (2001)

PRÉSENTÉE AU DÉPARTEMENT DE MATHÉMATIQUES

ÉCOLE POLYTECHNIQUE FÉDÉRALE DE LAUSANNE

POUR L'OBTENTION DU GRADE DE DOCTEUR ÈS SCIENCES

PAR

Daniel KESSLER

Ingénieur physicien diplômé EPF
de nationalité suisse

accaptée sur proposition du jury:

Prof. J. Rappaz, directeur de thèse
Dr E. Burman, rapporteur
Prof. P. Colli, rapporteur
Prof. A. Quarteroni, rapporteur
Prof. J.-F. Scheid, rapporteur

Lausanne, EPFL
2001

Version abrégée

Nous étudions un modèle de champ de phase solutal isotherme thermody-namiquement consistant décrivant la solidification d'un alliage binaire. Le système est caractérisé par deux variables: le champ de phase et la concentration. Le champ de phase décrit la phase dans laquelle se trouve locale-ment l'alliage (liquide, solide, intermédiaire). L'évolution de ces variables est décrite par un système parabolique avec conditions de bord de Neumann. Après avoir présenté la construction du modèle, nous cherchons des limites asymptotiques formelles lorsque l'épaisseur d'interface liquide-solide devient petite. Nous obtenons des modèles limites sous la forme de problèmes de Stefan généralisés, prenant en compte les effets de vitesse et courbure locales de l'interface. Ensuite, nous introduisons un schéma numérique de type élé-ments finis en espace et Euler semi-implicite en temps. Nous démontrons la convergence de ce schéma grâce à l'introduction d'un projecteur elliptique généralisé. Nous utilisons ce schéma pour simuler la croissance dendritique dans les alliages, et étudions la stabilité des simulations physiques par rap-port à plusieurs paramètres numériques.

iv

Abstract

We investigate a thermodynamically consistent isothermal solutal phase-field model describing the solidification of a binary alloy. The system is characterized by two variables: phase-field and concentration. The phase-field locally describes the phase state of the alloy (liquid, solid or intermediate). The evolution of these variables is described by a parabolic system with Neumann boundary conditions. After presenting the construction of the model, we investigate formal asymptotic limits when the liquid-solid interface width becomes small. Limit models are found in the form of generalized Stefan problems, which account for effects of the local interface curvature and velocity. We then introduce a finite element in space, semi-implicit Euler in time numerical scheme. The convergence of this scheme is proved thanks to the introduction of a generalized elliptic projector. We use this scheme to simulate dendritic growth in alloys, and investigate the stability of physical simulations with respect to various numerical parameters.

Acknowledgements

As any scientist knows, scientific research is never just an individual work performed in isolation. Individual contributions are made possible only by the interaction with a team, and with the rest of the scientific world. Some people have been of special help and inspiration during this thesis work, and I wish to thank them explicitly.

First of all, I am very grateful to Prof. Jacques Rappaz, who accepted me in his team both as a researcher and a teaching assistant. During all these years, he has shown me the landmarks of every aspect of scientific work, while at the same time granting me the freedom necessary to perform an original work.

I also want to especially thank Jean-François Scheid, who taught me the more technical aspects of the field while we closely collaborated during the first two years of my thesis. He has always been extremely encouraging, even when there seemed to be no way out of a mist of arcane formulae.

Several other people have been directly of help, notably Olivier Krüger with whom I collaborated at the beginning of this work, Marco Picasso who provided the finite element library used for the simulations, Erik Burman who started exploring the theoretical subtleties of the anisotropic problem and suggested interesting numerical investigations, and Prof. Michel Rappaz and Alain Jacot who provided important insight into the physical aspects of the problem.

I also thank Professors Pierluigi Colli and Alfio Quarteroni who honoured me by being part of the jury, and Prof. Peter Buser for presiding it.

Finally, I am grateful to all the people with whom I had fruitful discussions in Lausanne, Les Diablerets, Berlin and Pavia, as well as to my parents who have always been encouraging, and all to my friends who shared other aspects of my life.

Contents

Introduction

One of the main topics of modern physics, both theoretical and applied, is the study of phase transition problems, ranging from the description of solidification of metals to the study of magnetic properties of solid materials and percolation. Theoretical physicists are generally more interested in a microscopic description of the phenomena, usually based on stochastic theories (Ising's model, ...), whereas applied physicists (for example materials scientists) are usually more interested in macroscopic, deterministic models, such as the Stefan problem and other explicit descriptions of interface motion. Good reviews have been written on the topic. In particular, for the more specific case of solidification one may refer to Boettinger *et al.* [BCG$^+$00], whereas general reviews of mathematical models related to phase transition problems can be found in [Ell97] and in [Vis98]. Many of these models have been the topic of various mathematical investigations (see for instance [Cag86, CLS99, CNS00, DD95, DHL98, RS00]).

Asides from the more traditional microscopic (stochastic) and macroscopic (explicit interface) viewpoints, a third approach, called *mesoscopic*, has been developed to describe phase transitions. There are several reasons to adopt it. Mathematically, the direct macroscopic approach of explicit sharp interfaces can pose serious problems related to possible changes of topology and complex geometries, especially for numerical implementations of front tracking algorithms. Physically, a mesoscopic approach may allow a combined description of the phase transition phenomena at two scales simultaneously - at a large scale in the "pure phases", and at a smaller scale in a "diffuse interface". There are also several ways to implement a mesoscopic approach. Using a purely mathematical approach, one may artificially create an intermediate problem with an extra variable, which has a level set that describes the sharp interface of a macroscopic model (for the level set method, see [Set96]). This is essentially a mathematical trick, not satisfactory in that it provides only the practical mathematical benefits, not the theoretical physical interest, of a mesoscopic approach. To get both benefits, at the cost of more complex modelling, phase-field models have been intro-

1

duced, which can be totally coherent with thermodynamics and account for small-scale phenomena in a physically interpretable way.

In this work, we investigate a phase-field model describing the solidification of a binary alloy. We consider the case in which concentration effects dominate (which experimentally happens for instance in the case of Ni-Cu), and where thermal fluctuation effects can be neglected. Therefore, it is natural to consider an isothermal model. From the theory of thermodynamics, we know that the adequate potential for describing an isothermal situation is the free energy. Our model will consist in evolution equations for the local concentration c of the alloy, and the local phase field ϕ, such that the total free energy of the domain decreases with time and that matter is conserved:

$$
\begin{cases}
\dfrac{\partial \phi}{\partial t} = M \left(\triangle \phi + F(c, \phi) \right), & \text{(1a)} \\[2ex]
\dfrac{\partial c}{\partial t} = \mathrm{div} \left(D_1(\phi)\nabla c + D_2(c, \phi)\nabla \phi \right), & \text{(1b)}
\end{cases}
$$

where M is a positive constant, F, D_1 and D_2 are Lipschitz bounded functions, and D_1 is positive.

As the domain is considered to be physically closed to the exchange of matter and non-thermal free energy, the evolution equations will be naturally coupled with homogeneous Neumann boundary conditions. To completely specify the model, a free energy density has to be built and the evolution equations need to be adjusted to known physical limit models. For these two purposes, we follow closely the work of Warren and Boettinger [WB95], although they considered a model based on the entropy potential, in view of later accounting for thermal fluctuation effects. This choice is justified because they have striven to build a thermodynamically consistent model, at the expense of evolution equations more complex than their predecessor's. The details of the model construction can be found in chapter 1 and Appendix A. The resulting model can be formulated as the parabolic system (1) with lipschitzian non-linearities. More synthetically one may write an evolution equation for the vectorial variable $\vec{u} = (\phi, \zeta c)^T$ as

$$
\frac{\partial \vec{u}}{\partial t} = \mathrm{div} \left(D(\vec{u})\nabla \vec{u} \right) + \vec{F}(\vec{u}), \tag{2}
$$

where D and $\vec{F}$ are Lipschitz bounded functions, and ζ a positive constant chosen such that after the change of variables matrix D is positive definite uniformly in $\vec{u}$.

The model actually exists in two variants, a simpler isotropic model, presented above, and a more complex anisotropic model accounting for privileged directions in crystal growth. The well-posedness of the isotropic model has been investigated by J. F. Scheid and J. Rappaz [RS00].

For any physically relevant phase-field model, a natural question immediatly arises: Is it possible to recover a proper macroscopic sharp-interface model from this mesoscopic diffuse-interface model? This question has been investigated in great detail by Caginalp for thermal pure element phase-field models [Cag86, Cag89]. It has also been addressed in the case of a simple solutal model by Wheeler *et al* [WBM92]. Nevertheless, to our knowledge it has not been investigated in detail before for a thermodynamically consistent solutal model. We consider this problem for the isotropic model in chapter 2, which has been published in [Kes01]. The method used is a formal asymptotic analysis of the model, and it is based on the techniques originally used by Caginalp. Four different limit models are found, corresponding to different ways of going to the sharp-interface limit. They differ by the dependence on local interface normal velocity and curvature of the resulting generalized Stefan problems:

$$
\left\{
\begin{array}{lll}
\dfrac{\partial c}{\partial t} = D_l \triangle c, & \text{in} \quad \Omega_l, & \text{(3a)} \\[2.5ex]
\dfrac{\partial c}{\partial t} = D_s \triangle c, & \text{in} \quad \Omega_s, & \text{(3b)} \\[2.5ex]
-v_n \left[c \right]_l^s = \left[D \dfrac{\partial c}{\partial n} \right]_l^s, & \text{on} \quad \Gamma, & \text{(3c)} \\[2.5ex]
\left[\dfrac{\partial f}{\partial c} \right]_l^s = 0, & \text{on} \quad \Gamma, & \text{(3d)} \\[2.5ex]
\left[f - \dfrac{\partial f}{\partial c} \right]_l^s = \mathcal{A}(v_n, \kappa), & \text{on} \quad \Gamma, & \text{(3e)}
\end{array}
\right.
$$

where Ω_l and Ω_s are liquid and solid subdomains, Γ the interface between them, f the local free energy density, D_l and D_s positive constants, v_n the local normal velocity and κ the local interface curvature. The notation $[.]_l^s$ means the jump of a quantity between the solid and liquid sides of the interface, and $\mathcal{A}$ is an affine function which characterizes the different limits.

For the purpose of numerical simulations, O. Krüger originally introduced a finite-element in space, semi-implicit Euler in time numerical scheme [Krü99]. We investigate the convergence of this scheme for the isotropic model in chapter 3, which is the result of a joint work with J. F. Scheid,

presently submitted for publication. We introduce an elliptic projector in the finite element space, which is a generalization of V. Thomée's projector [Tho91] to a vectorial time-dependent problem with Neumann boundary conditions. A convergence result is obtained by combining this tool with problem-specific a priori error estimates and Gronwall's lemma. We find that if the solution $\vec{u}$ of the continuous problem (2) is sufficiently regular, then there exists a constant C independent of h and τ such that

$$\max_{0 \leqslant n \leqslant N} \|\vec{u}(t^n) - \vec{u}_h^n\|_{L^2(\Omega, \mathbb{R}^2)} \leqslant C(h^2 + \tau), \tag{4}$$

where $\vec{u}_h^n$, $n = 0, \ldots, N$ are the approximate solutions at discrete times $t_0, \ldots, t^n$, h the finite element mesh size and τ the time step of the numerical scheme.

We believe that the generalized vectorial elliptic projector we introduced might be useful in the study of convergence of a similar numerical scheme applied to other parabolic systems.

We have implemented the aforementioned numerical scheme as a `C++` program, based on M. Picasso's finite element code library and the USA National Institute of Standards (NIST) implementation of the GMRES algorithm for solving linear systems. Numerical results are presented in chapter 4. The theoretical order of convergence is verified for the isotropic model, and several stability questions are investigated for the anisotropic model. Finally, the physical validity of simulation results with the anisotropic model has been partially addressed with the example of a Ni-Cu alloy. The following figures show the phase-field and concentration in a simulation in the square adimensional domain $[-4, 4] \times [-4, 4]$. The computation was actually made in one quarter of that domain, with a two-percent anisotropy, after an adimensional time $t = 0.3$.
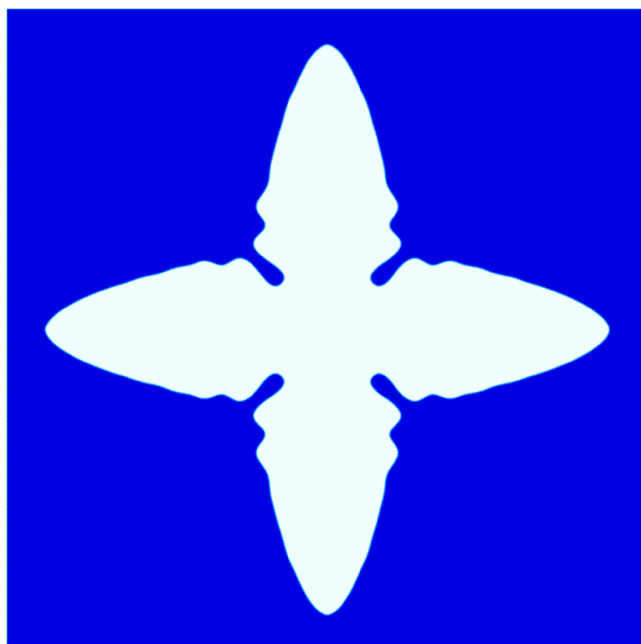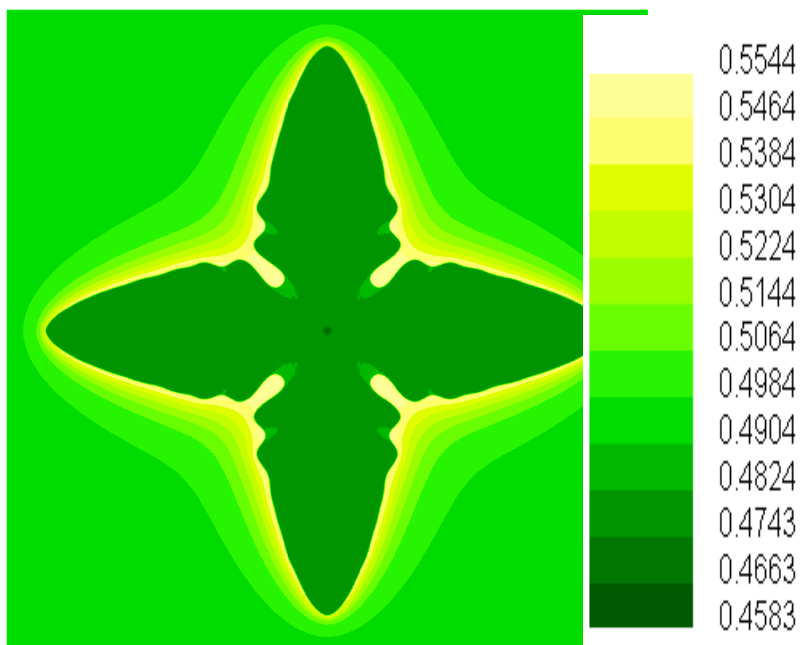
Figure 1: Phase-Field ϕ, $\bar{a} = 0.02$, $t = 0.3$

Figure 2: Concentration c, $\bar{a} = 0.02$, $t = 0.3$

Chapter 1

Model

1.1 Physical model

In this section we present the main steps of the construction of a solutal isothermal phase-field model. Some details have been omitted for the sake of readability, but can be found in appendix A. Both this section and the appendix are based on material originally presented in [KKS98], which aims to introduce a thermodynamically consistent model based on the works of Wheeler, Boettinger and McFadden [WBM92] and Warren and Boettinger [WB95].

1.1.1 Description of the physical system

We consider a mixture of two pure elements A and B, present both in liquid and solid states inside a space domain Ω whose border we call $\partial\Omega$. We consider the evolution of this system from an initial time 0 to a final time t_f. From now on, we will always denote by x space coordinates in Ω and by t time coordinates in $[0, t_f]$. The physical system can be characterized by a relative concentration $c : (x, t) \in \Omega \times [0, t_f] \longmapsto c(x, t) \in \mathbb{R}$ of element B with respect to the mixture. The relative concentration of element A will then be $1 - c$, and the variable c will take physical values in the interval $[0, 1]$. We further characterize the system with an order parameter for solidification, the phase field $\phi = \phi(x, t)$, which also takes values in the interval $[0, 1]$. A value of $\phi = 0$ corresponds to a pure solid region, and a value of $\phi = 1$ to a pure liquid region. Since we do not want to account for thermal effects, we assume temperature $T(t)$ to be homogenous in space, and we consider it as an external parameter. Note that all quantities in this section are considered with their proper physical dimension (e.g. t in seconds), whereas after section 1.2 and throughout the document, the same notations will be used to denote

the corresponding adimensionalized quantities. Also, let us point out that all functions introduced in the physical model make sense only for values of c and ϕ in $[0, 1]$. Continuation outside of the physical interval is the matter of mathematical modelling, examined in section 1.3.

To have a thermodynamical description of the evolution of variables c and ϕ, we introduce a Ginzburg-Landau free energy functional (see [CH58, PF90, WSW$^+$93])

$$\mathcal{F}(T, c, \phi) = \int_\Omega \left[f(T, c, \phi) + \frac{\varepsilon^2}{2} |\nabla \phi|^2 \right] dx, \tag{1.1}$$

where f is a free energy density and ε a small parameter (which is linked, as we shall see, to the solid-liquid interface thickness).

The second principle of thermodynamics tells us that the degrees of freedom of the system will evolve in a way that decreases the free energy of the system. We are considering temperature $T(t)$ as an externally imposed parameter. Therefore, we want the time evolution of both c and ϕ to be such that the time derivative at fixed T of $\mathcal{F}(T, c, \phi)$ be negative. We define this time derivative at fixed T as

$$\left. \frac{d}{dt} \mathcal{F}(T, c, \phi) \right|_{T=cst} = \int_\Omega \left(\frac{\partial f}{\partial c} \frac{\partial c}{\partial t} + \frac{\partial f}{\partial \phi} \frac{\partial \phi}{\partial t} + \varepsilon^2 \nabla \frac{\partial \phi}{\partial t} \cdot \nabla \phi \right) dx. \tag{1.2}$$

Furthermore, local conservation of matter implies that the evolution of c must be writeable in a divergence form, i.e. there is a flux of matter $J_c(T, c, \phi)$ such that

$$\frac{\partial c}{\partial t} = - \operatorname{div} \left(J_c(T, c, \phi) \right). \tag{1.3}$$

We may now integrate by parts the right-hand side of (1.2), thus naturally separating terms describing free energy production inside the domain from those describing free energy transport through the domain's boundary:

$$\left. \frac{d}{dt} \mathcal{F}(T, c, \phi) \right|_{T=cst} = \int_\Omega \left(J_c \cdot \nabla \frac{\partial f}{\partial c} + \left(\frac{\partial f}{\partial \phi} - \varepsilon^2 \triangle \phi \right) \frac{\partial \phi}{\partial t} \right) dx$$
$$+ \int_{\partial \Omega} \left(\varepsilon^2 \frac{\partial \phi}{\partial t} \nabla \phi - \frac{\partial f}{\partial c} J_c \right) \cdot n \, dx, \tag{1.4}$$

where n is the unit vector normal to the boundary $\partial \Omega$.

To fulfill the second principle of thermodynamics, the evolution of both c and ϕ inside the domain should tend to locally decrease the free energy. We

therefore ask that each term of the integrand in the first integral of (1.4) be non-positive:

$$\begin{cases} J_c \cdot \nabla \dfrac{\partial f}{\partial c} \leqslant 0, & \text{in} \quad \Omega, & \text{(1.5a)} \\[2mm] \left(\dfrac{\partial f}{\partial \phi} - \varepsilon^2 \triangle \phi \right) \dfrac{\partial \phi}{\partial t} \leqslant 0, & \text{in} \quad \Omega. & \text{(1.5b)} \end{cases}$$

Conservation of matter (1.3) and decrease of free energy inside the domain (1.5b) can be fulfilled by evolution equations which are reasonably simple, yet flexible enough to allow for fitting of the resulting model to specific situations: Let $\eta(T, c, \phi)$ and $\mu(T, c, \phi)$ be positive functions. We choose

$$J_c(T, c, \phi) = -\mu(T, c, \phi) \nabla \frac{\partial f}{\partial c}, \tag{1.6}$$

and we describe the evolution of quantities c and ϕ in the domain Ω for positive times by the following set of equations:

$$\begin{cases} \dfrac{\partial \phi}{\partial t} = \eta \left(\varepsilon^2 \triangle \phi - f_\phi \right), & \text{in} \quad \Omega, & \text{(1.7a)} \\[2mm] \dfrac{\partial c}{\partial t} = \text{div} \left(\mu \left(f_{cc} \nabla c + f_{c\phi} \nabla \phi \right) \right), & \text{in} \quad \Omega, & \text{(1.7b)} \end{cases}$$

where $f_\phi = \dfrac{\partial f}{\partial \phi}$, $f_{cc} = \dfrac{\partial^2 f}{\partial c^2}$, $f_{c\phi} = \frac{\partial^2 f}{\partial c \, \partial \phi}$ and f, η and μ depend on T, c and ϕ.

Finally, in an isothermal system closed to exchange of matter, neither concentration flux, nor non-thermal free energy flux should cross the domain boundary. We interpret the latter requirement by asking that the integrand of the righternmost term in (1.4) be equal to zero throughout the boundary. Therefore, the two aforementioned conditions can be written as:

$$\begin{cases} \left(\varepsilon^2 \dfrac{\partial \phi}{\partial t} \nabla \phi - \dfrac{\partial f}{\partial c} J_c \right) \cdot n = 0, & \text{on} \quad \partial \Omega, & \text{(1.8a)} \\[2mm] J_c \cdot n = 0, & \text{on} \quad \partial \Omega, & \text{(1.8b)} \end{cases}$$

These boundary conditions can be simplified to

$$\frac{\partial \phi}{\partial n} = \frac{\partial c}{\partial n} = 0, \quad \text{on} \quad \partial \Omega. \tag{1.9}$$

The general form (1.7) of isothermal solutal phase-field evolution equations is used both by Wheeler, Boettinger and McFadden [WBM92] and

Warren and Boettinger [WB95]. To completely determine the evolution equations (1.7), a free energy density $f(T, c, \phi)$ has to be constructed and functions $\eta(T, c, \phi)$ and $\mu(T, c, \phi)$ must be determined by fitting to known limit situations.

1.1.2   Free energy density

The free energy density $f(T, c, \phi)$ for a solutal phase-field model is given by a convex combination of the pure element free energies $f^A(T, \phi)$ and $f^B(T, \phi)$, plus a mixture term (see [BK97]):

$$f(T, c, \phi) = (1 - c)f^A(T, \phi) + cf^B(T, \phi) + \frac{RT}{v_m}\big((1 - c)\ln(1 - c) + c\ln(c)\big),$$
$$(1.10)$$

where R is Boltzman's constant and v_m the molar volume.

The specification of a particular form of pure element free energies is the most important step in defining a particular solutal phase-field model. We chose to work using variants of Warren and Boettinger's thermodynamically consistent free energy density [WB95]. We justify this choice in appendix A, given by

$$f^\xi(T, \phi) = L^\xi \frac{T_m^\xi - T}{T_m^\xi} p(\phi) + W^\xi \frac{T}{T_m^\xi} g(\phi) + f^\xi(T, 0), \qquad (1.11)$$

where ξ stands for either A or B.

The function $g(\phi)$ is a standard double-well potential

$$g(\phi) = \phi^2(1 - \phi)^2. \qquad (1.12)$$

The constants L^ξ and T_m^ξ are respectively the latent heat and melting temperature for pure element ξ, while W^ξ is a model parameter for the potential barrier height at melting temperature (which we shall see is linked to both interface thickness and surface tension).

Function $p(\phi)$ is introduced in [WB95] as a regularization of the solid-liquid discontinuity. Whereas Warren and Boettinger specify a choice of p as a fifth-degree polynomial, in appendix A we investigate possible generalizations of this choice. To get the simplest possible model, p must follow at least these constraints:

$$\begin{cases} p(0) = 0, & (1.13a) \\[2mm] p(1) = 1, & (1.13b) \\[2mm] p'(\phi) > 0, \quad \forall \phi \in]0, 1[, & (1.13c) \end{cases}$$

but in order to get a completely thermodynamically consistent model, we require also the following extra constraints on the function p (see appendix A):

$$\begin{cases} p'(0) = p'(1) = 0, & \text{(1.14a)} \\ p''(0) = p''(1) = 0. & \text{(1.14b)} \end{cases}$$

Warren and Boettinger [WB95] have chosen the polynomial of smallest degree satisfying both constraints 1.13 and 1.14, which is

$$p(\phi) = 6\phi^5 - 15\phi^4 + 10\phi^3. \tag{1.15}$$

For numerical simulations in chapter 4, we have chosen to use exactly Warren and Boettinger's nonlinear functions. However, on the more theoretical chapters 2 and 3, results are valid for a more general family of models. For instance, we will only need the constraints, and not a specific choice of p, in order to derive asymptotic limits of the model in chapter 2. Actually, we are also interested in knowing whether the extra constraints (1.14) that ensure thermodynamic consistency are necessary for the model to have meaningful sharp-interface limits or if constraints (1.13) are sufficient, therefore allowing for a simpler choice of p. We are motivated in this by Kim *et al.* [KPGD98], who have numerical reasons to believe that (another class of) phase-field models yield the same asymptotic limits whether they are thermodynamically consistent or not. As for the numerical scheme convergence in chapter 3, the proof relies on assumptions made on the nonlinearities of the problem, which hold true for any sufficiently regular choice of p verifying constraints (1.13) and some extra mathematical assumptions outside of the physical domain for the variables. The convergence result even remains valid for a more general class of problems.

1.1.3 Fitting of model parameters

Pure element phase equation

The stationary one-dimensional pure element ($c \equiv 0$) equation for the phase-field at melting temperature $T = T_m^A$ is

$$\varepsilon^2 \frac{\partial^2 \phi}{\partial x^2} - W^A g'(\phi) = 0. \tag{1.16}$$

It has an infinite number of explicit solutions $\phi : \mathbb{R} \longrightarrow \mathbb{R}$ for limit conditions $\phi(-\infty) = 1$, $\phi(+\infty) = 0$, obtained by translations of coordinate
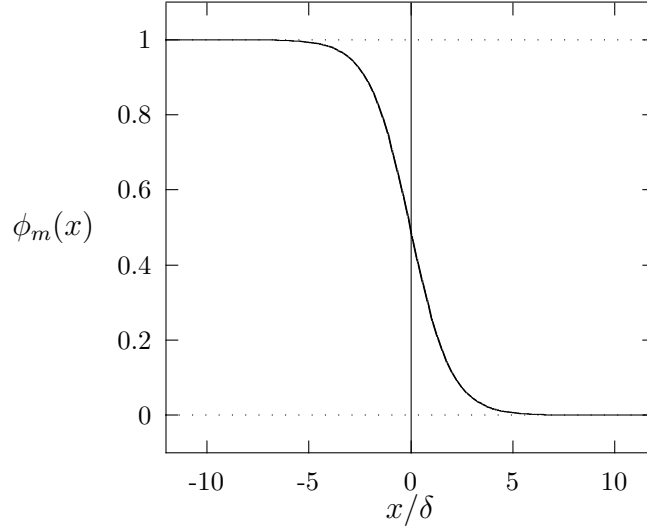
Figure 1.1: one-dimensional pure element stationary solution

x. A particular function ϕ_m can be chosen by fixing $\phi_m(0) = \frac{1}{2}$. It is explicitly given by

$$\phi_m(x) = \frac{1}{1 + e^{\frac{\sqrt{2W^A}}{\varepsilon}x}}, \tag{1.17}$$

and its graph is represented in figure 1.1.

The quantity

$$\delta = \varepsilon/\sqrt{2W^A} \tag{1.18}$$

can be easily interpreted as the interface thickness, and should be given numerical values of the order of atomic distances (see [WBM92]), such as $\delta = 5.10^{-8}$ cm.

Moreover, we can compute the total free energy (1.1) for the specific solution $c \equiv 0$, $\phi = \phi_m$. If we give the one-dimensional solution the interpretation of a planar three-dimensional solution, then the total free energy of the one-dimensional solution can be given the interpretation of a surface energy

$$\sigma^A = \mathcal{F}(T_m^A, 0, \phi_m) = \frac{\varepsilon\sqrt{2W^A}}{6}, \tag{1.19}$$

where $\mathcal{F}$ is given by equation (1.1). Such surface tensions for stationary planar solutions at melting temperature are experimentally known and can be used to fit the model.

For a pure metal A, we can therefore link model parameters W^A and ε to physically known quantities using equations (1.18) and (1.19), resulting in

$$W^A = 3\frac{\sigma^A}{\delta} \quad \text{and} \quad \varepsilon^2 = 6\sigma^A\delta \qquad \text{when} \quad c = 0. \tag{1.20}$$

Analogous parameter adjustments also hold for pure element B when $c = 1$.

For the alloy, we will keep the adjusted values for the potential barrier heights

$$W^A = 3\frac{\sigma^A}{\delta} \quad \text{and} \quad W^B = 3\frac{\sigma^B}{\delta}. \tag{1.21}$$

We want however to keep ε^2 a constant, so we arbitrarily define it as the average of the pure element values:

$$\varepsilon^2 = 3(\sigma^A + \sigma^B)\delta. \tag{1.22}$$

This approximation is reasonable under the assumption that c remains bounded on a small interval. Note that we make a similar assumption for the molar volume v_m.

Pure phase concentration equation

We want to ensure that the evolution equation for c on a pure solid ($\phi \equiv 0$) or a pure liquid ($\phi \equiv 1$) is a classical diffusion equation of the form

$$\begin{cases} \dfrac{\partial c}{\partial t} = D_s \triangle c, & \text{if} \quad \phi \equiv 0, & \text{(1.23a)} \\[2mm] \dfrac{\partial c}{\partial t} = D_l \triangle c, & \text{if} \quad \phi \equiv 1, & \text{(1.23b)} \end{cases}$$

where D_s and D_l are the solid and liquid diffusion coefficients (assumed to be independent of c).

Generalizing these particular cases, we want the equation for c on a homogeneous phase (i.e. on regions where $\nabla\phi = 0$) to be of the form

$$\frac{\partial c}{\partial t} = D_1(\phi)\triangle c, \tag{1.24}$$

where

$$D_1(\phi) = D_s + q(\phi)(D_l - D_s) \tag{1.25}$$

is a variable diffusion coefficient, such that q is a monotonous increasing function of $\phi \in [0, 1]$ with values $q(0) = 0$ and $q(1) = 1$. For instance, Warren and Boettinger choose $q(\phi) = p(\phi)$, since these two functions play analogous roles in the regularization of the solid-liquid transition. Again, the particular choices for p and q won't play any role either in the asymptotic limits (chapter 2), which depend only on some of the physical properties that were imposed on these functions during the construction of the model, or in the convergence result (chapter 3), which relies on more general mathematical assumptions. We do however also use Warren and Boettinger's specific choice of function q for the numerical simulations in chapter 4.

Equation (1.24) determines the positive model function μ in (1.7) as

$$\mu(T, c, \phi) = \frac{D_1(\phi)}{f_{cc}(T, c, \phi)}, \tag{1.26}$$

We will also assume that the phase-field diffusion coefficient defined by

$$M = \eta \varepsilon^2 \tag{1.27}$$

is a positive constant, where η is one of the positive model functions in (1.7) and ε the Ginzburg-Landau coefficient in (1.1).

1.1.4   Anisotropy

The model we have introduced is isotropic: there is no privileged direction for solidification. The more theoretical chapters 2 and 3 will deal with this simple isotropic model. However, real alloys grow anisotropically, and we want to take this in into consideration for numerical simulations in chapter 4. This anisotropy is due to crystallographic properties of the solid phase of an alloy: whereas the liquid is disordered in the microscopic scale, the solid will appear as an ordered lattice of atoms. In two dimensions, it will thus typically have four or six privileged directions of growth.

To account for this anisotropy effect, we change the behaviour of the phase-field equation according to phenomenological laws, as did Warren and Boettinger [WB95]. First we introduce an angle $\psi \in [0, 2\pi[$ depending on the local gradient of ϕ, such that

$$\nabla \phi = |\nabla \phi| \begin{pmatrix} \cos(\psi(\nabla \phi)) \\ \sin(\psi(\nabla \phi)) \end{pmatrix}. \tag{1.28}$$

This is the angle between the direction normal to the solidification front and an arbitrary axis. If $\nabla \phi = 0$, then we may arbitrarily fix $\psi = 0$.

Anisotropy is introduced in the model through an anisotropy factor $a(\psi)$, taking values near 1, maximal when ψ indicates a privileged solidification direction. The anisotropy factor is introduced in the Ginzburg-Landau free energy (1.1), which is modified as follows:

$$\frac{\varepsilon^2}{2}|\nabla\phi|^2 \longrightarrow \frac{\varepsilon^2}{2}a^2(\psi(\nabla\phi))|\nabla\phi|^2. \tag{1.29}$$

This induces the following modification in the integrand of the right-hand side of (1.2):

$$\varepsilon^2\nabla\frac{\partial\phi}{\partial t}\cdot\nabla\phi \longrightarrow \frac{\partial}{\partial t}\left(\frac{\varepsilon^2}{2}a^2(\psi(\nabla\phi))|\nabla\phi|^2\right). \tag{1.30}$$

We can write the previous quantity more explicitly as

$$\frac{\partial}{\partial t}\left(\frac{\varepsilon^2}{2}a^2(\psi(\nabla\phi))|\nabla\phi|^2\right)$$
$$= \varepsilon^2 a^2(\psi(\nabla\phi))\nabla\frac{\partial\phi}{\partial t}\cdot\nabla\phi + \varepsilon^2 a'(\psi(\nabla\phi))a(\psi(\nabla\phi))\frac{\partial\psi(\nabla\phi)}{\partial t}|\nabla\phi|^2. \tag{1.31}$$

We now need to find an explicit expression for the time derivative of $\psi(\nabla\phi)$. Differentiating (1.28) with respect to t we find that

$$\nabla\frac{\partial\phi}{\partial t} = \frac{\partial|\nabla\phi|}{\partial t}\begin{pmatrix}\cos(\psi(\nabla\phi))\\\sin(\psi(\nabla\phi))\end{pmatrix} + |\nabla\phi|\,J^T\begin{pmatrix}\cos(\psi(\nabla\phi))\\\sin(\psi(\nabla\phi))\end{pmatrix}\frac{\partial\psi(\nabla\phi)}{\partial t}, \tag{1.32}$$

where J is the rotation matrix

$$J = \begin{pmatrix} 0 & 1 \\ -1 & 0 \end{pmatrix}, \tag{1.33}$$

which verifies $J^T J = Id$, $J^2 = -Id$ and $\vec{w}^T J\vec{w} = 0, \forall\vec{w}\in\mathbb{R}^2$.

If we take the scalar product of (1.32) and $J\nabla\phi/|\nabla\phi|$, we find, using definition (1.28), that

$$\frac{\partial\psi(\nabla\phi)}{\partial t} = -\frac{1}{|\nabla\phi|^2}\nabla\frac{\partial\phi}{\partial t}\cdot J\nabla\phi. \tag{1.34}$$

Using (1.34) we can further explicit (1.31) as

$$\frac{\partial}{\partial t}\left(\frac{\varepsilon^2}{2}a^2(\psi(\nabla\phi))|\nabla\phi|^2\right) = \varepsilon^2\nabla\frac{\partial\phi}{\partial t}\cdot\Theta(\nabla\phi)\nabla\phi, \tag{1.35}$$

where

$$\Theta(\nabla\phi) = \begin{pmatrix} a^2(\psi(\nabla\phi)) & -a'(\psi(\nabla\phi))a(\psi(\nabla\phi)) \\ a'(\psi(\nabla\phi))a(\psi(\nabla\phi)) & a^2(\psi(\nabla\phi)) \end{pmatrix}. \qquad (1.36)$$

We now consider the modification (1.30) in the time derivative of the total free energy, together with equality (1.35). Replacing this in the derivation of the model (equations (1.2)-(1.8)), we find that when anisotropy is introduced into the free energy, equation (1.7a) describing the evolution of ϕ should be replaced by

$$\frac{\partial \phi}{\partial t} = \eta \left(\varepsilon^2 \operatorname{div} (\Theta(\nabla\phi)\nabla\phi) - f_\phi \right), \quad \text{in} \quad \Omega, \qquad (1.37)$$

and boundary condition (1.8a) for ϕ by

$$\left(\varepsilon^2 \frac{\partial \phi}{\partial t} \Theta(\nabla\phi)\nabla\phi - \frac{\partial f}{\partial c} J_c \right) \cdot n = 0, \quad \text{on} \quad \partial\Omega, \qquad (1.38)$$

while equations (1.7b) and (1.8b) are kept in their original form.

Finally, we have to define an anisotropy function $a(\psi)$. We choose as Warren and Boettinger [WB95]:

$$a(\psi) = 1 + \bar{a}\cos(k\psi), \qquad (1.39)$$

where k is the order of anisotropy (usually 4 or 6) and $\bar{a} \in [0, 1[$ its amplitude.

Note that the natural limit conditions associated with the anisotropic evolution equations are more complex than simple homogeneous Neumann conditions. Nevertheless, they are still the physically relevant conditions, as they guarantee conservation of matter in the physical domain, and forbid transfer of free energy through the phase, allowing only free energy transfer through the thermal flux that intrinsically keeps the system isothermal.

1.2   Adimensional model

Combining all the steps of the model construction, we obtain evolution equations for c and ϕ, which can be adimensionalized by changing space coordinates to $\tilde{x} = \frac{x}{l}$, where l is a characteristic length of the domain Ω, and time coordinates to $\tilde{t} = \frac{D_l t}{l^2}$, where $\frac{l^2}{D_l}$ is the characteristic liquid diffusion time associated with the characteristic length l. Furthermore, we won't explicitly write the temperature T anymore, since it plays the role of a parameter. The

evolution equations then become, in the isotropic case, for $\tilde{\phi}(\tilde{x}, \tilde{t}) = \phi(x, t)$ and $\tilde{c}(\tilde{x}, \tilde{t}) = c(x, t)$,

$$
\begin{cases}
\dfrac{\partial \tilde{\phi}}{\partial \tilde{t}} = \widetilde{M} \left(\widetilde{\triangle} \tilde{\phi} - \dfrac{1}{\tilde{\delta}} \tilde{f}_{\tilde{\phi}}(\tilde{c}, \tilde{\phi}) \right), & \text{(1.40a)} \\[3mm]
\dfrac{\partial \tilde{c}}{\partial \tilde{t}} = \widetilde{\mathrm{div}} \left[\tilde{\mu}(\tilde{c}, \tilde{\phi}) \left(\tilde{f}_{\tilde{c}\tilde{c}}(\tilde{c}, \tilde{\phi}) \widetilde{\nabla} \tilde{c} + \tilde{f}_{\tilde{c}\tilde{\phi}}(\tilde{c}, \tilde{\phi}) \widetilde{\nabla} \tilde{\phi} \right) \right], & \text{(1.40b)}
\end{cases}
$$

where $\widetilde{M} = \frac{M}{D_l}$, $\tilde{\delta} = \frac{\delta}{l}$,

$$
\begin{aligned}
\tilde{f}(c, \phi) &= \frac{\delta l}{\varepsilon^2} f(c, \phi) \\
&= \frac{\alpha(c)}{\tilde{\delta}} g(\phi) + \beta(c) p(\phi) + \frac{1}{\gamma} \left[(1 - c) \ln(1 - c) + c \ln c \right] + \tilde{f}_0(c)
\end{aligned} \qquad \text{(1.41)}
$$

and

$$
\tilde{\mu}(c, \phi) = \frac{\varepsilon^2}{D_l \delta l} \mu(c, \phi) = \gamma c (1 - c) \widetilde{D}_1(\phi). \qquad \text{(1.42)}
$$

On the definition of $\tilde{\mu}$ we used the variable adimensional concentration diffusivity defined by

$$
\widetilde{D}_1(\phi) = \tilde{D}_s + q(\phi) \left(\tilde{D}_l - \tilde{D}_s \right), \qquad \text{(1.43)}
$$

where $\tilde{D}_l = 1$ and $\tilde{D}_s = \frac{D_s}{D_l}$.

On the definition of $\tilde{f}$ we used the notation $\tilde{f}_0(c)$ to describe an affine function, which is actually irrelevant since f appears in the evolution equations only through derivatives on ϕ and second derivatives on c.

The constant γ used for defining both $\tilde{f}$ and $\tilde{\mu}$ is linked to physical parameters by

$$
\gamma = 3 \frac{v_m}{RT} \frac{\sigma^A + \sigma^B}{l} \qquad \text{(1.44)}
$$

Finally, the auxiliary functions α and β used in (1.41) are defined by

$$
\begin{cases}
\alpha(c) = (1 - c)\alpha^A + c\alpha^B & \text{(1.45a)} \\[2mm]
\beta(c) = (1 - c)\beta^A + c\beta^B & \text{(1.45b)}
\end{cases}
$$

where

$$
\begin{cases}
\alpha^\xi = \dfrac{\sigma^\xi}{\sigma^A + \sigma^B}\dfrac{T}{T_m^\xi} & \text{(1.46a)} \\[4mm]
\beta^\xi = \dfrac{l}{3}\dfrac{L_\xi}{\sigma^A + \sigma^B}\dfrac{T_m^\xi - T}{T_m^\xi}, & \text{(1.46b)}
\end{cases}
$$

for $\xi = A$ or B.

   We will omit the tildes from now on in all quantities throughout the rest of this document. We will be always implicitly considering the adimensional quantities, except where explicitly stated otherwise. Note that the phase-field diffusion coefficient M is the only model parameter yet to be linked to physical quantities. This will be done in chapter 2 through asymptotic limits of the model.

1.3   Mathematical formulation

1.3.1   Mathematical problem

Expanding evolution equations (1.40) (without the tildes) and combining them with physical boundary conditions (1.9) and initial conditions, we can write the mathematical problem corresponding to the physical model derived in section 1.1 as:

   Find $\phi, c : \Omega \times [0, t_f] \longrightarrow \mathbb{R}$ such that:

$$
\begin{cases}
\dfrac{1}{M}\dfrac{\partial \phi}{\partial t} - \triangle\phi = F(c, \phi), & \text{in} \quad \Omega \times (0, t_f), & \text{(1.47a)} \\[3mm]
\dfrac{\partial c}{\partial t} - \operatorname{div}\left(D_1(\phi)\nabla c + D_2(c, \phi)\nabla\phi\right) = 0, & \text{in} \quad \Omega \times (0, t_f), & \text{(1.47b)} \\[3mm]
\dfrac{\partial \phi}{\partial n} = \dfrac{\partial c}{\partial n} = 0 & \text{on} \quad \partial\Omega \times (0, t_f), & \text{(1.47c)} \\[2mm]
\phi(0) = \phi_0 & \text{in} \quad \Omega, & \text{(1.47d)} \\[2mm]
c(0) = c_0 & \text{in} \quad \Omega, & \text{(1.47e)}
\end{cases}
$$

where

$$
F(c, \phi) = -\frac{1}{\delta^2}\alpha(c)g'(\phi) - \frac{1}{\delta}\beta(c)p'(\phi), \tag{1.48}
$$

$$
D_2(c, \phi) = \gamma c(1 - c)D_1(\phi)\left(\frac{\alpha'}{\delta}g'(\phi) + \beta'p'(\phi)\right) \tag{1.49}
$$

Figure 1.2: Non-linear source term for phase-field equation
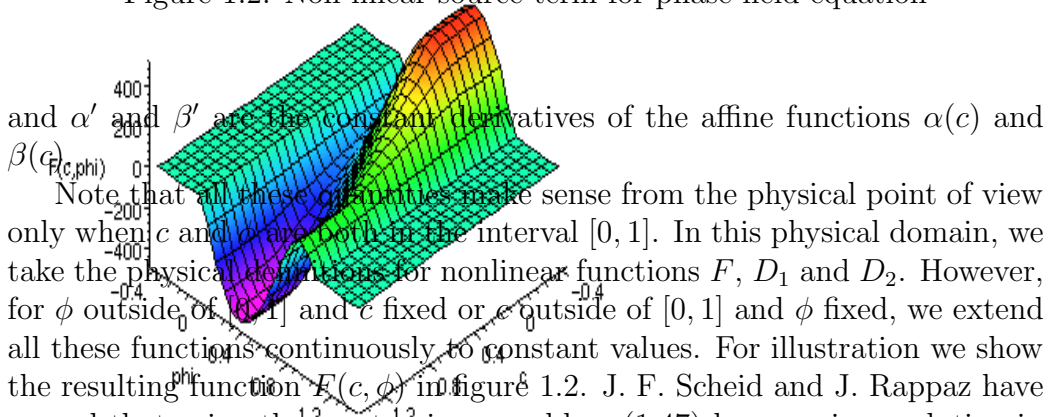
and α' and β' are the constant derivatives of the affine functions $\alpha(c)$ and $\beta(c)$.

Note that all these quantities make sense from the physical point of view only when c and ϕ are both in the interval $[0, 1]$. In this physical domain, we take the physical definitions for nonlinear functions F, D_1 and D_2. However, for ϕ outside of $[0, 1]$ and c fixed or c outside of $[0, 1]$ and ϕ fixed, we extend all these functions continuously to constant values. For illustration we show the resulting function $F(c, \phi)$ in figure 1.2. J. F. Scheid and J. Rappaz have proved that using these extensions, problem (1.47) has a unique solution in $L^2(0, t_f; H^2(\Omega))$ with time derivative in $L^2(0, t_f; L^2(\Omega))$ when the initial condition is in $H^2(\Omega)$. Furthermore, they proved a maximum principle: under the same assumptions, the solution stays in the physical domain throughout the evolution if the initial condition was in the physical domain.

1.3.2 Vectorial formulation

We transform problem (1.47) to a vectorial form by defining the vectorial variable

$$\vec{u} = \begin{pmatrix} \phi \\ \zeta c \end{pmatrix}, \tag{1.50}$$

where ζ is an arbitrary positive parameter that will be fixed later. Then problem (1.47) reads as a vectorial problem of the form:

Find $\vec{u} : (x,t) \in \Omega \times [0, t_f] \longmapsto \vec{u}(x,t) = (u_1(x,t), u_2(x,t)) \in \mathbb{R}^2$ such that

$$\begin{cases} \dfrac{\partial \vec{u}}{\partial t} = \operatorname{div}\left(D(\vec{u})\nabla\vec{u}\right) + \vec{F}(\vec{u}) & \text{in} \quad \Omega \times (0, t_f), & (1.51\text{a}) \\[2mm] \dfrac{\partial \vec{u}}{\partial n} = 0 & \text{on} \quad \partial\Omega \times (0, t_f), & (1.51\text{b}) \\[2mm] \vec{u}(0) = \vec{u}_0 & \text{in} \quad \Omega, & (1.51\text{c}) \end{cases}$$

where the 2×2 triangular matrix D is given by

$$D(\vec{u}) = \begin{pmatrix} M & 0 \\ \zeta D_2\left(\frac{u_2}{\zeta}, u_1\right) & D_1(u_1) \end{pmatrix} \tag{1.52}$$

and the vector $\vec{F}$ by

$$\vec{F}(\vec{u}) = \begin{pmatrix} MF\left(\frac{u_2}{\zeta}, u_1\right) \\ 0 \end{pmatrix}. \tag{1.53}$$

where

$$\operatorname{div}\left(D(\vec{u})\nabla\vec{u}\right) = \sum_{i=1,2} \frac{\partial}{\partial x_i}\left(D(\vec{u})\frac{\partial}{\partial x_i}\vec{u}\right).$$

The nonlinear functions of the vectorial problem, defined from the physical functions extended to constants outside the physical domain, verify the following assumptions:

(H1.1) $\vec{F}$ is a 2-vector of Lipschitz bounded components. We call $\mathcal{L}_{\vec{F}}$ the maximum of the components' Lipschitz constants.

(H1.2) D is a 2x2 lower triangular matrix whose coefficients are given by $d_{11} = M > 0$, $d_{12} = 0$, $d_{21} = \zeta D_2(\vec{u})$ and $d_{22} = D_1(\vec{u}) \geqslant D_s > 0$. The functions $D_1(\vec{u})$ and $D_2(\vec{u})$ are Lipschitz bounded functions. We call D_M the maximum of the components' absolute bounds and $\mathcal{L}_D$ the maximum of the components' Lipschitz constants.

Since $M > 0$ and $D_1(\vec{u}) \geqslant D_s > 0$ for all $\vec{u} \in \mathbb{R}^2$, we can choose the parameter ζ small enough for $D(\vec{u})$ to be definite positive uniformly in $\vec{u}$. Indeed, if we choose

$$\zeta < \frac{2(MD_s)^{1/2}}{\|D_2\|_\infty}, \tag{1.54}$$

where

$$\|D_2\|_\infty = \sup_{\vec{u} \in \mathbb{R}^2} |D_2(\vec{u})|, \tag{1.55}$$

then it can be shown that

$$\vec{w}^T D(\vec{v}) \vec{w} \geqslant \min(M, D_s) \vec{w}^T \vec{w}, \quad \forall \vec{v}, \vec{w} \in \mathbb{R}^2, \tag{1.56}$$

so in addition to (H1.1) and (H1.2), it is plainly justified to make an extra assumption on the positiveness of the matrix:

(H1.3) The matrix $D(\vec{v})$ is definite positive uniformly with $\vec{v}$, i.e. there exists a constant $D_m > 0$ independent of $\vec{v}$ such that $\vec{w}^T D(\vec{v}) \vec{w} \geqslant D_m \vec{w}^T \vec{w}$ for all $\vec{v}, \vec{w} \in \mathbb{R}^2$.

1.3.3 Variational formulation

We recall some basic properties about vectorial calculus that will be useful later on. If $\vec{v} : \Omega \in \mathbb{R}^2 \longrightarrow \mathbb{R}^2$ is a differentiable function, we define its gradient by the matrix

$$\nabla \vec{v} = \left(\frac{\partial v_i}{\partial x_j} \right)_{i,j=1,2}. \tag{1.57}$$

We introduce the notation $\mathcal{M}_2$ to denote the set of 2×2 matrices with real components.

From now on we shall denote by a colon the tensorial product in $\mathbb{R}^2 \otimes \mathbb{R}^2$, such that for any $A = (a_{ij})_{i,j=1,2}$ in $\mathcal{M}_2$ we have

$$A \nabla \vec{v} : \nabla \vec{w} = \sum_{\mu,\nu=1,2} a_{\nu\mu} \nabla v_\mu \cdot \nabla w_\nu = \sum_{i=1,2} \sum_{\mu,\nu=1,2} a_{\nu\mu} \frac{\partial v_\mu}{\partial x_i} \frac{\partial w_\nu}{\partial x_i}, \tag{1.58}$$

where $\vec{v}, \vec{w}$ are differentiable functions from Ω to $\mathbb{R}^2$.

Let us remark that if a 2×2 matrix $A = (a_{ij})_{i,j=1,2}$ is positive definite, i.e. if there exists $\lambda > 0$ such that $\vec{w}^T A \vec{w} \geqslant \lambda |\vec{w}|^2$ for all $\vec{w} \in \mathbb{R}^2$, then for a differentiable function $\vec{v} : \Omega \in \mathbb{R}^2 \longrightarrow \mathbb{R}^2$ we have

$$A \nabla \vec{v} : \nabla \vec{v} \geqslant \lambda \left(|\nabla v_1|^2 + |\nabla v_2|^2 \right). \tag{1.59}$$

This can be immediately proved if we notice that

$$A \nabla \vec{v} : \nabla \vec{v} = a_{11} |\nabla v_1|^2 + a_{22} |\nabla v_2|^2 + (a_{12} + a_{21}) \nabla v_1 \cdot \nabla v_2 \tag{1.60}$$

$$\geqslant a_{11} |\nabla v_1|^2 + a_{22} |\nabla v_2|^2 - |a_{12} + a_{21}| |\nabla v_1| |\nabla v_2|. \tag{1.61}$$

and choose $w_1 = |\nabla v_1|$ and $w_2 = -\operatorname{sign}(a_{12} + a_{21}) |\nabla v_2|$ in the above definition of positive definiteness.

It is also clear from (1.58) that for any matrix $A \in \mathcal{M}_2(\mathbb{R})$ with bounded components, we have

$$\int_\Omega A\nabla\vec{v} : \nabla\vec{w} = \int_\Omega A^T\nabla\vec{w} : \nabla\vec{v}, \qquad \forall\, \vec{v}, \vec{w} \in H^1(\Omega, \mathbb{R}^2). \qquad (1.62)$$

Furthermore, for any matrix $A \in \mathcal{M}_2$ with components in $W^{1,\infty}(\Omega)$, the following Green's formula

$$\int_\Omega A\nabla\vec{v} : \nabla\vec{w} = -\int_\Omega \operatorname{div}(A\nabla\vec{v}) \cdot \vec{w} + \int_{\partial\Omega} A\frac{\partial\vec{v}}{\partial n} \cdot \vec{w} \qquad (1.63)$$

holds for all $\vec{v} \in H^2(\Omega, \mathbb{R}^2)$ and $\vec{w} \in H^1(\Omega, \mathbb{R}^2)$.

Using the notations we just introduced and defining $V = H^1(\Omega)$, the vectorial problem (1.51) can be rewritten in a weak form as:

Find $\vec{u} \in L^2(0, t_f; V^2)$ s.t. $\dfrac{\partial\vec{u}}{\partial t} \in L^2(0, t_f; (V')^2)$ and

$$\begin{cases} \displaystyle\int_\Omega \frac{\partial\vec{u}}{\partial t}(t) \cdot \vec{v} + \int_\Omega D(\vec{u}(t))\nabla\vec{u}(t) : \nabla\vec{v} = \int_\Omega \vec{F}(\vec{u}(t)) \cdot \vec{v}, & (1.64a) \\ \qquad\qquad\qquad\qquad \forall\vec{v} \in V^2, \quad \text{a.e. } t \in (0, t_f), & \\ \vec{u}(0) = \vec{u}_0. & (1.64b) \end{cases}$$

This variational formulation will be useful for the expression of the numerical scheme in section 3.1, and consequently for the error analysis.

1.3.4 Anisotropic problem

When anisotropy is added to the model, as explained at the end of section 1.1, the previous formulations remain the same, except that now the diffusion matrix D is given by:

$$D(\vec{u}) = \begin{pmatrix} M\Theta(\nabla u_1) & 0 \\ \zeta D_2\left(\frac{u_2}{\zeta}, u_1\right) & D_1(\phi) \end{pmatrix}. \qquad (1.65)$$

where Θ is defined by (1.36).

The well-posedness of the anisotropic problem has been studied in [BR]. The main result of that paper is the existence of weak solutions when the following condition is fulfilled by the anisotropy parameters:

$$\bar{a} \leqslant \frac{1}{k^2 - 1}. \qquad (1.66)$$

This condition is directly linked to the convexity of the anisotropy operator.

This theoretical result has prompted us to look for a change of behaviour for values of $\bar{a}$ below and above this critical number, by performing several numerical tests, which are presented in section 4.3.

Chapter 2

Sharp-interface limits

Our goal in this chapter is to establish formal asymptotic limits for the problem defined by the set of equations (1.40) [1] for a two-dimensional space domain Ω when $\delta \longrightarrow 0$, using when needed assumptions (1.13) and (1.14) on function p, but never a specific choice of this function. Four different limits will be considered, characterized by the dependence of the surface tensions σ^A and σ^B and model parameter M on δ. This approach is analog to Caginalp's in [Cag89], where he considers various limits of a thermal phase-field model differing by the behaviour of several model parameters while the limit is taken. The results of this chapter have already been published in [Kes01].

We assume the boundedness of ϕ and c in the following way:

$$
\begin{cases}
0 \leqslant \phi(x,t) \leqslant 1, \quad x \in \Omega, \quad t \geqslant 0, & \text{(2.1a)} \\[2mm]
0 < c_{\min} \leqslant c(x,t) \leqslant c_{\max} < 1, \quad x \in \Omega, \quad t \geqslant 0. & \text{(2.1b)}
\end{cases}
$$

We also assume that

$$ D_s > 0, \tag{2.2} $$

which means that a pure solid inhomogenous in c is not a stationary solution of (1.40). We shall only consider the case of two-dimensional space domains.

Finally, we define liquid and solid free energy densities by

$$
\begin{cases}
f^{\text{liq}}(c) = f(c,1), & \text{(2.3a)} \\[2mm]
f^{\text{sol}}(c) = f(c,0). & \text{(2.3b)}
\end{cases}
$$

---

[1]Notice that in this chapter we are omitting the tildes from the adimensional quantities defined in section 1.2, so that for instance the parameters we now call δ and M were called $\tilde{\delta}$ and $\tilde{M}$ in (1.40).

2.1   Small surface tension limit: classical Stefan-like problem

We consider the limit where δ, σ^A and σ^B tend to zero with δ/σ^A, δ/σ^B, and M kept fixed. Let us define a modified adimensional free energy density that will be independent of δ in this particular limit (except for the irrelevant last term that doesn't contribute to the derivatives of f appearing in (1.40)):

$$
\begin{aligned}
\hat{f}(c,\phi) &= \delta f(c,\phi) \\
&= \alpha(c)g(\phi) + \hat{\beta}(c)p(\phi) + \frac{1}{\hat{\gamma}}\left[(1-c)\ln(1-c) + c\ln c\right] + \delta f_0(c),
\end{aligned} \tag{2.4}
$$

where $\hat{\beta}(c) = \delta\beta(c)$ and $\hat{\gamma} = \gamma/\delta$.

Since δ/σ^A and δ/σ^B are kept fixed, $\alpha(c)$, $\hat{\beta}(c)$ and $\hat{\gamma}$ are independent of δ (see definitions (1.44-1.46)). We also define

$$
\hat{\mu}(c,\phi) = \frac{\mu(c,\phi)}{\delta} = \hat{\gamma}c(1-c)D(\phi). \tag{2.5}
$$

and

$$
\begin{cases}
\hat{f}^{\mathrm{liq}}(c) = \hat{f}(c,1) = \delta f^{\mathrm{liq}}(c), & \text{(2.6a)} \\[2mm]
\hat{f}^{\mathrm{sol}}(c) = \hat{f}(c,0) = \delta f^{\mathrm{sol}}(c). & \text{(2.6b)}
\end{cases}
$$

Equation system (1.40) can then be written:

$$
\begin{cases}
\dfrac{\delta^2}{M}\dfrac{\partial \phi}{\partial t} = \delta^2 \triangle\phi - \hat{f}_\phi(c,\phi), & \text{(2.7a)} \\[4mm]
\dfrac{\partial c}{\partial t} = \operatorname{div}\left[\hat{\mu}(c,\phi)\left(\hat{f}_{cc}(c,\phi)\nabla c + \hat{f}_{c\phi}(c,\phi)\nabla\phi\right)\right]. & \text{(2.7b)}
\end{cases}
$$

2.1.1   Outer solution

We now consider the previous equations when δ tends to zero at the macroscopic scale: the first equation becomes

$$
\hat{f}_\phi(c,\phi) = 0. \tag{2.8}
$$

If we assume the constraints (1.14) on function p, pure liquid $\phi \equiv 1$ and solid $\phi \equiv 0$ are possible solutions independently of the behaviour of c. These solutions can be proved to be stable with respect to small perturbations for

positive temperatures. Putting them into the second equation, we get (using definition (1.26)) respectively

$$\begin{cases} \dfrac{\partial c}{\partial t} = D_l \triangle c, & \text{on regions where } \phi \equiv 1, & \text{(2.9a)} \\[2ex] \dfrac{\partial c}{\partial t} = D_s \triangle c, & \text{on regions where } \phi \equiv 0. & \text{(2.9b)} \end{cases}$$

Let us now consider the case when both a liquid region Ω_l and a solid region Ω_s are present, delimited by an interface Γ. Such a configuration might locally look like figure 2.1.
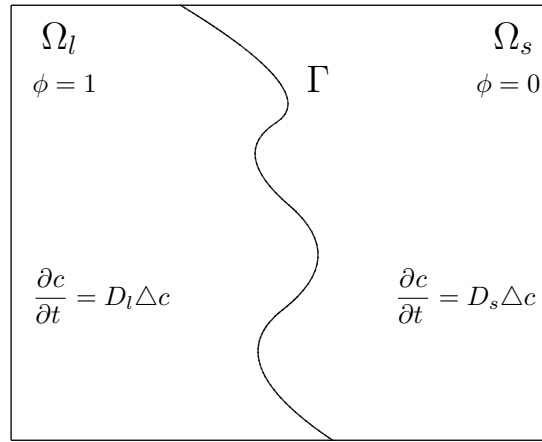

Figure 2.1: macroscopic domains

We expect to be able to study the transition between the pure phase regions at a space scale of order δ on the direction normal to the interface. To be able to do this, we assume that the interface (formally defined as the level set $\phi = 0.5$) can be described by a C^2 parametrization $\Gamma(s,t)$, and that a normal velocity $v_n(s,t)$ and a mean curvature $\kappa(s,t)$ can be defined at the macroscopic scale. Under these assumptions, we may define a time-dependent local invertible change of space coordinates $(x,y) \leftrightarrow (r,s)$, where r denotes the normal distance to the interface and s is a curvilinear coordinate of the interface. Using Frenet formulae we can then establish the properties:

$$\begin{cases} \dfrac{\partial r}{\partial t} = -v_n, & \text{(2.10a)} \\[2ex] |\nabla r|^2 = 1, & \text{(2.10b)} \\[2ex] \nabla r . \nabla s = 0, & \text{(2.10c)} \\[2ex] \triangle r = \dfrac{\kappa}{1 + \kappa r}. & \text{(2.10d)} \end{cases}$$

Let us assume that the system is liquid at the left ($r < 0$) and solid at the right ($r > 0$) of the interface. We call $c_l(s,t)$ and $c_s(s,t)$ the left and right limits of the "outer" function c when r tends to zero, and $\left(\dfrac{\partial c}{\partial r}\right)_{liq}(s,t)$ and $\left(\dfrac{\partial c}{\partial r}\right)_{sol}(s,t)$ the corresponding limits of $\dfrac{\partial c}{\partial r} = \dfrac{\partial}{\partial r}\left[c(x(r,s,t),t)\right]$. These values provide limit conditions for the diffusion equations (2.9).

2.1.2   Inner solution

To link the "outer" quantities across the interface, we will formally examine problem (2.7) near the interface by re-scaling the r coordinate as

$$r = \delta\rho. \tag{2.11}$$

Let us now consider the "inner" functions $\bar{\phi}$ and $\bar{c}$ inside the interface region as functions of the new set of space-time coordinates (ρ, s, t), and formally develop them with respect to the small parameter δ as:

$$
\begin{cases}
\bar{\phi}(\rho, s, t) = \phi_0(\rho, s, t) + \delta\phi_1(\rho, s, t) + \dots & \text{(2.12a)} \\[2ex]
\bar{c}(\rho, s, t) = c_0(\rho, s, t) + \delta c_1(\rho, s, t) + \dots & \text{(2.12b)}
\end{cases}
$$

As $\rho \longrightarrow \pm\infty$, we take limit conditions for the inner functions that are C^1-compatible with the outer functions:

$$
\begin{cases}
\lim_{\rho\longrightarrow-\infty}\phi_0(\rho,s,t) = 1, \ \lim_{\rho\longrightarrow+\infty}\phi_0(\rho,s,t) = 0, & \text{(2.13a)} \\[2ex]
\lim_{\rho\longrightarrow\pm\infty}\dfrac{\partial\phi_0}{\partial\rho}(\rho,s,t) = 0, & \text{(2.13b)} \\[2ex]
\lim_{\rho\longrightarrow\pm\infty}\phi_1(\rho,s,t) = \lim_{\rho\longrightarrow\pm\infty}\dfrac{\partial\phi_1}{\partial\rho}(\rho,s,t) = 0, & \text{(2.13c)} \\[2ex]
\lim_{\rho\longrightarrow-\infty}c_0(\rho,s,t) = c_l(s,t), \quad \lim_{\rho\longrightarrow+\infty}c_0(\rho,s,t) = c_s(s,t), & \text{(2.13d)} \\[2ex]
\lim_{\rho\longrightarrow-\infty}\dfrac{\partial c_1}{\partial\rho}(\rho,s,t) = \left(\dfrac{\partial c}{\partial r}\right)_{liq}(s,t), & \text{(2.13e)} \\[2ex]
\lim_{\rho\longrightarrow+\infty}\dfrac{\partial c_1}{\partial\rho}(\rho,s,t) = \left(\dfrac{\partial c}{\partial r}\right)_{sol}(s,t), & \text{(2.13f)} \\[2ex]
\lim_{\rho\longrightarrow\pm\infty}c_1(\rho,s,t) = \lim_{\rho\longrightarrow\pm\infty}\dfrac{\partial c_0}{\partial\rho}(\rho,s,t) = 0. & \text{(2.13g)}
\end{cases}
$$

Inside the re-scaled domain, we can use the interface properties (2.10)

combined with the rescaling (2.11) and the asymptotic series (2.12) to establish the following series in δ

$$\begin{cases} \delta \dfrac{\partial \bar{\phi}}{\partial t} = -v_n \dfrac{\partial \phi_0}{\partial \rho} + \dots, & \text{(2.14a)} \\[4mm] \delta^2 \triangle \bar{\phi} = \dfrac{\partial^2 \phi_0}{\partial \rho^2} + \delta \left(\dfrac{\partial^2 \phi_1}{\partial \rho^2} + \kappa \dfrac{\partial \phi_0}{\partial \rho} \right) + \dots, & \text{(2.14b)} \end{cases}$$

as well as analogous formal series for $\dfrac{\partial \bar{c}}{\partial t}$ and $\triangle \bar{c}$, and also

$$\nabla \bar{c} \cdot \nabla \bar{\phi} = \frac{\partial c_0}{\partial \rho} \frac{\partial \phi_0}{\partial \rho} + \delta^2 (\dots) + \dots . \tag{2.15}$$

Order 0 in δ

The equations (2.7) therefore become at lowest order in δ:

$$\begin{cases} \dfrac{\partial^2 \phi_0}{\partial \rho^2} - \hat{f}_\phi(c_0, \phi_0) = 0, & \text{(2.16a)} \\[4mm] \dfrac{\partial}{\partial \rho} \left[\hat{\mu}(c_0, \phi_0) \left(\hat{f}_{cc}(c_0, \phi_0) \dfrac{\partial c_0}{\partial \rho} + \hat{f}_{c\phi}(c_0, \phi_0) \dfrac{\partial \phi_0}{\partial \rho} \right) \right] = 0 & \text{(2.16b)} \end{cases}$$

Let us first look at the second equation. Under assumptions (2.1),(2.2), the function $\hat{\mu}(c_0, \phi_0)$ defined in (2.5) remains strictly positive in the whole domain. We know however by (2.13) that $\dfrac{\partial c_0}{\partial \rho}$ and $\dfrac{\partial \phi_0}{\partial \rho}$ both become zero on the limits when ρ tends to plus or minus infinity. We may therefore conclude that

$$\hat{f}_{cc}(c_0, \phi_0) \frac{\partial c_0}{\partial \rho} + \hat{f}_{c\phi}(c_0, \phi_0) \frac{\partial \phi_0}{\partial \rho} = 0 \tag{2.17}$$

inside all the rescaled interface.

This can be rewritten as

$$\frac{\partial}{\partial \rho} \hat{f}_c(c_0, \phi_0) = 0. \tag{2.18}$$

In particular, this gives us a first interface condition,

$$\boxed{\hat{f}_c^{\text{liq}}(c_l) = \hat{f}_c^{\text{sol}}(c_s),} \tag{2.19}$$

where $\hat{f}_c^{\text{liq}}$ and $\hat{f}_c^{\text{sol}}$ are defined by (2.6), and c_l and c_s are the limit conditions given in (2.13d)

Actually, equation (2.18) also tells us that

$$\hat{f}_c(c_0, \phi_0) \equiv \hat{C} \tag{2.20}$$

is a constant for all values of ρ (at fixed s and t), and this gives us an algebraic relationship between c_0 and ϕ_0. Writing this relationship explicitly, one may be convinced that it can be described with a uniquely determined function

$$c_0 = \lambda(\phi_0), \tag{2.21}$$

which we do not need to write explicitly for our purposes. Therefore,

$$\frac{\partial}{\partial\phi}\left[\hat{f}\left(\lambda(\phi), \phi\right) - \hat{C}\lambda(\phi)\right]\bigg|_{\phi=\phi_0} = \hat{f}_\phi\left(\lambda(\phi_0), \phi_0\right), \tag{2.22}$$

and the first equation of (2.16) can be rewritten as

$$\frac{\partial^2\phi_0}{\partial\rho^2} = \frac{\partial}{\partial\phi}\left[\hat{f}\left(\lambda(\phi), \phi\right) - \hat{C}\lambda(\phi)\right]\bigg|_{\phi=\phi_0}. \tag{2.23}$$

By multiplying this equation by $\dfrac{\partial\phi_0}{\partial\rho}$ and integrating with respect to ρ we then obtain

$$\frac{1}{2}\left|\frac{\partial\phi_0}{\partial\rho}\right|^2\Bigg|_{\rho=-\infty}^{\rho=+\infty} = \left[\hat{f}\left(\lambda(\phi), \phi\right) - \hat{C}\lambda(\phi)\right]\Bigg|_{\rho=-\infty}^{\rho=+\infty}, \tag{2.24}$$

which, by using limit conditions (2.13) and the definition of $\lambda(\phi_0)$, gives us a second interface condition:

$$\boxed{\hat{f}^{\text{liq}}(c_l) - \hat{f}_c^{\text{liq}}(c_l)c_l = \hat{f}^{\text{sol}}(c_s) - \hat{f}_c^{\text{sol}}(c_s)c_s.} \tag{2.25}$$

The two conditions (2.19) and (2.25) mean that there is a common tangent to the graphs of the functions $\hat{f}^{\text{liq}}(c)$ and $\hat{f}^{\text{sol}}(c)$, tangent to the graphs at respectively concentrations $c = c_l$ and $c = c_s$ (see figure 2.2). Actually, if the temperature T of the system is inside the interval delimited by the melting temperatures of the two pure elements A and B, then there is a single set of concentrations (c_s, c_l) allowing for such a geometric construction, and these concentrations, as functions of T, provide the (T,c) equilibrium "lens-type" phase diagram for the alloy (see figure 2.3, which has been computed using the same model parameter values as in chapter 4).
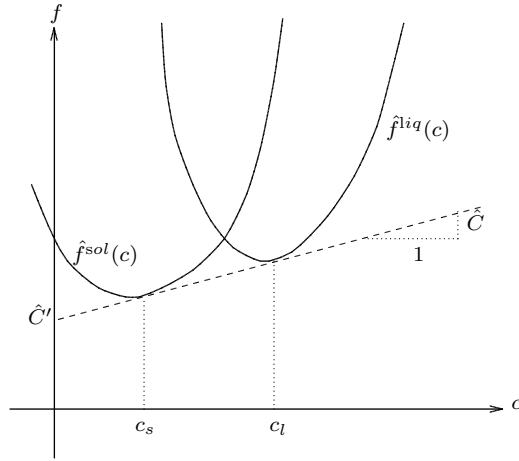
Figure 2.2: Common tangent construction, where $\hat{C} = \hat{f}_c^{\mathrm{sol}}(c_s) = \hat{f}_c^{\mathrm{liq}}(c_l)$ and $\hat{C}' = \hat{f}^{\mathrm{liq}}(c_l) - \hat{f}_c^{\mathrm{liq}}(c_l)c_l = \hat{f}^{\mathrm{sol}}(c_s) - \hat{f}_c^{\mathrm{sol}}(c_s)c_s$.
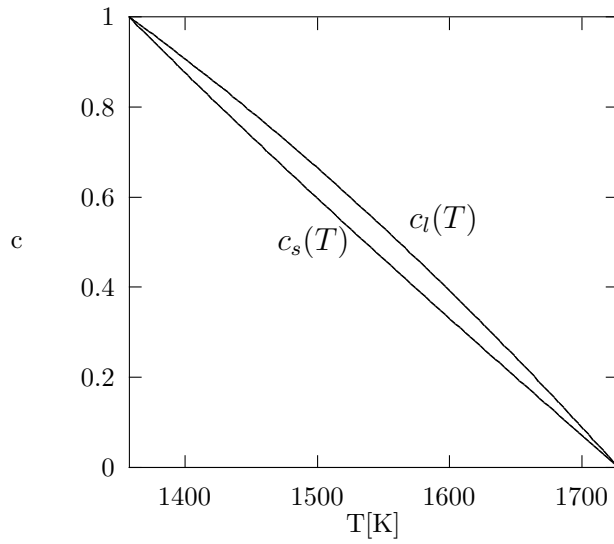

Figure 2.3: Equilibrium phase diagram derived from the phase-field model, using parameters for a Ni-Cu alloy.

Order 1 **in** δ

Using properties (2.14) and (2.15), we can write the equation for c in (2.7) at order 1 in δ, greatly simplified by relationship (2.18):

$$-v_n \frac{\partial c_0}{\partial \rho} = \frac{\partial}{\partial \rho} \left\{ \hat{\mu}(c_0, \phi_0) \frac{\partial}{\partial \rho} \left[\hat{f}_{cc}(c_0, \phi_0)c_1 + \hat{f}_{c\phi}(c_0, \phi_0)\phi_1 \right] \right\}. \qquad (2.26)$$

We may simply integrate with respect to ρ from $-\infty$ to $+\infty$ to obtain a third interface condition. Assuming that the normal velocity v_n, a macroscopic quantity, is uniform in ρ, we obtain, using (1.25), (1.26) and limit conditions (2.13):

$$\boxed{-v_n(c_s - c_l) = D_s \frac{\partial c_s}{\partial n} - D_l \frac{\partial c_l}{\partial n}.} \qquad (2.27)$$

This corresponds to the conservation of matter through the interface.

Note that throughout the steps used to derive interface conditions (2.19), (2.25) and (2.27), we implicitly used constraints (1.13) on function p, but never needed the extra constraints (1.14).

2.1.3   Stefan-like problem

Regrouping results (2.9), (2.19), (2.25), (2.27), and recalling the definitions of $\hat{f}$ and f, we can write the sharp-interface small surface tension asymptotic limit when δ, σ^A and σ^B tend to zero with δ/σ^A, δ/σ^B, and M kept fixed as the following Stefan problem:

$$\begin{cases} \dfrac{\partial c}{\partial t} = D_l \triangle c, & \text{in} \quad \Omega_l, & (2.28a) \\[2mm] \dfrac{\partial c}{\partial t} = D_s \triangle c, & \text{in} \quad \Omega_s, & (2.28b) \\[2mm] -v_n \left[c\right]_l^s = \left[D \dfrac{\partial c}{\partial n} \right]_l^s, & \text{on} \quad \Gamma & (2.28c) \\[2mm] \left[f_c\right]_l^s = 0, & \text{on} \quad \Gamma & (2.28d) \\[1mm] \left[f - f_c c\right]_l^s = 0, & \text{on} \quad \Gamma, & (2.28e) \end{cases}$$

where $[.]_l^s$ denotes the jump of a quantity across the liquid-solid interface. This limit can be easily interpreted: on liquid and solid regions there is a classical diffusion of matter, while through the interface on one hand there is conservation of matter as the interface moves, and on the other hand concentration takes liquid and solid equilibrium values on respective sides of the interface.

This is the simplest limit we will consider in this chapter, and it is the concentration problem's analogue of the classical Stefan problem obtained as the simplest sharp-interface limit of a thermal phase-field model in [Cag89]. The interface conditions are different in the thermal and solutal problems, which can be explained by the fact that concentration is a globally conserved quantity that is discontinuous at the interface, whereas temperature is a non-conserved quantity that is continuous at the interface, but whose normal derivative is not.

2.2 Small surface tension, low phase-field diffusivity limit: kinetic effects

We now consider the limit when $\delta, \sigma^A, \sigma^B$ and M tend to zero with δ/σ^A, δ/σ^B, and δ/M kept fixed. We use the same modified free energy density $\hat{f}$ defined by (2.4) on the last section. We define a new quantity independent of δ:

$$\hat{M} = \frac{M}{\delta}, \tag{2.29}$$

and the evolution equations (2.7) can then be written

$$
\begin{cases}
\dfrac{\delta}{\hat{M}} \dfrac{\partial \phi}{\partial t} = \delta^2 \triangle \phi - \hat{f}_\phi(c, \phi), & \text{(2.30a)} \\[2mm]
\dfrac{\partial c}{\partial t} = \text{div} \left[\hat{\mu}(c, \phi) \left(\hat{f}_{cc}(c, \phi)\nabla c + \hat{f}_{c\phi}(c, \phi)\nabla \phi \right) \right], & \text{(2.30b)}
\end{cases}
$$

The outer solutions will be the same as (2.9), and the macroscopic behaviour still corresponds to figure 2.1. All the steps to obtain interface conditions (2.19) and (2.27) depend only on the second equation in (2.30), and are therefore unmodified; equation (2.18) also still holds. However, the first equation in (2.16) now becomes

$$-\frac{v_n}{\hat{M}} \frac{\partial \phi_0}{\partial \rho} = \frac{\partial^2 \phi_0}{\partial \rho^2} - \hat{f}_\phi(c_0, \phi_0), \tag{2.31}$$

from which we can derive an analogous of (2.23):

$$\frac{\partial^2 \phi_0}{\partial \rho^2} + \frac{v_n}{\hat{M}} \frac{\partial \phi_0}{\partial \rho} = \frac{\partial}{\partial \phi} \left[\hat{f}\left(\lambda(\phi), \phi\right) - \hat{C}\lambda(\phi) \right]\Big|_{\phi=\phi_0}. \tag{2.32}$$

Finally, multiplying (2.32) by $\dfrac{\partial \phi_0}{\partial \rho}$, integrating on ρ and recalling definitions (2.20) and (2.21), we get the following interface condition:

$$\left[\hat{f} - \hat{f}_c c \right]_l^s = \frac{\chi}{\hat{M}} v_n, \tag{2.33}$$

where

$$\chi = \int_{-\infty}^{+\infty} \left| \frac{\partial \phi_0}{\partial \rho} \right|^2 d\rho. \tag{2.34}$$

The limit as $\delta, \sigma^A, \sigma^B$ and M tend to zero therefore corresponds to a modified Stefan problem, equivalent to (2.28) where the last interface condition is to be replaced by (2.33). There is still classical diffusion on pure phase regions, separed by δ-width interfaces, through which the concentration and its normal derivative jump in such a way that matter is conserved. However, the values of concentration on both sides of the interface are no longer equilibrium values, but are obtained through a "parallel tangent construction" dependent upon the local interface velocity. On regions where the interface is static, we find again the equilibrium values of c_l and c_s corresponding to the phase diagram. Note that this limit does not correspond to any of Caginalp's limits in [Cag89].
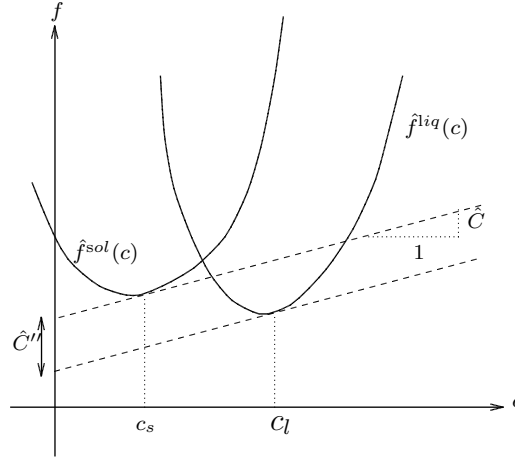

Figure 2.4: Common tangent construction, where $\hat{C} = \hat{f}_c^{\mathrm{sol}}(c_s) = \hat{f}_c^{\mathrm{liq}}(c_l)$ and $\hat{C}'' = (\hat{f}^{\mathrm{sol}}(c_s) - \hat{f}_c^{\mathrm{sol}}(c_s)c_s) - (\hat{f}^{\mathrm{liq}}(c_l) - \hat{f}_c^{\mathrm{liq}}(c_l)c_l) = \frac{\chi}{\hat{M}} v_n.$

2.3 Similar elements limit: kinetic and curvature effects

We now want to consider a sharp-interface limit with finite surface tension. However, taking the limit as δ tends to zero with all other quantities fixed does not yield valid interface conditions using Caginalp [Cag86, Cag89] methods as we did in preceding subsections. We therefore choose to have an extra constraint: we want the coefficient $\alpha(c)$ defined in (1.45) to be a constant at lowest order in δ:

$$\alpha(c) = \bar{\alpha} + \delta \Delta \alpha c. \tag{2.35}$$

This is equivalent to assuming that the quantity

$$\alpha^B - \alpha^A = \frac{T}{\sigma^A + \sigma^B} \left(\frac{\sigma^B}{T_m^B} - \frac{\sigma^A}{T_m^A} \right) = \delta \Delta \alpha \tag{2.36}$$

is of order δ, i.e. that the two components of the alloy are similar enough in the sense of (2.36). Another interpretation of this assumption can be given using the potential barrier heights W^A and W^B defined in (1.21): as δ tends to zero, both potential barriers become infinite, but their difference (weighted by respective melting temperatures) is kept fixed.

We introduce yet another modified free energy density:

$$
\begin{aligned}
\check{f}(c, \phi) &= f(c, \phi) - \frac{\bar{\alpha}}{\delta} g(\phi) \\
&= \Delta \alpha c g(\phi) + \beta(c) p(\phi) + \frac{1}{\gamma} \left[(1 - c) \ln(1 - c) + c \ln c \right] + f_0(c).
\end{aligned}
\tag{2.37}
$$

The equations (1.40) can then be written as

$$
\begin{cases}
\dfrac{\delta^2}{M} \dfrac{\partial \phi}{\partial t} = \delta^2 \triangle \phi - \bar{\alpha} g'(\phi) - \delta \check{f}_\phi(c, \phi), & \text{(2.38a)} \\[2mm]
\dfrac{\partial c}{\partial t} = \operatorname{div} \left[\mu(c, \phi) \left(\check{f}_{cc}(c, \phi) \nabla c + \check{f}_{c\phi}(c, \phi) \nabla \phi \right) \right]. & \text{(2.38b)}
\end{cases}
$$

In the asymptotic limit as δ tends to zero, for the outer solution, equation (2.8) is now replaced by

$$g'(\phi) = 0. \tag{2.39}$$

This still gives the same behaviour as (2.9) outside the interface, but we no longer need to assume that the constraints (1.14) on function p are satisfied.

As for the inner solution, the second equation in (2.38) is analogous to the second equation in (2.7), and will therefore yield interface conditions analogous to (2.19) and (2.27). Noting that

$$\check{f}_c = f_c = \frac{\hat{f}_c}{\delta}, \tag{2.40}$$

we conclude that the two interface conditions on c obtained in this case are actually strictly equivalent to (2.19) and (2.27).

We must now look at the evolution equation for ϕ in (2.38). At lowest order in δ it becomes simply

$$\frac{\partial^2 \phi_0}{\partial \rho^2} = \bar{\alpha} g'(\phi_0). \tag{2.41}$$

With the limit conditions (2.13), and fixing $\phi_0(0) = \frac{1}{2}$, this equation (which is essentially the same as (1.16)) has a unique solution:

$$\phi_0(\rho) = \frac{1}{1 + e^{\sqrt{2\bar{\alpha}}\rho}}. \tag{2.42}$$

This doesn't give us an interface condition yet, so we must look at the next order in δ of the first equation in (2.38). Using formal series (2.12), and definition (2.21), we get:

$$-\frac{v_n}{M} \frac{\partial \phi_0}{\partial \rho} = \frac{\partial^2 \phi_1}{\partial \rho^2} + \kappa \frac{\partial \phi_0}{\partial \rho} - \bar{\alpha} g''(\phi_0)\phi_1 - \check{f}_\phi \left(\lambda(\phi_0), \phi_0 \right). \tag{2.43}$$

Let's call Λ the operator

$$\Lambda = \bar{\alpha} g''(\phi_0) - \frac{\partial^2}{\partial \rho^2}. \tag{2.44}$$

We can then rewrite (2.43) as

$$\Lambda \phi_1 = \left(\kappa + \frac{v_n}{M} \right) \frac{\partial \phi_0}{\partial \rho} - \check{f}_\phi \left(\lambda(\phi_0), \phi_0 \right), \tag{2.45}$$

and by differentiating (2.41) with respect to ρ we find that

$$\Lambda \frac{\partial \phi_0}{\partial \rho} = 0. \tag{2.46}$$

In fact, Λ is a self-adjoint operator on functions satisfying limit conditions (2.13), for the L^2 scalar product on variable ρ. Therefore, we have an orthogonality condition for (2.45) to be solvable when (2.46) is true:

$$\left(\kappa + \frac{v_n}{M}\right) \int_{-\infty}^{+\infty} \left|\frac{\partial \phi_0}{\partial \rho}\right|^2 d\rho - \int_{-\infty}^{+\infty} \check{f}_\phi \left(\lambda(\phi_0), \phi_0\right) \frac{\partial \phi_0}{\partial \rho} d\rho = 0. \qquad (2.47)$$

Using limit conditions (2.13) and equation (2.22) with definitions (2.20) and (2.21), we then find the following interface condition:

$$\boxed{\left[\check{f} - \check{f}_c c\right]_l^s = \check{\chi} \left(\kappa + \frac{v_n}{M}\right),} \qquad (2.48)$$

where the explicit form of constant $\check{\chi}$ can be obtained using (2.42):

$$\check{\chi} = \int_{-\infty}^{+\infty} \left|\frac{\partial \phi_0}{\partial \rho}\right|^2 d\rho = \frac{1}{3}\sqrt{\frac{\bar{\alpha}}{2}}. \qquad (2.49)$$

The limit where δ tends to zero with $\Delta\alpha$ fixed therefore also corresponds to a modified Stefan problem, similar to (2.28) where the last interface condition is to be replaced by (2.48). There is also still classical diffusion on pure phase regions, separed by δ-width interfaces, through which the normal derivative of concentration jumps in such a way that matter is conserved. However, the values of concentration on both sides of the interface are now obtained through a "parallel tangent construction" dependent upon both local interface velocity and local curvature. On regions where the interface is both planar and static, we find again the equilibrium values of c_l and c_s corresponding to the phase diagram.

This limit corresponds to Caginalp's "modified Stefan model" in [Cag89] and is equivalent to Warren's fixed surface tension limit in [War95]. An expansion of f and f_c in interface conditions (2.19) and (2.48) results in conditions very similar to (C) and (D) in [War95, p. 42]. They differ in certain factors T/T_m^A and T/T_m^B, due to the fact that Warren and Boettinger's original model was derived from an entropy formulation, while we used a free energy formulation. Note also that Warren[War95] remarked that $\frac{\sigma_A}{T_m^A} - \frac{\sigma_B}{T_m^B}$ as a consequence of asymptotics obtained before adjusting model parameters, whereas we found that such a requirement was technically needed to be able to derive this particular asymptotic limit after adjusting model parameters.

Note that the solvability condition technique implemented through the operator Λ can also be used to obtain an interesting limit in the case of a pure element ($c \equiv 0$ or $c \equiv 1$). We then have only the equation for the evolution of ϕ in (2.38). The outer solutions will still be chosen as liquid

($\phi \equiv 1$) on the left and solid ($\phi \equiv 0$) on the right of the interface. The inner development will however now yield only one interface condition, which in the case of pure element A would be:

$$\kappa + \frac{v_n}{M} = \frac{[\check{f}]_l^s}{\check{\chi}} = \frac{L^A}{l\sigma^A}\frac{T - T_m^A}{T_m^A}. \tag{2.50}$$

This describes an interface moving by mean curvature. The preceeding equation can also be compared, when $\kappa = 0$, to phenomenological laws, in order to adjust M with a known kinetic coefficient, and have a numerical value to use on the original phase-field model. For instance, Warren and Boettinger [WB95] choose M to fit Coriell-Turnbull's model kinetic coefficient.

2.4   Similar elements limit with large phase-field diffusivity: curvature effects only

We consider the same conditions as in the last subsection, except that now the quantity

$$\check{M} = M\delta \tag{2.51}$$

is supposed to be fixed.

With analogous steps, we find a similar limit problem as in the last paragraph. It is also a modified version of problem (2.28), where the last equation is replaced by

$$\boxed{\left[\check{f} - \check{f}_c c\right]_l^s = \check{\Gamma}\kappa.} \tag{2.52}$$

The "parallel tangent construction" is now dependent upon local curvature only, and the equilibrium values of c_l and c_s corresponding to the phase diagram can now be found on all regions where the interface is planar, even if it moves. This last limit corresponds to what Caginalp [Cag89] called an "alternative modified Stefan model" in the thermal case.

2.5   Summary of the results and physical interpretation of the limits

The limit problems for the evolution equations (1.40) when the interface thickness δ vanishes, as seen in sections 2.1-2.4, all have the generic form of

generalized Stefan problems:

$$
\begin{cases}
\dfrac{\partial c}{\partial t} = D_l \triangle c, & \text{in} \quad \Omega_l, & (2.53a) \\[2mm]
\dfrac{\partial c}{\partial t} = D_s \triangle c, & \text{in} \quad \Omega_s, & (2.53b) \\[2mm]
-v_n \left[c\right]_l^s = \left[D \dfrac{\partial c}{\partial n}\right]_l^s, & \text{on} \quad \Gamma, & (2.53c) \\[2mm]
\left[f_c\right]_l^s = 0, & \text{on} \quad \Gamma, & (2.53d) \\[1mm]
\left[f - f_c c\right]_l^s = \mathcal{A}(v_n, \kappa), & \text{on} \quad \Gamma. & (2.53e)
\end{cases}
$$

In all of these limits, pure liquid (2.53a) and pure solid (2.53b) regions with classical diffusion coexist, separed by sharp interfaces that evolve ensuring the conservation of matter (2.53c). Moreover, the values of concentration at the interface can be obtained through a "parallel tangent construction" ((2.53d) and (2.53e)), using solid and liquid free energy densities, and dependent either on the local interface velocity, the local interface curvature, both or none, through the generic affine function $\mathcal{A}(v_n, \kappa)$. This function is dependent on the type of limit:

section	σ_A, σ_B	$\dfrac{\sigma_A}{T_m^A} - \dfrac{\sigma_B}{T_m^B}$	M	$\mathcal{A}$
2.1	$O(\delta)$	$O(\delta)$	$O(1)$	0
2.2	$O(\delta)$	$O(\delta)$	$O(\delta)$	$\propto \quad v_n$
2.3	$O(1)$	$O(\delta)$	$O(1)$	$\propto \quad \kappa + \frac{v_n}{M}$
2.4	$O(1)$	$O(\delta)$	$O(\frac{1}{\delta})$	$\propto \quad \kappa$

$$(2.54)$$

For the asymptotic limits presented on sections 2.3 and 2.4, all the steps of the asymptotic analysis and all the results depend on the choice of a function p only through its regularity (it should be at least C^1) and through its values at $\phi = 0$ and $\phi = 1$. The constraints (1.13) are therefore sufficient to get the proper limits. The extra constraints (1.14), while necessary to have a thermodynamically consistent mesoscopic model, are not necessary to get these limits. Therefore, instead of the function (1.15), we could simply define p as

$$p(\phi) = \phi \qquad (2.55)$$

and still get the same limits.

However, to get the low interface thickness at low surface tensions asymptotic limits presented on sections 2.1 and 2.2, the extra constraints (1.14) on function p are also required.

We now give a concise interpretation of each limit. Limit 2.1 clearly corresponds to an equilibrium state, and is of little interest for the solidification at finite speed of alloys. Limit 2.4 can describe solidification of microstructures at low speed in which the curvature contribution is dominant and the attachment kinetics is negligible. This typically occurs for metallic alloys solidified under conventional conditions and for systems which are undergoing coarsening. This situation can be approximated by choosing a high value for parameter M in the phase-field model. Limit 2.3 describes the case of fast solidification of metallic alloys or more generally the solidification of complex alloy systems (e.g., molecules such as oxides) in which both curvature effects and attachment kinetics are playing a role. Finally, limit 2.2 can describe the solidification of complex alloys in which the curvature contribution can be neglected (e.g., Bridgeman solidification under planar front conditions of a complex alloy system).

Chapter 3

Numerical scheme and convergence

The main goal of this chapter is to prove the convergence of a finite element in space, semi-implicit Euler in time numerical scheme for the isotropic problem (1.51). This is the result of a joint work with J. F. Scheid, presently submitted for publication.The key ingredient of the proof is the introduction of a generalized vectorial elliptic projector.

3.1 Numerical scheme

We want to approximate the isotropic problem (1.51) by a $\mathbb{P}_1$ finite element in space, semi-implicit Euler in time discretization. This scheme was first used for this problem by O. Krüger in his Ph.D. thesis [Krü99].

To begin with, let us introduce some notations. We denote by $\mathcal{T}_h$ a regular triangulation of the domain Ω (see [Cia78, p. 132]), where h is the diameter of the biggest triangle in $\mathcal{T}_h$. From now, we shall assume that the domain Ω is a convex polygonal subset of $\mathbb{R}^2$.

We will need the following extra assumption for some properties of the elliptic projector and for the convergence theorem:

(H3.1) The triangulation $\mathcal{T}_h$ verifies an inverse assumption i.e. there exists a constant C such that $h/h_K \leqslant C, \quad \forall K \in \mathcal{T}_h$, where h_K stands for the diameter of the triangle K.

We now define the finite element spaces

$$V_h = \left\{ v_h \in C^0(\overline{\Omega}); \quad v_h|_K \in \mathbb{P}_1(K), \quad \forall K \in \mathcal{T}_h \right\}, \tag{3.1}$$

and

$$V_h^2 = V_h \times V_h, \tag{3.2}$$

where $\mathbb{P}_1(K)$ denotes the set polynomials of degree 1 in the triangle K.

As in the previous chapters, we denote by t_f a final time. For a given integer $N \geqslant 1$, we denote by $\tau = t_f/N$ the time step and by $t^n = n\tau$, the current time for $n = 0, ..., N$. From now on, we assume that the initial data $\vec{u}_0$ belongs to $H^2(\Omega; \mathbb{R}^2)$ so that it is a continuous function. We denote by r_h the Lagrange interpolation operator both in V_h and in V_h^2, and remark that $r_h \vec{u}_0$ is well defined. Based on the variational formulation (1.64), we now introduce an approximate problem for $\vec{u}_h^n$, approximation of the exact solution $\vec{u}(t^n)$:

$$\begin{cases} \text{For } n = 1, \dots, N, \text{ find } \vec{u}_h^n \in V_h^2 \text{ such that for all } \vec{v}_h \in V_h^2, \\[2mm] \displaystyle\int_\Omega \frac{\vec{u}_h^n - \vec{u}_h^{n-1}}{\tau}.\vec{v}_h + \int_\Omega D(\vec{w}_h^{\theta n})\nabla \vec{u}_h^n : \nabla \vec{v}_h = \int_\Omega \vec{F}(\vec{u}_h^{n-1}).\vec{v}_h, \quad (3.3\text{a}) \\[2mm] \vec{u}_h^0 = r_h \vec{u}_0, \hspace{7.5cm} (3.3\text{b}) \end{cases}$$

where $\theta \in [0,1]$ and the vector $\vec{w}_h^{\theta n}$ is defined from $\vec{u}_h^n = (u_{1h}^n, u_{2h}^n)^T$ and $\vec{u}_h^{n-1}$ by

$$\vec{w}_h^{\theta n} = \begin{pmatrix} (1-\theta)u_{1h}^{n-1} + \theta u_{1h}^n \\ u_{2h}^{n-1} \end{pmatrix}. \tag{3.4}$$

It is easy to see that for all $\theta \in [0,1]$, the discrete problem (3.3) has a unique solution. This is clear from the fact that the matrix $D(\vec{u})$ is lower triangular and that its diagonal is positive. So, at first, from $\vec{u}_h^{n-1} = (u_{1h}^{n-1}, u_{2h}^{n-1})^T$ we determine u_{1h}^n by restricting (3.3a) to the case of $\vec{v}_h = (v_h, 0)^T$, for all $v_h \in V_h$; then since the second element of $\vec{w}_h^{\theta n}$ does not depend on $\vec{u}_h^n$ at all, we determine u_{2h}^n by restricting (3.3a) to $\vec{v}_h = (0, v_h)^T$, for all $v_h \in V_h$. Also, for any $\theta \in [0,1]$, we do not have to solve nonlinear algebraic equations at each time step, while still granting convergence without a condition linking h and τ, as we will see in the next section. Finally, note that in the approximate problem (3.3) we consider, no numerical integration is assumed.

In section 3.2 we will introduce a generalized elliptic projector, which will be the main tool used in section 3.3 to derive a priori error estimates for the scheme (3.3).

3.2   Generalized elliptic projector

We introduce a vectorial elliptic projector which is a generalization of the scalar elliptic projector used for instance by V. Thomée [Tho91]. Throughout this section, we deal with a 2×2 matrix which is neither assumed to be triangular nor symmetric. In particular, Theorems 3.1-3.3 are valid for a general 2×2 matrix.

   We consider a time dependent matrix D that will depend on both space $x \in \Omega$ and time $t \in [0, t_f]$ coordinates, and we define a time dependent generalized vectorial projector. We will assume that:

(H3.2) $D \in C^0\left([0, t_f]; L^\infty\left(\Omega, \mathcal{M}_2\right)\right)$.

(H3.3) D is uniformly positive definite, i.e. there exists a constant $\hat{\beta}$ independent of x and t such that $\vec{w}^T D(x,t)\vec{w} \geqslant \hat{\beta}\,\vec{w}^T\vec{w}$ for all $\vec{w} \in \mathbb{R}^2$ and a.e. $x \in \Omega$, $\forall t \in [0, t_f]$.

We introduce a time dependent bilinear form in $H^1(\Omega, \mathbb{R}^2)$ defined for all $t \in [0, t_f]$ by

$$\vec{\xi_1}, \vec{\xi_2} \in H^1(\Omega, \mathbb{R}^2) \longmapsto a_t(\vec{\xi_1}, \vec{\xi_2}) = \int_\Omega D(t)\nabla\vec{\xi_1} : \nabla\vec{\xi_2} + \int_\Omega \vec{\xi_1} \cdot \vec{\xi_2}, \qquad (3.5)$$

Assumption (H3.2) implies that a_t is continuous in $H^1(\Omega, \mathbb{R}^2)$ uniformly in t, i.e.

$$a_t(\vec{\xi_1}, \vec{\xi_2}) \leqslant \alpha\|\vec{\xi_1}\|_{H^1(\Omega,\mathbb{R}^2)}\|\vec{\xi_2}\|_{H^1(\Omega,\mathbb{R}^2)}, \quad \forall \vec{\xi_1}, \vec{\xi_2} \in H^1(\Omega, \mathbb{R}^2), \quad \forall t > 0,$$
$$(3.6)$$

where $\alpha = \max(\|D\|_{L^\infty(0,t_f;L^\infty(\Omega,\mathcal{M}_2))}, 1)$ is independent of t.

   Furthermore, under assumption (H3.3), using equation (1.59), one can also see that a_t is coercive uniformly in t, i.e.

$$a_t(\vec{\xi}, \vec{\xi}) \geqslant \beta\|\vec{\xi}\|_{H^1(\Omega,\mathbb{R}^2)}, \quad \forall \vec{\xi} \in H^1(\Omega, \mathbb{R}^2), \quad \forall t > 0, \qquad (3.7)$$

where $\beta = \min(\hat{\beta}, 1)$ is independent of t.
We can now define the time-dependent generalized vectorial elliptic projector.

Definition 3.1 *Under assumptions* (H3.2) *and* (H3.3)*, we define the time-dependent generalized vectorial elliptic projector (GVP)*

$$\pi_h \quad : \quad C^0\left([0, t_f]; H^1(\Omega, \mathbb{R}^2)\right) \longrightarrow L^\infty\left(0, t_f; V_h^2\right)$$
$$\vec{\xi} \longmapsto \pi_h\vec{\xi}$$

by the relation

$$a_t(\vec{\xi}(t) - \pi_h\vec{\xi}(t), \vec{v}_h) = 0, \quad \forall \vec{v}_h \in V_h^2, \quad \forall t \in [0, t_f], \tag{3.8}$$

where we introduced the short notation $\pi_h\vec{\xi}(t)$ for $(\pi_h\vec{\xi})(t)$.

Lax-Milgram's lemma together with (3.6) and (3.7) ensures that π_h is well-defined.

We now state some important properties of the time-dependent GVP, which will be proved after introducing a lemma. In particular, we derive error bounds that will be key ingredients for the proof of Theorem 3.4 in section 3.3 .

Theorem 3.1 *We assume* (H3.2) *and* (H3.3)*. If in addition we assume that $D \in L^\infty\left(0, t_f; W^{1,\infty}\left(\Omega, \mathcal{M}_2\right)\right)$, and also that $\vec{\xi} \in C^0\left([0, t_f]; H^2(\Omega, \mathbb{R}^2)\right)$, then $\pi_h\vec{\xi}$ is an element of $C^0\left([0, t_f]; V_h^2\right)$, and there exists a positive constant C_1 independent of h, such that*

$$\|\vec{\xi} - \pi_h\vec{\xi}\|_{L^\infty\left(0, t_f; L^2(\Omega, \mathbb{R}^2)\right)} + h\|\vec{\xi} - \pi_h\vec{\xi}\|_{L^\infty\left(0, t_f; H^1(\Omega, \mathbb{R}^2)\right)} \leqslant C_1 h^2. \tag{3.9}$$

Theorem 3.2 *We assume* (H3.2) *and* (H3.3)*. If in addition we assume that $D \in L^\infty\left(0, t_f; W^{1,\infty}\left(\Omega, \mathcal{M}_2\right)\right) \cap H^1\left(0, t_f; L^\infty(\Omega, \mathcal{M}_2)\right)$ and also that $\vec{\xi} \in H^1\left(0, t_f; H^2(\Omega, \mathbb{R}^2)\right)$ then $\pi_h\vec{\xi} \in H^1\left(0, t_f; V_h^2\right)$ and there exists a positive constant C_2 independent of h, such that*

$$\left\|\frac{\partial}{\partial t}\left(\vec{\xi} - \pi_h\vec{\xi}\right)\right\|_{L^2\left(0, t_f; L^2(\Omega, \mathbb{R}^2)\right)} + h\left\|\frac{\partial}{\partial t}\left(\vec{\xi} - \pi_h\vec{\xi}\right)\right\|_{L^2\left(0, t_f; H^1(\Omega, \mathbb{R}^2)\right)} \leqslant C_2 h^2.$$
$$\tag{3.10}$$

Theorem 3.3 *Let assumptions* (H3.1)*,* (H3.2) *and* (H3.3) *be fulfilled. If $\vec{\xi} \in H^1\left(0, t_f; H^2(\Omega, \mathbb{R}^2)\right) \cap L^\infty\left(0, t_f; W^{1,\infty}(\Omega, \mathbb{R}^2)\right)$ then there exists a positive constant C_3 independent of h, such that*

$$\|\nabla \pi_h\vec{\xi}\|_{L^\infty\left(0, t_f; L^\infty(\Omega, \mathcal{M}_2)\right)} \leqslant C_3. \tag{3.11}$$

Remark: Theorems 3.1 and 3.2 are still valid in space dimension 3. However, Theorem 3.3 is not. Indeed, in that case the right-hand side C_3 in (3.11) would no longer be a constant but would depend on $h^{-1/2}$.

We will need a lemma for proving Theorems 3.1-3.3. This lemma extends a regularity result of [Gri85] from scalar elliptic problems to elliptic systems.

Lemma 3.1 *Let $A \in W^{1,\infty}(\Omega, \mathcal{M}_2)$ be a uniformly positive definite matrix and let $\vec{b} \in L^2(\Omega, \mathbb{R}^2)$. Then the solution $\vec{w} \in H^1(\Omega, \mathbb{R}^2)$ to the equation*

$$\int_\Omega A\nabla\vec{w} : \nabla\vec{v} + \int_\Omega \vec{w} \cdot \vec{v} = \int_\Omega \vec{b} \cdot \vec{v}, \quad \forall \vec{v} \in H^1(\Omega, \mathbb{R}^2), \tag{3.12}$$

is actually in $H^2(\Omega, \mathbb{R}^2)$ and satisfies $\partial\vec{w}/\partial n = 0$ a.e. on $\partial\Omega$. Furthermore, there exists a constant C_4 independent of $\vec{b}$ such that

$$\|\vec{w}\|_{H^2(\Omega,\mathbb{R}^2)} \leqslant C_4 \|\vec{b}\|_{L^2(\Omega,\mathbb{R}^2)}. \tag{3.13}$$

Proof of Lemma 3.1

•Let $\vec{b} = (b_1, b_2) \in L^2(\Omega) \times L^2(\Omega)$. According to Lax-Milgram's lemma, there exists a unique solution $\vec{w} = (w_1, w_2) \in H^1(\Omega) \times H^1(\Omega)$ to the equation (3.12). We call a_{ij}, $i, j = 1, 2$, the coefficients of A, and we notice that they are elements of $W^{1,\infty}(\Omega)$. Since A is uniformly positive definite, there are three positive constants β_i, $i = 1, 2, 3$, such that $0 < \beta_1 \leqslant a_{11} \leqslant \beta_2$ and $a_{11}a_{22} - a_{12}a_{21} \geqslant \beta_3 > 0$. Under the lemma's assumptions, Grisvard's result [Gri85, Thm. 3.2.1.3] tells us that there exists a unique $\tilde{w}_2 \in H^2(\Omega)$ verifying homogeneous Neumann boundary conditions such that in Ω

$$-\operatorname{div}\left(\left(a_{22} - \frac{a_{21}}{a_{11}}a_{12}\right)\nabla\tilde{w}_2\right) + \tilde{w}_2$$
$$= b_2 - \frac{a_{21}}{a_{11}}(b_1 - w_1) + \nabla\left(\frac{a_{21}}{a_{11}}\right) \cdot (a_{11}\nabla w_1 + a_{12}\nabla w_2). \tag{3.14}$$

For the same reasons, once $\tilde{w}_2 \in H^2(\Omega)$ is given, there exists a unique $\tilde{w}_1 \in H^2(\Omega)$ verifying homogeneous Neumann boundary conditions such that in Ω

$$-\operatorname{div}(a_{11}\nabla\tilde{w}_1) + \tilde{w}_1 = b_1 + \operatorname{div}(a_{12}\nabla\tilde{w}_2). \tag{3.15}$$

•Let us write a weak form of (3.14): For all v in $H^1(\Omega)$,

$$\int_\Omega \left(a_{22} - \frac{a_{21}}{a_{11}}a_{12}\right)\nabla\tilde{w}_2 \cdot \nabla v + \int_\Omega \left(\tilde{w}_2 - \frac{a_{21}a_{11}}{w_1}\right)v$$
$$= \int_\Omega (a_{11}\nabla w_1 + a_{12}\nabla w_2) \cdot \nabla\left(\frac{a_{21}}{a_{11}}\right)v + \int_\Omega \left(b_2 - \frac{a_{21}}{a_{11}}b_1\right)v. \tag{3.16}$$

Furthermore, if we choose $\vec{v} = (\frac{a_{21}}{a_{11}}v, -v)^T$ as a test function in (3.12), we obtain that for all v in $H^1(\Omega)$,

$$\int_\Omega \left(\frac{a_{21}}{a_{11}}a_{12} - a_{22}\right)\nabla w_2 \cdot \nabla v + \int_\Omega \left(\frac{a_{21}a_{11}}{w_1} - w_2\right)v$$
$$= -\int_\Omega (a_{11}\nabla w_1 + a_{12}\nabla w_2) \cdot \nabla\left(\frac{a_{21}}{a_{11}}\right)v + \int_\Omega \left(\frac{a_{21}}{a_{11}}b_1 - b_2\right)v. \tag{3.17}$$

Adding (3.16) and (3.17), we find that

$$\int_\Omega \left(a_{22} - \frac{a_{21}}{a_{11}} a_{12} \right) \nabla(w_2 - \tilde{w}_2) \cdot \nabla v + (w_2 - \tilde{w}_2)v = 0, \qquad (3.18)$$

for all v in $H^1(\Omega)$.

• Let us now write a weak form of (3.15): For all v in $H^1(\Omega)$,

$$\int_\Omega a_{11} \nabla \tilde{w}_1 \cdot \nabla v + \int_\Omega \tilde{w}_1 v = \int_\Omega b_1 v - \int_\Omega a_{12} \nabla \tilde{w}_2 \cdot \nabla v. \qquad (3.19)$$

If we then choose $\vec{v} = (v, 0)^T$ as a test function in (3.12), we obtain that for all v in $H^1(\Omega)$,

$$\int_\Omega (a_{11} \nabla w_1 + a_{12} \nabla w_2) \cdot \nabla v + \int_\Omega w_1 v = \int_\Omega b_1 v. \qquad (3.20)$$

Substracting (3.19) from (3.20), we find that for all v in $H^1(\Omega)$,

$$\int_\Omega a_{11} \nabla(w_1 - \tilde{w}_1) \cdot \nabla v + a_{12} \nabla(w_2 - \tilde{w}_2) \cdot \nabla v + (w_1 - \tilde{w}_1)v = 0. \quad (3.21)$$

• By first chosing $v = w_2 - \tilde{w}_2$ in (3.18) and then $v = w_1 - \tilde{w}_1$ in (3.21), we conclude that $w_1 \equiv \tilde{w}_1$ and $w_2 \equiv \tilde{w}_2$. Therefore $\vec{w} = (w_1, w_2) \in H^2(\Omega, \mathbb{R}^2)$ and $\vec{w}$ satisfies

$$-\operatorname{div}(A \nabla \vec{w}) + \vec{w} = \vec{b}, \qquad \text{a.e. in } \Omega, \qquad (3.22)$$

$$\frac{\partial \vec{w}}{\partial n} = 0, \qquad \text{a.e. on } \partial\Omega. \qquad (3.23)$$

• Using the assumptions on matrix A, it follows from (3.14) and (3.15), using theorems 3.1.3.3 and 3.2.1.3 from [Gri85], that there exists a constant $C_5 > 0$, depending only on the $W^{1,\infty}$ norm and the positive definiteness constant of matrix A, such that

$$\|\vec{w}\|_{H^2(\Omega,\mathbb{R}^2)} \leqslant C_5 \left(\|\vec{w}\|_{H^1(\Omega,\mathbb{R}^2)} + \|\vec{b}\|_{L^2(\Omega,\mathbb{R}^2)} \right). \qquad (3.24)$$

On the other hand, we obtain from (3.12) with $\vec{v} = \vec{w}$ that there exists a constant $C_6 > 0$ such that

$$\|\vec{w}\|_{H^1(\Omega,\mathbb{R}^2)} \leqslant C_6 \|\vec{b}\|_{L^2(\Omega,\mathbb{R}^2)}. \qquad (3.25)$$

Combining (3.24) and (3.25) we find the estimate (3.13) stated in the lemma.

∎

Remark: We believe that this proof could be generalized to an elliptic system with more than two unknowns, the guiding principle being the *LU* decomposition of matrix A.

We will now proceed to prove Theorems 3.1-3.3.

Proof of Theorem 3.1

• We note $r_h : C^0(\Omega, \mathbb{R}^2) \longrightarrow V_h^2$ the $\mathbb{P}_1$-Lagrange interpolation operator on V_h^2. It is well known (see e.g. [Cia78]) that the interpolation error on H^1 norm can be estimated by

$$\|\vec{w} - r_h\vec{w}\|_{L^2(\Omega,\mathbb{R}^2)} + h\,\|\vec{w} - r_h\vec{w}\|_{H^1(\Omega,\mathbb{R}^2)} \leqslant C_7\,h^2\,|\vec{w}|_{H^2(\Omega,\mathbb{R}^2)},$$
$$\forall \vec{w} \in H^2(\Omega, \mathbb{R}^2), \quad (3.26)$$

where $|.|_{H^2(\Omega,\mathbb{R}^2)}$ denotes the H^2 semi-norm and C_7 is a positive constant independent of $\vec{w}$ and h.

With the previously introduced notations, we can write that for all $t \in [0, t_f]$, using first the coercivity (3.6) of a_t, then Definition 3.1 and finally the continuity (3.7) of a_t,

$$\beta\|\vec{\xi}(t) - \pi_h\vec{\xi}(t)\|_{H^1}^2 \leqslant a_t(\vec{\xi}(t) - \pi_h\vec{\xi}(t), \vec{\xi}(t) - \pi_h\vec{\xi}(t)) \quad (3.27)$$

$$\leqslant a_t(\vec{\xi}(t) - \pi_h\vec{\xi}(t), \vec{\xi}(t) - r_h\vec{\xi}(t)) \quad (3.28)$$

$$\leqslant \alpha\|\vec{\xi}(t) - \pi_h\vec{\xi}(t)\|_{H^1}\|\vec{\xi}(t) - r_h\vec{\xi}(t)\|_{H^1}. \quad (3.29)$$

. Using the interpolation error estimate (3.26), and since $\vec{\xi}(t)$ is in $H^2(\Omega, \mathbb{R}^2)$ for all $t \in [0, t_f]$, bounded independently of t we find that

$$\|\vec{\xi}(t) - \pi_h\vec{\xi}(t)\|_{L^\infty\left(0, t_f; H^1(\Omega,\mathbb{R}^2)\right)} \leqslant C_8 h, \quad (3.30)$$

where C_8 depends on $\|\vec{\xi}\|_{L^\infty\left(0, t_f; H^2(\Omega,\mathbb{R}^2)\right)}$ and is independent of h.

• For the L^2-error estimate, we use Aubin-Nitsche's technique, by introducing the dual problem to the definition of $\pi_h\vec{\xi}(t)$. We define, for a fixed $t \in [0, t_f]$, the auxiliary function $\vec{w} \in H^1(\Omega, \mathbb{R}^2)$ as the solution to the adjoint equation:

$$a_t(\vec{v}, \vec{w}) = \int_\Omega \left(\vec{\xi}(t) - \pi_h\vec{\xi}(t)\right) \cdot \vec{v}, \quad \text{for all } \vec{v} \in H^1(\Omega, \mathbb{R}^2). \quad (3.31)$$

Once again, Lax-Milgram's lemma ensures that $\vec{w}$ is well-defined. Using (3.7), the regularity of D and $\vec{\xi}$, and Lemma 3.1 with $A = D^T$, we obtain that $\vec{w} \in H^2(\Omega, \mathbb{R}^2)$ and that there exists a constant C_9 independent of $\vec{\xi}$ and h, such that

$$|\vec{w}|_{H^2(\Omega, \mathbb{R}^2)} \leqslant C_9 \|\vec{\xi} - \pi_h \vec{\xi}\|_{L^2(\Omega, \mathbb{R}^2)}. \tag{3.32}$$

From equation (3.31), Definition 3.1 and the continuity (3.6) of a_t, we find that

$$\|\vec{\xi}(t) - \pi_h \vec{\xi}(t)\|_{L^2}^2 = a_t(\vec{\xi}(t) - \pi_h \vec{\xi}(t), \vec{w}) \tag{3.33}$$

$$= a_t(\vec{\xi}(t) - \pi_h \vec{\xi}(t), \vec{w} - r_h \vec{w}) \tag{3.34}$$

$$\leqslant \alpha \|\vec{\xi}(t) - \pi_h \vec{\xi}(t)\|_{H^1} \|\vec{w} - r_h \vec{w}\|_{H^1} \tag{3.35}$$

Using result (3.30), interpolation estimate (3.26) and the dual H^2-bound (3.32), we find that there exists a positive constant C_{10} such that

$$\left\| \vec{\xi}(t) - \pi_h \vec{\xi}(t) \right\|_{L^2(\Omega, \mathbb{R}^2)} \leqslant C_{10} h^2, \tag{3.36}$$

and since this last inequality is valid for any fixed $t \in [0, t_f]$, we obtain

$$\|\vec{\xi} - \pi_h \vec{\xi}\|_{L^\infty(0, t_f; L^2(\Omega, \mathbb{R}^2))} \leqslant C_{11} h^2, \tag{3.37}$$

where C_{11} depends on $\|\vec{\xi}\|_{L^\infty(0, t_f; H^2(\Omega, \mathbb{R}^2))}$ and is independent of h.

This last inequality, together with (3.30), proves inequality (3.9). To complete the proof of the theorem we still need to verify that $\pi_h \vec{\xi}$ is indeed continuous in t.

• Let $s, t \in (0, t_f)$. From (3.7) we find that

$$\beta \|\pi_h \vec{\xi}(t) - \pi_h \vec{\xi}(s)\|_{H^1(\Omega, \mathbb{R}^2)}^2 \leqslant a_t(\pi_h \vec{\xi}(t) - \pi_h \vec{\xi}(s), \pi_h \vec{\xi}(t) - \pi_h \vec{\xi}(s)). \tag{3.38}$$

From Definition 3.1, it follows that

$$\beta \|\pi_h \vec{\xi}(t) - \pi_h \vec{\xi}(s)\|_{H^1(\Omega, \mathbb{R}^2)}^2$$
$$\leqslant a_t(\vec{\xi}(t), \pi_h \vec{\xi}(t) - \pi_h \vec{\xi}(s)) - a_s(\vec{\xi}(s), \pi_h \vec{\xi}(t) - \pi_h \vec{\xi}(s))$$
$$+ a_s(\pi_h \vec{\xi}(s), \pi_h \vec{\xi}(t) - \pi_h \vec{\xi}(s)) - a_t(\pi_h \vec{\xi}(s), \pi_h \vec{\xi}(t) - \pi_h \vec{\xi}(s)). \tag{3.39}$$

Using (3.5) and regrouping some terms we find that

$$\beta \|\pi_h \vec{\xi}(t) - \pi_h \vec{\xi}(s)\|^2_{H^1(\Omega, \mathbb{R}^2)}$$
$$\leqslant \int_\Omega \left(D(t) \nabla \vec{\xi}(t) - D(s) \nabla \vec{\xi}(s) \right) : \nabla \left(\pi_h \vec{\xi}(t) - \pi_h \vec{\xi}(s) \right)$$
$$+ \int_\Omega \left(D(s) - D(t) \right) \nabla \pi_h \vec{\xi}(s) : \nabla \left(\pi_h \vec{\xi}(t) - \pi_h \vec{\xi}(s) \right)$$
$$+ \int_\Omega \left(\vec{\xi}(t) - \vec{\xi}(s) \right) \cdot \left(\pi_h \vec{\xi}(t) - \pi_h \vec{\xi}(s) \right) \quad (3.40)$$

Using Hölder's theorem we then find that

$$\beta \|\pi_h \vec{\xi}(t) - \pi_h \vec{\xi}(s)\|_{H^1(\Omega, \mathbb{R}^2)} \leqslant \|D(t) \nabla \vec{\xi}(t) - D(s) \nabla \vec{\xi}(s)\|_{L^2 \Omega, \mathbb{R}^2}$$
$$+ \|D(t) - D(s)\|_{L^\infty(\mathcal{M}_2)} \|\pi_h \vec{\xi}(s)\|_{H^1(\Omega, \mathbb{R}^2)} + \|\vec{\xi}(t) - \vec{\xi}(s)\|_{L^2 \Omega, \mathbb{R}^2}. \quad (3.41)$$

This last inequality holds for any $s, t \in (0, t_f)$. We know, by (3.9), that $\|\pi_h \vec{\xi}(s)\|_{H^1(\Omega, \mathbb{R}^2)}$ is bounded independently of h, so it becomes an immediate consequence of (3.41) and the theorem's assumptions that $\pi_h \vec{\xi} \in C^0(0, t_f; V_h^2)$.

∎

Proof of Theorem 3.2

• We take advantage of the fact that V_h is a finite dimensional space. Let's call $\pi_i(t)$ for $i = 1, \ldots, 2n_h$, the coordinates of $\pi_h \vec{\xi}(t)$ in a basis of V_h^2 defined by a set of linearly independent elements $\left\{ \vec{\psi}_1, \ldots, \vec{\psi}_{2n_h} \right\}$, where n_h is the dimension of V_h, i.e.

$$\pi_h \vec{\xi}(t) = \sum_{i=1}^{2n_h} \pi_i(t) \vec{\psi}_i \quad (3.42)$$

Definition 3.1 can then be translated as:

$$A(t) \vec{\pi}(t) = \vec{b}(t), \qquad \forall t \in [0, t_f], \quad (3.43)$$

where

$$\vec{\pi}(t) = (\pi_j(t))_{1 \leqslant j \leqslant 2n_h}, \quad (3.44)$$

$$\vec{b}(t) = (b_k(t))_{1 \leqslant k \leqslant 2n_h} = \left(\int_\Omega D(t) \nabla \vec{\xi}(t) : \nabla \vec{\psi}_k + \int_\Omega \vec{\xi}(t) \cdot \vec{\psi}_k \right)_{1 \leqslant k \leqslant 2n_h}, \quad (3.45)$$

and

$$\vec{A}(t) = (a_{kj}(t))_{1 \leqslant k,j \leqslant 2n_h} = \left(\int_\Omega D(t) \nabla \vec{\psi}_j : \nabla \vec{\psi}_k + \int_\Omega \vec{\psi}_j . \vec{\psi}_k \right)_{1 \leqslant k,j \leqslant 2n_h}.$$
(3.46)

By the existence and uniqueness of $\vec{\pi}(t)$ (Lax-Milgram's lemma), we know that $A(t)$ is invertible for all $t \in [0, t_f]$ and we get

$$\vec{\pi}(t) = A^{-1}(t)\vec{b}(t), \qquad \forall t \in [0, t_f].$$
(3.47)

Since $H^1(0, t_f)$ is an algebra and $A(t)$ is invertible for all $t \in [0, t_f]$, it is clear that $\vec{b} \in H^1(0, t_f; \mathbb{R}^{2n_h})$ and $A^{-1} \in H^1(0, t_f; \mathcal{M}_{2n_h})$, and therefore $\vec{\pi} \in H^1(0, t_f; \mathbb{R}^{2n_h})$. Thus we have that $\pi_h \vec{\xi} \in H^1(0, t_f; V_h^2)$.

- We now differentiate equation (3.8) with respect to t and obtain

$$\int_\Omega \frac{\partial D}{\partial t}(t) \nabla \left(\vec{\xi}(t) - \pi_h \vec{\xi}(t) \right) : \nabla \vec{v}_h + \int_\Omega D(t) \nabla \frac{\partial}{\partial t} \left(\vec{\xi}(t) - \pi_h \vec{\xi}(t) \right) : \nabla \vec{v}_h$$
$$+ \int_\Omega \frac{\partial}{\partial t} \left(\vec{\xi}(t) - \pi_h \vec{\xi}(t) \right) . \vec{v}_h = 0, \quad \forall \, \vec{v}_h \in V_h^2, \quad \text{a.e. in } (0, t_f).$$
(3.48)

From now on we will be writing inequalities valid for almost every $t \in (0, t_f)$. From (3.7) we infer that

$$\beta \left\| \frac{\partial}{\partial t} \left(\vec{\xi}(t) - \pi_h \vec{\xi}(t) \right) \right\|_{H^1(\Omega, \mathbb{R}^2)}^2$$
$$\leqslant a_t \left(\frac{\partial}{\partial t} \left(\vec{\xi}(t) - \pi_h \vec{\xi}(t) \right), \frac{\partial}{\partial t} \left(\vec{\xi}(t) - \pi_h \vec{\xi}(t) \right) \right).$$
(3.49)

Using the definition of a_t and equation (3.48) with $\vec{v}_h = r_h \vec{\xi}(t) - \pi_h \vec{\xi}(t)$, it follows that

$$\beta \left\| \frac{\partial}{\partial t} \left(\vec{\xi}(t) - \pi_h \vec{\xi}(t) \right) \right\|_{H^1(\Omega, \mathbb{R}^2)}^2$$
$$\leqslant \int_\Omega D(t) \nabla \frac{\partial}{\partial t} \left(\vec{\xi}(t) - \pi_h \vec{\xi}(t) \right) : \nabla \frac{\partial}{\partial t} \left(\vec{\xi}(t) - r_h \vec{\xi}(t) \right)$$
$$+ \int_\Omega \frac{\partial}{\partial t} \left(\vec{\xi}(t) - \pi_h \vec{\xi}(t) \right) \cdot \frac{\partial}{\partial t} \left(\vec{\xi}(t) - r_h \vec{\xi}(t) \right)$$
$$+ \int_\Omega \frac{\partial D}{\partial t}(t) \nabla \left(\vec{\xi}(t) - \pi_h \vec{\xi}(t) \right) : \nabla \left(\pi_h \vec{\xi}(t) - r_h \vec{\xi}(t) \right).$$
(3.50)

Using Cauchy-Schwarz's inequality and the triangle inequality it follows that

$$
\beta \left\| \frac{\partial}{\partial t} \left(\vec{\xi}(t) - \pi_h \vec{\xi}(t) \right) \right\|_{H^1(\Omega,\mathbb{R}^2)}^2
$$
$$
\leqslant \left(\|D(t)\|_{L^\infty(\Omega,\mathcal{M}_2)} + 1 \right)
$$
$$
\left\| \frac{\partial}{\partial t} \left(\vec{\xi}(t) - \pi_h \vec{\xi}(t) \right) \right\|_{H^1(\Omega,\mathbb{R}^2)} \left\| \frac{\partial}{\partial t} \left(\vec{\xi}(t) - r_h \vec{\xi}(t) \right) \right\|_{H^1(\Omega,\mathbb{R}^2)}
$$
$$
+ \left\| \frac{\partial D}{\partial t}(t) \right\|_{L^\infty(\Omega,\mathcal{M}_2)} \left\| \vec{\xi}(t) - \pi_h \vec{\xi}(t) \right\|_{H^1(\Omega,\mathbb{R}^2)}
$$
$$
\left(\left\| \vec{\xi}(t) - r_h \vec{\xi}(t) \right\|_{H^1(\Omega,\mathbb{R}^2)} + \left\| \vec{\xi}(t) - \pi_h \vec{\xi}(t) \right\|_{H^1(\Omega,\mathbb{R}^2)} \right). \quad (3.51)
$$

The operator $\partial/\partial t$, which acts on time and the operator r_h, which acts on space, commute, so from (3.26) we find that

$$
\left\| \frac{\partial}{\partial t} \left(\vec{\xi}(t) - r_h \vec{\xi}(t) \right) \right\|_{H^1(\Omega,\mathbb{R}^2)} \leqslant C_7 h \left| \frac{\partial \vec{\xi}}{\partial t}(t) \right|_{H^2(\Omega,\mathbb{R}^2)}. \quad (3.52)
$$

From (3.51) together with Theorem 3.1 and estimates (3.26) and (3.52), we find using Young's inequality that there exists a constant C_{12} such that for almost every $t \in [0, t_f]$,

$$
\left\| \frac{\partial}{\partial t} \left(\vec{\xi}(t) - \pi_h \vec{\xi}(t) \right) \right\|_{H^1(\Omega,\mathbb{R}^2)}^2 \leqslant C_{12} \left(\left| \frac{\partial \vec{\xi}}{\partial t}(t) \right|_{H^2(\Omega,\mathbb{R}^2)}^2 + \left\| \frac{\partial D}{\partial t}(t) \right\|_{L^\infty(\Omega,\mathcal{M}_2)} \right) h^2,
$$
$$
(3.53)
$$

where we used the theorem's assumptions stating that $\vec{\xi}(t)$ is bounded in $H^2(\Omega, \mathbb{R}^2)$ and $D(t)$ in $L^\infty(\Omega, \mathcal{M}_2)$, independently of t.

Equations (3.49) to (3.53) are valid almost everywhere in $(0, t_f)$ and both sides of inequality (3.53) are elements of $L^2(0, t_f)$. We therefore integrate inequality (3.53) to conclude from the regularity assumptions on $\vec{\xi}$ and on D that there exists a constant C_{13}, which depends in particular on $\|\partial \vec{\xi}/\partial t\|_{L^2\left(0,t_f;H^2(\Omega,\mathbb{R}^2)\right)}$ and on $\|\partial D/\partial t\|_{L^1\left(0,t_f;L^\infty(\Omega,\mathbb{R}^2)\right)}$, and is independent of h, such that

$$
\left\| \frac{\partial}{\partial t} \left(\vec{\xi} - \pi_h \vec{\xi} \right) \right\|_{L^2\left(0,t_f;H^1(\Omega,\mathbb{R}^2)\right)} \leqslant C_{13} h, \quad (3.54)
$$

• In order to get an L^2-error estimate, again we use Aubin-Nitsche's technique. This time we define $\vec{w}(t) \in H^1(\Omega, \mathbb{R}^2)$ as the solution to the adjoint equation:

$$a_t(\vec{v}, \vec{w}(t)) = \int_\Omega \frac{\partial}{\partial t}\left(\vec{\xi}(t) - \pi_h\vec{\xi}(t)\right) \cdot \vec{v}, \quad \forall \vec{v} \in H^1(\Omega, \mathbb{R}^2), \quad \text{a.e. } t \in (0, t_f).$$
(3.55)

Thus $\vec{w}(t)$ is well-defined a.e. in $(0, t_f)$ and applying Lemma 3.1, we find that $\vec{w}(t) \in H^2(\Omega, \mathbb{R}^2)$ and $\partial\vec{w}/\partial n(t) = 0$ a.e. on $\partial\Omega$, for a.e. $t \in (0, t_f)$ and that there exists a constant $C_{14} > 0$ such that,

$$\|\vec{w}(t)\|_{H^2(\Omega,\mathbb{R}^2)} \leqslant C_{14} \left\|\frac{\partial}{\partial t}\left(\vec{\xi}(t) - \pi_h\vec{\xi}(t)\right)\right\|_{L^2(\Omega,\mathbb{R}^2)}, \quad \text{a.e. } t \in (0, t_f).$$
(3.56)

Using (3.55) and (3.48), we find that, a.e. in $(0, t_f)$,

$$\left\|\frac{\partial}{\partial t}\left(\vec{\xi}(t) - \pi_h\vec{\xi}(t)\right)\right\|_{L^2(\Omega,\mathbb{R}^2)}^2 = a_t\left(\frac{\partial}{\partial t}\left(\vec{\xi}(t) - \pi_h\vec{\xi}(t)\right), \vec{w}(t) - r_h\vec{w}(t)\right)$$

$$+ \int_\Omega \frac{\partial D}{\partial t}(t)\nabla(\vec{\xi}(t) - \pi_h\vec{\xi}(t)) : \nabla(\vec{w}(t) - r_h\vec{w}(t))$$

$$- \int_\Omega \frac{\partial D}{\partial t}(t)\nabla(\vec{\xi}(t) - \pi_h\vec{\xi}(t)) : \nabla\vec{w}(t). \quad (3.57)$$

Applying Green's formula (1.63) with property (1.62) to the last term of the right-hand side, and using the continuity (3.6) of a_t, we find that, a.e. in $(0, t_f)$,

$$\left\|\frac{\partial}{\partial t}\left(\vec{\xi}(t) - \pi_h\vec{\xi}(t)\right)\right\|_{L^2(\Omega,\mathbb{R}^2)}^2$$

$$\leqslant \|\vec{w}(t) - r_h\vec{w}(t)\|_{H^1(\Omega,\mathbb{R}^2)}\left(\alpha \left\|\frac{\partial}{\partial t}\left(\vec{\xi}(t) - \pi_h\vec{\xi}(t)\right)\right\|_{H^1(\Omega,\mathbb{R}^2)}\right.$$

$$\left.+ \left\|\frac{\partial D}{\partial t}(t)\right\|_{L^\infty(\Omega,\mathcal{M}_2)} \|\vec{\xi}(t) - \pi_h\vec{\xi}(t)\|_{H^1(\Omega,\mathbb{R}^2)}\right)$$

$$+ \int_\Omega \left(\nabla\frac{\partial D}{\partial t}(t)^T\nabla\vec{w} + \frac{\partial D}{\partial t}(t)^T\Delta\vec{w}\right) \cdot \left(\vec{\xi}(t) - \pi_h\vec{\xi}(t)\right). \quad (3.58)$$

Integrating on time and using Cauchy-Schwarz's inequality, we find that

$$
\left\| \frac{\partial}{\partial t} \left(\vec{\xi} - \pi_h \vec{\xi} \right) \right\|^2_{L^2\left(0,t_f;L^2(\Omega,\mathbb{R}^2)\right)}
$$
$$
\leqslant \left\| \vec{w} - r_h \vec{w} \right\|_{L^2\left(0,t_f;H^1(\Omega,\mathbb{R}^2)\right)} \left(\alpha \left\| \frac{\partial}{\partial t} \left(\vec{\xi} - \pi_h \vec{\xi} \right) \right\|_{L^2\left(0,t_f;H^1(\Omega,\mathbb{R}^2)\right)} \right.
$$
$$
\left. + \left\| \frac{\partial D}{\partial t} \right\|_{L^2\left(0,t_f;L^\infty(\Omega,\mathcal{M}_2)\right)} \left\| \vec{\xi} - \pi_h \vec{\xi} \right\|_{L^\infty\left(0,t_f;H^1(\Omega,\mathbb{R}^2)\right)} \right) \tag{3.59}
$$
$$
+ 2 \left\| \frac{\partial D}{\partial t} \right\|_{L^2\left(0,t_f;W^{1,\infty}(\Omega,\mathcal{M}_2)\right)} \left\| \vec{w} \right\|_{L^2\left(0,t_f;H^2(\Omega,\mathbb{R}^2)\right)}
$$
$$
\cdot \left\| \vec{\xi} - \pi_h \vec{\xi} \right\|_{L^\infty\left(0,t_f;L^2(\Omega,\mathbb{R}^2)\right)} .
$$

Using then (3.54) and Theorem 3.1, we obtain that there exists a positive constant C_{15} which depends on $\|D\|_{H^1\left(0,t_f;W^{1,\infty}(\Omega,\mathcal{M}_2)\right)}$ but independent of h such that

$$
\left\| \frac{\partial}{\partial t} \left(\vec{\xi} - \pi_h \vec{\xi} \right) \right\|^2_{L^2\left(0,t_f;L^2(\Omega,\mathbb{R}^2)\right)}
$$
$$
\leqslant C_{15} \left(h \left\| \vec{w} - r_h \vec{w} \right\|_{L^2\left(0,t_f;H^1(\Omega,\mathbb{R}^2)\right)} + h^2 \left\| \vec{w} \right\|_{L^2\left(0,t_f;H^2(\Omega,\mathbb{R}^2)\right)} \right) . \tag{3.60}
$$

From interpolation estimate (3.26) and the H^2-norm estimate (3.56) together with (3.60), we conclude that there exists a positive constant C_{16} independent of h such that

$$
\left\| \frac{\partial}{\partial t} \left(\vec{\xi} - \pi_h \vec{\xi} \right) \right\|_{L^2\left(0,t_f;L^2(\Omega,\mathbb{R}^2)\right)} \leqslant C_{16}\, h^2. \tag{3.61}
$$

$\blacksquare$

Proof of Theorem 3.3:

Using assumption (H3.1), we can write the following inverse inequality in V_h (see [Cia78], p.140): there exists a positive constant C_{17} independent of h such that

$$
\left\| \nabla v_h \right\|_{L^\infty(\Omega,\mathbb{R}^2)} \leqslant C_{17} h^{-1} \left\| \nabla v_h \right\|_{L^2(\Omega,\mathbb{R}^2)}, \quad \forall v_h \in V_h. \tag{3.62}
$$

Remark: In the case of space dimension 3, estimate (3.62) would actually go as $h^{-3/2}$.

Therefore, since $\pi_h\vec{\xi}(t) - r_h\vec{\xi}(t) \in V_h^2$, we have for a.e $t \in (0, t_f)$:

$$\|\nabla(\pi_h\vec{\xi}(t) - r_h\vec{\xi}(t))\|_{L^\infty(\Omega,\mathcal{M}_2)}$$
$$\leqslant C_{17}h^{-1}\|\nabla(\pi_h\vec{\xi}(t) - r_h\vec{\xi}(t))\|_{L^2(\Omega,\mathcal{M}_2)}$$
$$\leqslant C_{17}h^{-1}\Big(\|\nabla(\pi_h\vec{\xi}(t) - \vec{\xi}(t))\|_{L^2(\Omega,\mathcal{M}_2)}$$
$$+ \|\nabla(\vec{\xi}(t) - r_h\vec{\xi}(t))\|_{L^2(\Omega,\mathcal{M}_2)}\Big).$$

Then using interpolation estimate (3.26) and (3.30), we infer that for a.e. $t \in (0, t_f)$

$$\|\nabla(\pi_h\vec{\xi}(t) - r_h\vec{\xi}(t))\|_{L^\infty(\Omega,\mathcal{M}_2)} \leqslant C_{18}, \tag{3.63}$$

where C_{18} is independent of h, and depends on $\|\vec{\xi}\|_{L^\infty\left(0,t_f;H^2(\Omega,\mathbb{R}^2)\right)}$.

On the other hand, we can estimate a $W^{1,\infty}$-interpolation error for $\vec{\xi}$. For the Lagrange interpolation operator, we have that (see [Cia78], p.121) there exists a constant C_{19} independent of h and $\vec{\xi}$ such that, for a.e. $t \in (0, t_f)$,

$$\|\vec{\xi}(t) - r_h\vec{\xi}(t)\|_{W^{1,\infty}(\Omega,\mathbb{R}^2)} \leqslant C_{19}\|\vec{\xi}(t)\|_{W^{1,\infty}(\Omega,\mathbb{R}^2)}, \tag{3.64}$$

and therefore

$$\|\nabla r_h\vec{\xi}(t)\|_{L^\infty(\Omega,\mathcal{M}_2)} \leqslant \|\nabla(r_h\vec{\xi}(t) - \vec{\xi}(t))\|_{L^\infty(\Omega,\mathcal{M}_2)} + \|\nabla\vec{\xi}(t)\|_{L^\infty(\Omega,\mathcal{M}_2)}$$
$$\leqslant (1 + C_{19})\|\vec{\xi}(t)\|_{W^{1,\infty}(\Omega,\mathbb{R}^2)}. \tag{3.65}$$

Finally, using (3.63) and (3.65), we find that there exists a constant C_{20} independent of h such that for a.e. $t \in (0, t_f)$

$$\|\nabla\pi_h\vec{\xi}(t)\|_{L^\infty(\Omega,\mathcal{M}_2)} \leqslant \|\nabla(\pi_h\vec{\xi}(t) - r_h\vec{\xi}(t))\|_{L^\infty(\Omega,\mathcal{M}_2)} + \|\nabla r_h\vec{\xi}(t)\|_{L^\infty(\Omega,\mathcal{M}_2)}$$
$$\leqslant C_{20}. \tag{3.66}$$

Theorem 3.3 is thus proved. ∎

3.3 Convergence result

The following theorem states the main result of this chapter, concerning the convergence of the solution $\vec{u}_h^n$ of the discrete problem (3.3) to the exact solution $\vec{u}$ of the continuous problem (1.51).

Theorem 3.4 *Let assumptions* (H1.1),(H1.2), (H1.3) *and* (H3.1) *be fulfilled. If the solution $\vec{u}$ of problem* (1.51) *belongs to $H^1\left(0, t_f; H^2(\Omega, \mathbb{R}^2)\right)$ and to $L^\infty\left(0, t_f; W^{1,\infty}(\Omega, \mathbb{R}^2)\right)$, then there exist two positive constants C and τ^* independent of h and τ such that for $0 < \tau \leqslant \tau*$,*

$$\max_{0 \leqslant n \leqslant N} \|\vec{u}(t^n) - \vec{u}_h^n\|_{L^2(\Omega, \mathbb{R}^2)} \leqslant C(h^2 + \tau). \tag{3.67}$$

The proof of Theorem 3.4 relies on the introduction of the generalized vectorial elliptic projector from section 3.2, in whose definition we choose matrix D to be in fact $D(\vec{u})$, where $\vec{u}$ is the solution of problem (1.51) and $D(\cdot)$ is defined by (1.53). First of all, let us remark that the assumptions of Theorem 3.4 imply the assumptions of theorems 3.1, 3.2 and 3.3, so we can define $\pi_h \vec{u} \in H^1\left(0, t_f; V_h^2\right)$ and use all the properties implied by those theorems. Also, from now on, $\|.\|_0$ will denote the norm of $L^2(\Omega, \mathbb{R}^2)$ or $L^2(\Omega, \mathcal{M}_2)$, as appropriate, and Q_n the space-time domain $(t^{n-1}, t^n) \times \Omega$. We also introduce the notation

$$\bar{g}^n = \frac{1}{\tau} \int_{t^{n-1}}^{t^n} g(t) dt \tag{3.68}$$

for the average of an integrable function g on $[t^{n-1}, t^n]$. Finally, let us define the auxiliary function

$$\delta \vec{u}_h^n = \pi_h \vec{u}(t^n) - \vec{u}_h^n, \tag{3.69}$$

for $n = 0, \dots, N$.

We now proceed by introducing four lemmata, which will be used for proving Theorem 3.4.

Lemma 3.2 *Under the assumptions of Theorem 3.4,*

$$\left\| \overline{\frac{\partial}{\partial t} (\pi_h \vec{u} - \vec{u})}^{\,n} \right\|_0^2 \leqslant \frac{1}{\tau} \left\| \frac{\partial}{\partial t} (\vec{u} - \pi_h \vec{u}) \right\|_{L^2(Q_n)}^2 \tag{3.70}$$

Proof
Using Cauchy-Schwarz's inequality, we get

$$
\begin{aligned}
\left\| \overline{\frac{\partial}{\partial t} (\pi_h \vec{u} - \vec{u})}^{\,n} \right\|_0^2 &= \int_\Omega \left| \frac{1}{\tau} \int_{t^{n-1}}^{t^n} \frac{\partial}{\partial t} (\pi_h \vec{u} - \vec{u}) dt \right|^2 dx \\
&\leqslant \int_\Omega \frac{1}{\tau} \int_{t^{n-1}}^{t^n} \left| \frac{\partial}{\partial t} (\pi_h \vec{u} - \vec{u}) \right|^2 dt \, dx,
\end{aligned}
\tag{3.71}
$$

where $|.|$ stands for the vectorial norm. ∎

Lemma 3.3 *Under the assumptions of Theorem 3.4,*

$$\left\|\overrightarrow{\vec{u} - \pi_h \vec{u}}^n\right\|_0^2 \leqslant \frac{1}{\tau}\left\|\vec{u} - \pi_h\vec{u}\right\|_{L^2(Q_n)}^2. \tag{3.72}$$

Proof
The result is straightforward with a computation similar to the one used to prove Lemma 3.2. ∎

Lemma 3.4 *Under the assumptions of Theorem 3.4, there exists a constant C_{21} independent of h such that*

$$\left\|\overrightarrow{\vec{F}(\vec{u})}^n - \vec{F}(\vec{u}_h^{n-1})\right\|_0^2$$
$$\leqslant C_{21}\left(\tau\left\|\frac{\partial\vec{u}}{\partial t}\right\|_{L^2(Q_n)}^2 + \left\|\vec{u}(t^{n-1}) - \pi_h\vec{u}(t^{n-1})\right\|_0^2 + \left\|\delta\vec{u}_h^{n-1}\right\|_0^2\right). \tag{3.73}$$

Proof
The left-hand side of the inequality we want to prove can be read as

$$\left\|\overrightarrow{\vec{F}(\vec{u})}^n - \vec{F}(\vec{u}_h^{n-1})\right\|_0^2 = \int_\Omega\left|\frac{1}{\tau}\int_{t^{n-1}}^{t^n}\left(\vec{F}(\vec{u}(t)) - \vec{F}(\vec{u}_h^{n-1})\right)dt\right|^2 dx. \tag{3.74}$$

We use Cauchy-Schwarz's inequality and the Lipschitz assumption (H1.1) on $\vec{F}$ in order to get

$$\left\|\overrightarrow{\vec{F}(\vec{u})}^n - \vec{F}(\vec{u}_h^{n-1})\right\|_0^2$$
$$\leqslant \int_\Omega\frac{1}{\tau}\int_{t^{n-1}}^{t^n}\left|\vec{F}(\vec{u}(t)) - \vec{F}(\vec{u}_h^{n-1})\right|^2 dt\,dx$$
$$\leqslant \frac{\mathcal{L}_{\vec{F}}^2}{\tau}\int_\Omega\int_{t^{n-1}}^{t^n}\left|\vec{u}(t) - \vec{u}_h^{n-1}\right|^2 dt\,dx$$
$$\leqslant \frac{2\mathcal{L}_{\vec{F}}^2}{\tau}\int_\Omega\int_{t^{n-1}}^{t^n}\left(\left|\vec{u}(t) - \vec{u}(t^{n-1})\right|^2 + \left|\vec{u}(t^{n-1}) - \vec{u}_h^{n-1}\right|^2 dt\,dx\right). \tag{3.75}$$

Now, since we have the following relation $\vec{u}(t) - \vec{u}(t^{n-1}) = \int_{t^{n-1}}^t\frac{\partial\vec{u}}{\partial t}(s)\,ds$, for all $t\in[t^{n-1}, t^n]$, it is easy to see that

$$\int_\Omega\int_{t^{n-1}}^{t^n}\left|\vec{u}(t) - \vec{u}(t^{n-1})\right|^2 dt\,dx \leqslant \tau^2\left\|\frac{\partial\vec{u}}{\partial t}\right\|_{L^2(Q_n)}^2. \tag{3.76}$$

Then we infer from (3.75) and (3.76) that

$$\left\| \overline{\vec{F}(\vec{u})}^n - \vec{F}(\vec{u}_h^{n-1}) \right\|_0^2 \leqslant 2\tau \mathcal{L}_{\vec{F}}^2 \left\| \frac{\partial \vec{u}}{\partial t} \right\|_{L^2(Q_n)}^2 + 2\mathcal{L}_{\vec{F}}^2 \left\| \vec{u}(t^{n-1}) - \vec{u}_h^{n-1} \right\|_0^2. \quad (3.77)$$

Finally, introducing projector $\pi_h \vec{u}(t^{n-1})$ in the above estimate, we obtain the wanted inequality, with $C_{21} = 4\mathcal{L}_{\vec{F}}^2$. ∎

Lemma 3.5 *Under the assumptions of Theorem 3.4, there exist two constants C_{22} and C_{23} independent of h such that*

$$\left\| D(\vec{w}_h^{\theta n}) \nabla \pi_h \vec{u}(t^n) - \overline{D(\vec{u})\nabla \pi_h \vec{u}}^n \right\|_0^2$$
$$\leqslant C_{22} \left(2 \|\vec{u} - \pi_h \vec{u}\|_{L^\infty\left(0,t_f;L^2(\Omega,\mathbb{R}^2)\right)}^2 + \left\| \delta \vec{u}_h^{n-1} \right\|_0^2 + \theta^2 \left\| \delta \vec{u}_h^n \right\|_0^2 \right)$$
$$+ C_{23}\tau \left(\left\| \frac{\partial \vec{u}}{\partial t} \right\|_{L^2(Q_n)}^2 + \left\| \nabla \frac{\partial \pi_h \vec{u}}{\partial t} \right\|_{L^2(Q_n)}^2 \right). \quad (3.78)$$

Proof
Using Cauchy-Schwarz and Young's inequalities, we can separate the left-hand side of inequality (3.78) in two terms as

$$\left\| D(\vec{w}_h^{\theta n}) \nabla \pi_h \vec{u}(t^n) - \overline{D(\vec{u})\nabla \pi_h \vec{u}}^n \right\|_0^2$$
$$\leqslant 2 \left\| \left(D(\vec{w}_h^{\theta n}) - \overline{D(\vec{u})}^n \right) \nabla \pi_h \vec{u}(t^n) \right\|_0^2$$
$$+ 2 \left\| \overline{D(\vec{u})}^n \nabla \pi_h \vec{u}(t^n) - \overline{D(\vec{u})\nabla \pi_h \vec{u}}^n \right\|_0^2. \quad (3.79)$$

- We will start by estimating the first right-hand term of (3.79):

$$\left\| \left(D(\vec{w}_h^{\theta n}) - \overline{D(\vec{u})}^n \right) \nabla \pi_h \vec{u}(t^n) \right\|_0^2$$
$$\leqslant 2 \|\nabla \pi_h \vec{u}\|_{L^\infty(0,t_f;L^\infty(\Omega,\mathcal{M}_2))}^2 \sum_{i,j=1}^2 \left\| D_{ij}(\vec{w}_h^{\theta n}) - \overline{D_{ij}(\vec{u})}^n \right\|_0^2, \quad (3.80)$$

where D_{ij} stands for the components of matrix D.

We now introduce an auxiliary function

$$\vec{w}^\theta(t) = \begin{pmatrix} (1-\theta)u_1(t-\tau) + \theta u_1(t) \\ u_2(t-\tau) \end{pmatrix}, \quad \text{for } t \geqslant \tau. \quad (3.81)$$

For all combinations of $i, j = 1, 2$ and for $n \geqslant 1$, we have

$$
\left\| D_{ij}(\vec{w}_h^{\theta n}) - \overline{D_{ij}(\vec{u})}^n \right\|_0^2
$$
$$
\leqslant 2 \left(\left\| D_{ij}(\vec{w}_h^{\theta n}) - D_{ij}(\vec{w}^\theta(t^n)) \right\|_0^2 + \left\| D_{ij}(\vec{w}^\theta(t^n)) - \overline{D_{ij}(\vec{u})}^n \right\|_0^2 \right). \quad (3.82)
$$

Let us estimate the first term in the right-hand side of (3.82). By the use of the lipschitz assumption (H1.2) on matrix D, we have

$$
\left\| D_{ij}(\vec{w}_h^{\theta n}) - D_{ij}(\vec{w}^\theta(t^n)) \right\|_0^2 \leqslant \mathcal{L}_D^2 \left\| \vec{w}_h^{\theta n} - \vec{w}^\theta(t^n) \right\|_0^2. \quad (3.83)
$$

Moreover, Definition (3.81) for $\vec{w}^\theta$ leads to

$$
\left| \vec{w}_h^{\theta n} - \vec{w}^\theta(t^n) \right|^2 = \left((1-\theta)(u_{1h}^{n-1} - u_1(t^{n-1})) + \theta(u_{1h}^n - u_1(t^n)) \right)^2 \quad (3.84)
$$
$$
+ \left(u_{2h}^{n-1} - u_2(t^{n-1}) \right)^2
$$
$$
\leqslant 2 \left(\left| \vec{u}_h^{n-1} - \vec{u}(t^{n-1}) \right|^2 + \theta^2 \left| \vec{u}_h^n - \vec{u}(t^n) \right|^2 \right), \quad (3.85)
$$

from what we infer that

$$
\left\| \vec{w}_h^{\theta n} - \vec{w}^\theta(t^n) \right\|_0^2 \leqslant 4 \left(\left\| \delta \vec{u}_h^{n-1} \right\|_0^2 + \left\| \vec{u}(t^{n-1}) - \pi_h \vec{u}(t^{n-1}) \right\|_0^2 \right.
$$
$$
\left. + \theta^2 \left\| \delta \vec{u}_h^n \right\|_0^2 + \theta^2 \left\| \vec{u}(t^n) - \pi_h \vec{u}(t^n) \right\|_0^2 \right). \quad (3.86)
$$

Thus from (3.83) and (3.86), and since $0 \leqslant \theta \leqslant 1$ we obtain

$$
\left\| D_{ij}(\vec{w}_h^{\theta n}) - D_{ij}(\vec{w}^\theta(t^n)) \right\|_0^2
$$
$$
\leqslant 4\mathcal{L}_D^2 \left(\left\| \delta \vec{u}_h^{n-1} \right\|_0^2 + \theta^2 \left\| \delta \vec{u}_h^n \right\|_0^2 + \left\| \vec{u}(t^{n-1}) - \pi_h \vec{u}(t^{n-1}) \right\|_0^2 \right.
$$
$$
\left. + \left\| \vec{u}(t^n) - \pi_h \vec{u}(t^n) \right\|_0^2 \right). \quad (3.87)
$$

Now, we estimate the second term of the right-hand side of (3.82). First we have

$$
\left\| D_{ij}(\vec{w}^\theta(t^n)) - \overline{D_{ij}(\vec{u})}^n \right\|_0^2 = \int_\Omega \left(\frac{1}{\tau} \int_{t^{n-1}}^{t^n} \left(D_{ij}(\vec{w}^\theta(t^n)) - D_{ij}(\vec{u}(t)) \right) dt \right)^2 dx.
$$
$$
(3.88)
$$

By using Cauchy-Schwarz's inequality and the Lipschitz assumption (H1.2) on the matrix D, we then get

$$
\left\| D_{ij}(\vec{w}^\theta(t^n)) - \overline{D_{ij}(\vec{u})}^n \right\|_0^2 \leqslant \frac{\mathcal{L}_D^2}{\tau} \left\| \vec{w}^\theta(t^n) - \vec{u} \right\|_{L^2(Q_n)}^2. \quad (3.89)
$$

Furthermore we have for all $t \in [t^{n-1}, t^n]$

$$
\begin{aligned}
&\left|\vec{w}^\theta(t^n) - \vec{u}(t)\right|^2 \\
&= \left((1-\theta)u_1(t^{n-1}) + \theta u_1(t^n) - u_1(t)\right)^2 + \left(u_2(t^{n-1}) - u_2(t)\right)^2.
\end{aligned}
\tag{3.90}
$$

Thus, remarking that

$$
\begin{aligned}
(1-\theta)u_1(t^{n-1}) + \theta u_1(t^n) - u_1(t) \\
= (1-\theta) \int_t^{t^{n-1}} \frac{\partial u_1}{\partial t}(s)ds + \theta \int_t^{t^n} \frac{\partial u_1}{\partial t}(s)ds
\end{aligned}
\tag{3.91}
$$

and

$$
u_2(t^{n-1}) - u_2(t) = \int_t^{t^{n-1}} \frac{\partial u_2}{\partial t}(s)ds,
\tag{3.92}
$$

we infer by Cauchy-Schwarz's inequality that, since $0 \leqslant \theta \leqslant 1$,

$$
\left|\vec{w}^\theta(t^n) - \vec{u}(t)\right|^2 \leqslant \tau \int_{t^{n-1}}^{t^n} \left|\frac{\partial \vec{u}}{\partial t}\right|^2 dt, \quad \text{for all } t \in [t^{n-1}, t^n].
\tag{3.93}
$$

Then from (3.89) and (3.93), we obtain

$$
\left\|D_{ij}(\vec{w}^\theta(t^n)) - \overline{D_{ij}(\vec{u})}^n\right\|_0^2 \leqslant \tau \mathcal{L}_D^2 \left\|\frac{\partial \vec{u}}{\partial t}\right\|_{L^2(Q_n)}^2.
\tag{3.94}
$$

- The second right-hand term of (3.79) is estimated as follows. We have

$$
\begin{aligned}
&\left\|\overline{D(\vec{u})}^n \nabla \pi_h \vec{u}(t^n) - \overline{D(\vec{u})\nabla \pi_h \vec{u}}^n\right\|_0^2 \\
&= \int_\Omega \left|\frac{1}{\tau} \int_{t^{n-1}}^{t^n} D(\vec{u}(t)) \left(\nabla \pi_h \vec{u}(t^n) - \nabla \pi_h \vec{u}(t)\right) dt\right|^2 dx.
\end{aligned}
\tag{3.95}
$$

By Cauchy-Schwarz's inequality and the boundedness assumption of D in (H1.2), we obtain that

$$
\left\|\overline{D(\vec{u})}^n \nabla \pi_h \vec{u}(t^n) - \overline{D(\vec{u})\nabla \pi_h \vec{u}}^n\right\|_0^2 \leqslant \frac{D_M^2}{\tau} \|\nabla \pi_h \vec{u}(t^n) - \nabla \pi_h \vec{u}\|_{L^2(Q_n)}^2.
\tag{3.96}
$$

Since for all $t \in [t^{n-1}, t^n]$ we have $\nabla \pi_h \vec{u}(t^n) - \nabla \pi_h \vec{u}(t) = \int_t^{t^n} \nabla \frac{\partial \pi_h \vec{u}}{\partial t}(s)ds$, we infer, using Cauchy-Schwarz's inequality and estimate (3.96), that

$$
\left\|\overline{D(\vec{u})}^n \nabla \pi_h \vec{u}(t^n) - \overline{D(\vec{u})\nabla \pi_h \vec{u}}^n\right\|_0^2 \leqslant \tau D_M^2 \left\|\nabla \frac{\partial \pi_h \vec{u}}{\partial t}\right\|_{L^2(Q_n)}^2
\tag{3.97}
$$

- Grouping steps (3.79)-(3.97), we find that

$$
\left\| D(\vec{w}_h^{\theta n})\nabla\pi_h\vec{u}(t^n) - \overline{D(\vec{u})\nabla\pi_h\vec{u}}^{\,n} \right\|_0^2
$$

$$
\leqslant \; 128\mathcal{L}_D^2 \left\| \nabla\pi_h\vec{u} \right\|_{L^\infty\left(0,t_f;L^\infty(\Omega,\mathcal{M}_2)\right)}^2 \left(\left\| \vec{u}(t^{n-1}) - \pi_h\vec{u}(t^{n-1}) \right\|_0^2 \right.
$$

$$
\left. + \left\| \vec{u}(t^n) - \pi_h\vec{u}(t^n) \right\|_0^2 + \left\| \delta\vec{u}_h^{n-1} \right\|_0^2 + \theta^2 \left\| \delta\vec{u}_h^n \right\|_0^2 \right)
$$

$$
+32\tau\mathcal{L}_D^2 \left\| \nabla\pi_h\vec{u} \right\|_{L^\infty\left(0,t_f;L^\infty(\Omega,\mathbb{R}^2)\right)}^2 \left\| \frac{\partial\vec{u}}{\partial t} \right\|_{L^2(Q_n)}^2
$$

$$
+2\tau D_M^2 \left\| \nabla\frac{\partial\pi_h\vec{u}}{\partial t} \right\|_{L^2(Q_n)}^2 .
$$

(3.98)

Thanks to theorem 3.3 we know that $\left\| \nabla\pi_h\vec{u} \right\|_{L^\infty\left(0,t_f;L^\infty(\Omega,\mathcal{M}_2)\right)}^2$ is bounded independently of h. We then get the result of the lemma by defining $C_{22} = 128\mathcal{L}_D^2 \sup_{h>0} \left\| \nabla\pi_h\vec{u} \right\|_{L^\infty\left(0,t_f;L^\infty(\Omega,\mathcal{M}_2)\right)}^2$ and $C_{23} = \max\left(C_{22}/4, 2D_M^2\right)$. ∎

Proof of Theorem 3.4

From the numerical scheme (3.3a), for all $\vec{v}_h \in V_h^2$ and for $n = 1, \ldots, N$, we have:

$$
\int_\Omega \left(\delta\vec{u}_h^n - \delta\vec{u}_h^{n-1} \right) \cdot \vec{v}_h + \tau \int_\Omega D(\vec{w}_h^{\theta n})\nabla\delta\vec{u}_h^n : \nabla\vec{v}_h
$$

$$
= \int_\Omega \left(\pi_h\vec{u}(t^n) - \pi_h\vec{u}(t^{n-1}) \right) \cdot \vec{v}_h + \tau \int_\Omega D(\vec{w}_h^{\theta n})\nabla\pi_h\vec{u}(t^n) : \nabla\vec{v}_h
$$

$$
- \tau \int_\Omega \vec{F}(\vec{u}_h^{n-1}) \cdot \vec{v}_h . \quad (3.99)
$$

Furthermore, since both $\vec{u}$ and $\pi_h\vec{u}$ are in $H^1(0, t_f; L^2(\Omega, \mathbb{R}^2))$, we have

$$
\int_\Omega \left(\pi_h\vec{u}(t^n) - \pi_h\vec{u}(t^{n-1}) \right) \cdot \vec{v}_h
$$

$$
= \int_\Omega (\pi_h\vec{u}(t^n) - \vec{u}(t^n)) \cdot \vec{v}_h - \int_\Omega \left(\pi_h\vec{u}(t^{n-1}) - \vec{u}(t^{n-1}) \right) \cdot \vec{v}_h
$$

$$
+ \int_\Omega \left(\vec{u}(t^n) - \vec{u}(t^{n-1}) \right) \cdot \vec{v}_h
$$

$$
= \tau \int_\Omega \overline{\frac{\partial}{\partial t}(\pi_h\vec{u} - \vec{u})}^{\,n} \cdot \vec{v}_h + \tau \int_\Omega \overline{\frac{\partial\vec{u}}{\partial t}}^{\,n} \cdot \vec{v}_h .
$$

(3.100)

Now, using equation (1.64a) of the exact problem, we infer that

$$\int_\Omega \overline{\frac{\partial \vec{u}}{\partial t}}^n . \vec{v}_h = \int_\Omega \overline{\vec{F}(\vec{u})}^n . \vec{v}_h - \int_\Omega \overline{D(\vec{u})\nabla\vec{u}}^n : \nabla\vec{v}_h \ . \qquad (3.101)$$

Then from equations (3.100) and (3.101) together with equation (3.99), we obtain

$$\int_\Omega \left(\delta\vec{u}_h^n - \delta\vec{u}_h^{n-1}\right) \cdot \vec{v}_h + \tau \int_\Omega D(\vec{w}_h^{\theta n})\nabla\delta\vec{u}_h^n : \nabla\vec{v}_h$$
$$= \tau \int_\Omega \overline{\frac{\partial}{\partial t}(\pi_h\vec{u} - \vec{u})}^n . \vec{v}_h - \tau \int_\Omega \overline{D(\vec{u})\nabla\vec{u}}^n : \nabla\vec{v}_h$$
$$+ \tau \int_\Omega \left(\overline{\vec{F}(\vec{u})}^n - \vec{F}(\vec{u}_h^{n-1})\right) \cdot \vec{v}_h$$
$$+ \tau \int_\Omega D(\vec{w}_h^{\theta n})\nabla\pi_h\vec{u}(t^n) : \nabla\vec{v}_h \ . \quad (3.102)$$

Moreover, by the definition (3.8) of the GVP, we get for all $\vec{v}_h \in V_h^2$:

$$\int_\Omega \overline{D(\vec{u})\nabla\vec{u}}^n : \nabla\vec{v}_h = \int_\Omega \overline{D(\vec{u})\nabla\pi_h\vec{u}}^n : \nabla\vec{v}_h + \int_\Omega \overline{(\pi_h\vec{u}(t) - \vec{u}(t))}^n . \vec{v}_h \ .$$
$$(3.103)$$

Then using (3.103) in equation (3.102), we obtain that:

$$\int_\Omega \left(\delta\vec{u}_h^n - \delta\vec{u}_h^{n-1}\right) \cdot \vec{v}_h + \tau \int_\Omega D(\vec{w}_h^{\theta n})\nabla\delta\vec{u}_h^n : \nabla\vec{v}_h$$
$$= \tau \int_\Omega \overline{\frac{\partial}{\partial t}(\pi_h\vec{u} - \vec{u})}^n . \vec{v}_h + \tau \int_\Omega \overline{(\vec{u} - \pi_h\vec{u})}^n . \vec{v}_h$$
$$+ \tau \int_\Omega \left(D(\vec{w}_h^{\theta n})\nabla\pi_h\vec{u}(t^n) - \overline{D(\vec{u})\nabla\pi_h\vec{u}}^n\right) : \nabla\vec{v}_h$$
$$+ \tau \int_\Omega \left(\overline{\vec{F}(\vec{u})}^n - \vec{F}(\vec{u}_h^{n-1})\right) \cdot \vec{v}_h, \qquad \text{for all } \vec{v}_h \in V_h^2. \quad (3.104)$$

We may now choose $\vec{v}_h = \delta\vec{u}_h^n$ in equation (3.104). Using assumption (H1.3) and applying Cauchy-Schwarz and Young's inequalities five times to equation (3.104), we get the following inequality, valid for all $\varepsilon_0, \dots, \varepsilon_4 > 0$

and for $n = 1, \ldots, N$:

$$(1 - (\varepsilon_0 + \varepsilon_1 + \varepsilon_2 + \varepsilon_3)) \, \|\delta\vec{u}_h^n\|_0^2 - \frac{1}{4\varepsilon_0} \, \|\delta\vec{u}_h^{n-1}\|_0^2 + \tau(D_m - \varepsilon_4) \, \|\nabla\delta\vec{u}_h^n\|_0^2$$

$$\leqslant \frac{\tau^2}{4\varepsilon_1} \left\| \overline{\frac{\partial}{\partial t}(\pi_h\vec{u} - \vec{u})}^n \right\|_0^2 + \frac{\tau^2}{4\varepsilon_2} \left\| \overline{\vec{u} - \pi_h\vec{u}}^n \right\|_0^2$$

$$+ \frac{\tau^2}{4\varepsilon_3} \left\| \overline{\vec{F}(\vec{u})}^n - \vec{F}(\vec{u}_h^{n-1}) \right\|_0^2$$

$$+ \frac{\tau}{4\varepsilon_4} \left\| D(\vec{w}_h^{\theta n})\nabla\pi_h\vec{u}(t^n) - \overline{D(\vec{u})\nabla\pi_h\vec{u}}^n \right\|_0^2. \quad (3.105)$$

The four terms of the right-hand side of inequality (3.105) are estimated using Lemmata 3.2-3.5. We choose

$$\varepsilon_0 = \frac{1}{2}, \quad \varepsilon_1 = \varepsilon_2 = \varepsilon_3 = \frac{\tau}{3} \qquad \text{and} \qquad \varepsilon_4 = D_m. \quad (3.106)$$

Then from estimates (3.70), (3.72), (3.73) and (3.78), together with inequality (3.105), we get for $n = 1, ..., N$,

$$(\frac{1}{2} - C_{24}\tau) \, \|\delta\vec{u}_h^n\|_0^2 - (\frac{1}{2} + C_{25}\tau) \, \|\delta\vec{u}_h^{n-1}\|_0^2$$

$$\leqslant \frac{3}{4} \, \|\vec{u} - \pi_h\vec{u}\|_{H^1(t^{n-1},t^n;L^2(\Omega,\mathbb{R}^2))}^2 + C_{26}\tau^2 \left(\left\| \frac{\partial\vec{u}}{\partial t} \right\|_{L^2(Q_n)}^2 + \left\| \nabla\frac{\partial\pi_h\vec{u}}{\partial t} \right\|_{L^2(Q_n)}^2 \right)$$

$$+ C_{25}\tau \, \|\vec{u} - \pi_h\vec{u}\|_{L^\infty(0,t_f;L^2(\Omega,\mathbb{R}^2))}^2, \quad (3.107)$$

where $C_{24} = 1 + \theta^2 C_{22}/(4D_m)$, $C_{25} = 3C_{21}/4 + C_{22}/(4D_m)$ and $C_{26} = 3C_{21}/4 + C_{23}/(4D_m)$. Now, let us define

$$\tau^* = \frac{1}{4C_{24}} > 0. \quad (3.108)$$

In that way, for all $0 < \tau \leqslant \tau^*$, we have

$$\frac{1}{2} - C_{24}\tau \geqslant \frac{1}{4}. \quad (3.109)$$

In addition, it is straightforward to prove that for all $0 < \tau \leqslant \tau^*$, we have

$$(\frac{1}{2} + C_{25}\tau) \leqslant (\frac{1}{2} - C_{24}\tau)(1 + \omega\tau) \quad (3.110)$$

where

$$\omega = 4(C_{24} + C_{25}). \tag{3.111}$$

Remark also that ω depends neither on h nor on τ.

Then using (3.109) and (3.110), we infer from (3.107) that for all $n = 1, \dots, N$ and $0 < \tau \leqslant \tau^*$,

$$\|\delta \vec{u}_h^n\|_0^2 - (1 + \omega\tau) \|\delta \vec{u}_h^{n-1}\|_0^2 \leqslant \lambda_n \tag{3.112}$$

where

$$\begin{aligned}
\lambda_n = {}& 3 \|\vec{u} - \pi_h \vec{u}\|_{H^1(t^{n-1}, t^n; L^2(\Omega, \mathbb{R}^2))}^2 \\
&+ 4C_{26}\tau^2 \left(\left\| \frac{\partial \vec{u}}{\partial t} \right\|_{L^2(Q_n)}^2 + \left\| \nabla \frac{\partial \pi_h \vec{u}}{\partial t} \right\|_{L^2(Q_n)}^2 \right) \\
&+ 4C_{25}\tau \|\vec{u} - \pi_h \vec{u}\|_{L^\infty(0, t_f; L^2(\Omega, \mathbb{R}^2))}^2. \tag{3.113}
\end{aligned}$$

Now, we sum inequality (3.112) over n, in order to get

$$\|\delta \vec{u}_h^n\|_0^2 \leqslant \|\delta \vec{u}_h^0\|_0^2 + \sum_{k=1}^n \lambda_k + \omega\tau \sum_{k=1}^n \|\delta \vec{u}_h^{k-1}\|_0^2, \tag{3.114}$$

for all $1 \leqslant n \leqslant N$ and $0 < \tau \leqslant \tau^*$. We can then use the discrete Gronwall's lemma (see for instance [QV91], §1.4) on inequality (3.114) and find that, for $n = 1, \dots, N$,

$$\|\delta \vec{u}_h^n\|_0^2 \leqslant \left(\|\delta \vec{u}_h^0\|_0^2 + \sum_{k=1}^n \lambda_k \right) \exp(\omega t_f). \tag{3.115}$$

Furthermore, using the definition (3.113) of λ_k, we have that for all $1 \leqslant n \leqslant N$

$$\begin{aligned}
\sum_{k=1}^n \lambda_k \leqslant {}& 3 \|\vec{u} - \pi_h \vec{u}\|_{H^1(0, t_f; L^2(\Omega, \mathbb{R}^2))}^2 \\
&+ 4C_{26}\tau^2 \left(\left\| \frac{\partial \vec{u}}{\partial t} \right\|_{L^2(0, t_f; L^2(\Omega, \mathbb{R}^2))}^2 + \left\| \nabla \frac{\partial \vec{u}}{\partial t} \right\|_{L^2(0, t_f; L^2(\Omega, \mathbb{R}^2))}^2 \right. \\
&\left. + \left\| \nabla \frac{\partial \pi_h \vec{u}}{\partial t} - \nabla \frac{\partial \vec{u}}{\partial t} \right\|_{L^2(0, t_f; L^2(\Omega, \mathbb{R}^2))}^2 \right) \\
&+ 4C_{25} t_f \|\vec{u} - \pi_h \vec{u}\|_{L^\infty(0, t_f; L^2(\Omega, \mathbb{R}^2))}^2. \tag{3.116}
\end{aligned}$$

Then it is plain, using theorems 3.1 and 3.2 for the properties of the time dependent GVP, that there exists a positive constant C_{27} independent of h and τ, such that for all $1 \leqslant n \leqslant N$

$$\sum_{k=1}^{n} \lambda_k \leqslant C_{27}(h^4 + \tau^2). \tag{3.117}$$

Finally, using (3.3b), (3.9) and (3.26), we find that there exists a constant C_{28} independent of h and τ such that

$$\left\| \delta \vec{u}_h^0 \right\|_0 \leqslant C_{28} h^2. \tag{3.118}$$

Therefore, using inequalities (3.117) and (3.118) together in inequality (3.115), we find that there exists a constant C_{29} independent of h and τ such that, for any $0 < \tau \leqslant \tau^*$,

$$\left\| \delta \vec{u}_h^n \right\|_0 \leqslant C_{29}(h^2 + \tau), \quad \text{for } n = 1, \dots, N. \tag{3.119}$$

We complete the proof of convergence result by writing

$$\left\| \vec{u}(t^n) - \vec{u}_h^n \right\|_0 \leqslant \left\| \vec{u}(t^n) - \pi_h \vec{u}(t^n) \right\|_0 + \left\| \delta \vec{u}_h^n \right\|_0 \tag{3.120}$$

for all $1 \leqslant n \leqslant N$. Then we use theorem 3.1 and estimate (3.119) to conclude that there exists a constant C independent of h and τ such that

$$\left\| \vec{u}(t^n) - \vec{u}_h^n \right\|_0 \leqslant C(h^2 + \tau), \tag{3.121}$$

for all $0 < \tau \leqslant \tau^*$ and $n = 1, \dots, N$. The theorem is thus proved. ∎

Chapter 4

Numerical simulations

4.1 Implementation

To enable numerical simulations of problem (1.47), a program has been written in the `C++` computer language, based on the finite element library `FELIB`[1]. The program has been called `cdp` (from the french "champ de phase") and has been compiled and run on a Silicon Graphics server with a 250 MHZ IP27 Processor in a MIPS R10000 Processor Chip, and 2048 Mbytes main memory, running the SGI IRIX64 6.5 Unix-family operating system.

The program `cdp` implements numerical scheme (3.3) with $\theta = 1$, using mass lumping for the mass matrix and trapeze quadrature formulae for the source term in the phase-field equation, as well as for the coupling term in the concentration equation. The non-linear functions depending on ϕ have been implemented in their truncated versions, as explained in section 1.3.

For model parameter values, we have used physical values for the Ni-Cu alloy, adimensionalized as explained in section 1.2. We assume temperature T to be the mean value of nickel's and copper's melting temperatures, and the adimensional space unit to correspond to $l = 2 \times 10^{-6}m$. We recall that the adimensional time unit is chosen such that adimensional concentration diffusivity is equal to $D_l = 1$. These choices result in the following numerical

---

[1]The code library `FELIB` has been created by Marco Picasso, from the Department of Mathematics, EPFL. It uses the implementation of the algorithm `GMRES` from the library `IML++`, of the american National Institute of Standards and Technology (NIST), to solve linear systems.

values for the model parameters:

$$\begin{cases} \alpha^A = 0.508, \quad \alpha^B = 0.489, & \text{(4.1a)} \\ \beta^A = 258, \quad \beta^B = -241, & \text{(4.1b)} \\ \gamma = 5.62 \times 10^{-4}, & \text{(4.1c)} \\ D_s = 10^{-4}. & \text{(4.1d)} \end{cases}$$

We recall that adimensional phase-field diffusivity M might determine kinetic effects in the corresponding sharp-interface limit (see chapter 2). Although Warren and Boettinger [WB95] quote Coriell and Turnbull's model for kinetic effects, which would yield an adimensional $M = 63.5$, there is no generally accepted value for this parameter, so we have simply fixed it to

$$M = 1. \tag{4.2}$$

Finally, except in section 4.2, the adimensional interface thickness parameter has been arbitrarily fixed to

$$\delta = 10^{-2}. \tag{4.3}$$

This corresponds to an interface thickness of the order of $10^{-8}m$. Smaller values would yield very stiff terms in the equations (for instance the source term of the phase-field equation is of order $1/\delta^2$), making computations virtually impossible without mesh adaption techniques.

4.2   Numerical convergence tests

The first series of tests that were performed on the program `cdp` were quantifiable numerical convergence tests on the isotropic problem, to which artificial extra source terms were added. These first tests aim to experimentally quantify the numerical order of convergence, and compare it to the theoretical results of chapter 3.

To remain in the framework of chapter 3, the tests were performed on the isotropic problem. Computations were performed in the unit square, with a final adimensional time $t_f = 10^{-5}$ and an interface thickness $\delta = 0.05$. Note that big time steps and low interface thickness can create stability problems due to the stiffness of the source terms, i.e. the high values of their Lipschitz constants. Thus, for these tests we chose a small final time, so that even for a low number of time steps, results may already be relevant, and that all required computations can be done using a reasonably small cpu time. We added right hand sides to both evolution equations in problem (1.47), so that

j	h_j	e_{h_j}	s_j
1	$5.000E-2$	$3.700E-1$	
2	$2.500E-2$	$9.332E-2$	1.988
3	$1.667E-2$	$4.158E-2$	1.994
4	$1.250E-2$	$2.343E-2$	1.994
5	$1.000E-2$	$1.500E-2$	1.996
6	$8.333E-3$	$1.043E-2$	1.997
7	$7.143E-3$	$7.662E-3$	1.998
8	$6.250E-3$	$5.868E-3$	1.998
9	$5.556E-3$	$4.637E-3$	1.998

Table 4.1: Errors and convergence order for very regular test functions

given functions $\phi_e(x, y, t)$ and $c_e(x, y, t)$ (defined for (x, y) in $[0, 1] \times [0, 1]$ and $t \in [0, t_f]$) are solutions of the resulting modified problem.

For a first test we chose the infinitely differentiable functions

$$\phi_e(x, y, t) = c_e(x, y, t) = \frac{1}{2}\left(1 + \sin\left(2\pi\left(x + \frac{t}{t_f}\right)\right)\sin\left(2\pi\left(y + \frac{t}{t_f}\right)\right)\right)$$
(4.4)

We chose to relate the time step τ to the mesh size h of a regular mesh by the relationship $\tau = 40h^2$. The meshes used in these tests are based on a regular grid of squares, each square being randomly cut through either of its diagonals. Let us denote by $e_h = \max_{1 \leqslant n \leqslant N} \|\vec{u}(t^n) - \vec{u}_h^n\|_{L^2(\Omega, \mathbb{R}^2)}$ the error between the exact solution $\vec{u} = (\phi_e, c_e)$ and the computed solution $\vec{u}_h$.

We are interested in the local slope of the error with respect to h in logarithmic scale, which we define by

$$s_j = \frac{\ln(e_{h_j}) - \ln(e_{h_{j-1}})}{\ln(h_j) - \ln(h_{j-1})},$$
(4.5)

where h_{j-1} and h_j are choices of mesh sizes for two consecutive calculations, and e_{h_j} and $e_{h_{j-1}}$ the corresponding computed errors.

The results of these tests are given in table 4.1. Note that the slopes s_j take values very close to 2. This simple test therefore confirms our theoretical result of convergence order $h^2 + \tau$, with a very regular test function.

Nevertheless, on physical simulations, the solutions are not as regular as the product of two sines, and their main feature is that their values change very fast on regions of length scale δ (adimensional interface thickness). For this reason, we now present a second numerical test, with test functions

reproducing the features of the physical solutions, yet regular enough to be in the scope of our convergence theorem.

We define $\rho(t) = 0.15 + 0.5\dfrac{t}{t_f}$ and we choose

$$
\phi_e(x,t) = \begin{cases} 0 & \text{if } r(x) < \rho(t), \\ 0.5\left(1 - \cos\left(\frac{r(x)-\rho(t)}{2\delta}\pi\right)\right) & \text{if } \rho(t) < r(x) < \rho(t) + 2\delta, \\ 1 & \text{if } \rho(t) + 2\delta < r(x), \end{cases}
\tag{4.6}
$$

and

$$
c_e(x,t) =
$$
$$
\begin{cases} 0.3 & \text{if } r(x) < \rho(t), \\ 0.3 + 0.2\left(1 - \cos\left(\frac{r(x)-\rho(t)}{\delta}\pi\right)\right) & \text{if } \rho(t) < r(x) < \rho(t) + \delta, \\ 0.7 - 0.1\left(1 - \cos\left(\frac{r(x)-\rho(t)-\delta}{\delta}\pi\right)\right) & \text{if } \rho(t) + \delta < r(x) < \rho(t) + 2\delta, \\ 0.5 & \text{if } \rho(t) + 2\delta < r(x), \end{cases}
\tag{4.7}
$$

where $r(x)$ is the distance between x and the center of Ω. The isovalues of the solution are expanding concentric circles with a boundary layer of width 2δ.

We follow the same procedure as for the previous tests. The results are given in table 4.2.

Again, this test confirms the theoretical result of convergence order $h^2+\tau$.

4.3   Anisotropy tests

In this section, we want to qualitatively study the convergence and stability of the numerical scheme (3.3) applied to the anisotropic problem, i.e. with matrix D redefined as (1.65), for computations corresponding to the beginning of dendritic growth. In particular, we are looking for differences in behaviour when inequality (1.66) is fulfilled or not. Calculations are still perfomed for parameter values corresponding to a Ni-Cu alloy, and therefore we fix the anisotropy order to $k = 4$, since 4-fold anisotropy is experimentally observed in Ni-Cu dendrites. For this choice of k, the right-hand side of (1.66) is equal to 1/15. For the reminder of this section, we will therefore call *low anisotropy* values of $\bar{a}$ below 1/15, and *high anisotropy* values of $\bar{a}$ above 1/15.

j	h_j	e_{h_j}	s_j
1	$5.000E-2$	$2.561E-1$	
2	$2.500E-2$	$5.071E-2$	2.337
3	$1.667E-2$	$2.282E-2$	1.969
4	$1.250E-2$	$1.295E-2$	1.969
5	$1.000E-2$	$8.355E-3$	1.965
6	$8.333E-3$	$5.810E-3$	1.992
7	$7.143E-3$	$4.281E-3$	1.981
8	$6.250E-3$	$3.284E-3$	1.987
9	$5.556E-3$	$2.596E-3$	1.995

Table 4.2: Errors and convergence order for test functions similar to physical solutions

Throughout this section, for the sake of performance, computations are actually made over one quarter of the square adimensional domain $\Omega = [-0.6, +0.6] \times [-0.6, +0.6]$, i.e. on the domain $\tilde{\Omega} = [0, 0.6] \times [0, 0.6]$. For an anisotropy of degree four whose main axis are chosen as coordinate axis, natural boundary conditions occur on the extra "artificial" boundaries of the partial domain $\tilde{\Omega}$. Let us remark that once extrapolated to the whole domain Ω, the solutions we find will be symmetric with respect to both cartesian coordinate axis. However, there might exist other less symmetric solutions. Final time is set to $t_f = 0.02$.

The initial conditions are defined as follows:

$$\phi_0(x) = \begin{cases} 0 & \text{if } |x| < \rho_0, \\ 0.5\left(1 - \cos\left(\frac{|x|-\rho_0}{\delta}\pi\right)\right) & \text{if } \rho_0 < |x| < \rho_0 + \delta, \\ 1 & \text{if } \rho_0 + \delta < |x|, \end{cases} \qquad (4.8)$$

and

$$c_0(x) = \begin{cases} c_{s0} & \text{if } |x| < \rho_0, \\ c_{l0} + (c_0 - c_{l0})\frac{|x|-\rho_0}{\delta} & \text{if } \rho_0 < |x| < \rho_0 + \delta, \\ c_0 & \text{if } \rho_0 + 2\delta < |x|, \end{cases} \qquad (4.9)$$

where $\rho_0 = 0.01$ unless stated otherwise. This corresponds to a small disc of solid in the center of a liquid domain. The initial concentration values are determined by $c_{s0} = 0.482$, $c_{l0} = 0.510$ and $c_0 = 0.497$. This last value corresponds to an undercooling of $20K$, i.e. the value that the concentration at the liquid side of the interface would have if the temperature was $20K$ higher, according to the phase diagram represented in figure 2.3.

4.3.1   Behaviour at low anisotropy

We perform a series of tests for $\bar{a} = 0.05$, which is below but close to the critical value $1/15 = 0.0666\ldots$. We want to qualitatively study the space and time convergence as well as stability with respect to mesh shape and initial conditions.

We will consider two families of structured meshes in $\tilde{\Omega}$, consisting of regular meshes of squares split into triangles either by the descending diagonal (see figure 1(a)) or by the ascending diagonal (see figure 1(b)). These correspond respectively to meshes of type I (see figure 2(a)) and type II (see figure 2(b)) in Ω.

(a) Type I mesh   (b) Type II mesh
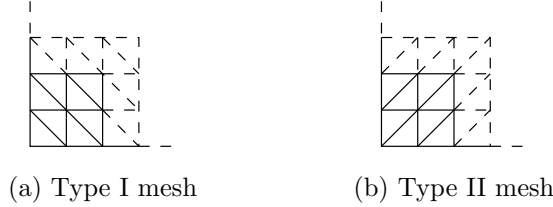
Figure 4.1: Meshes used for computations in domain $\tilde{\Omega}$

(a) Type I mesh   (b) Type II mesh
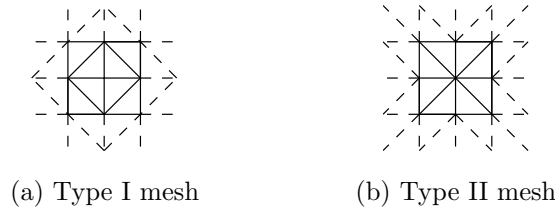
Figure 4.2: Meshes extrapolated to domain Ω

Our reference computations are done with 200×200 nodes in $\tilde{\Omega}$ and 1000 time steps with an initial condition of radius $\rho = 0.01$. For the remainder of this section we will show curves of the level set $\phi = 1/2$. It will thus be possible to qualitatively appraise the effect of numerical parameters by comparing several such curves, which can be superimposed on the same graphic. The black curves in figures 4.3, 4.4 and 4.5 are actually the same, corresponding to the reference coputations, whereas the other curves in each of these figures is obtained by varying numerical parameters one at a time.

Effect of initial condition

We first test stability with respect to initial conditions. For this we fix all physical and numerical parameters, and vary only the initial condition radius ρ_0 in (4.9) and (4.8). Results are represented in figure 4.3, where it can be clearly seen that the solution for low anisotropy is stable with respect to initial condition. [2] In this figure, level sets $\phi = 1/2$ have been represented both at initial and final times of the computations. Notice that the behaviour is the same for both mesh types.

(a) Type I mesh   (b) Type II mesh

Radius ρ_0 of initial condition: ▬ 0.1 ▬ 0.2 ▬ 0.3
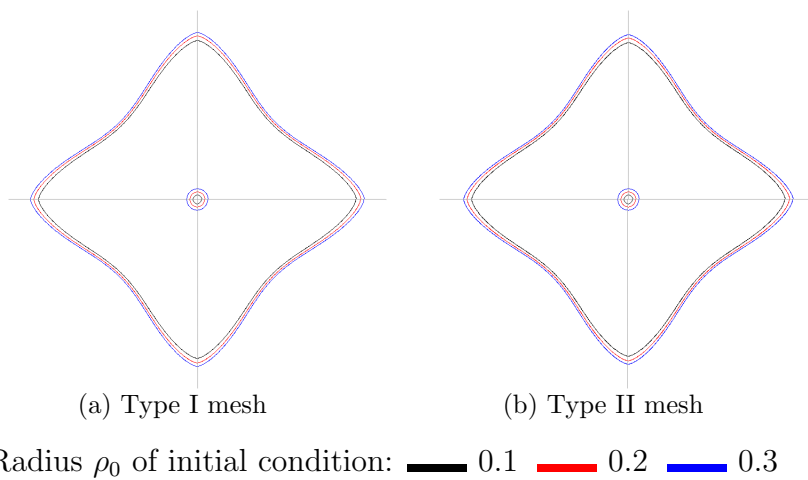
Figure 4.3: Different initial conditions in 200×200 meshes, 1000 time steps

Effect of mesh size

Now we fix the initial condition and the time step, and vary the mesh size. We qualitatively observe convergence in mesh, as seen in figure 4.4. Again, results are essentially independent of mesh type when the mesh is fine.

Effect of time step

Finally, we fix the initial condition and the mesh size, and vary the time step. We qualitatively observe convergence in time step, as seen in figure 4.5. Results are still essentially independent of the mesh type.

---

[2]We have also noticed that different shapes (circle, square, …) of initial conditions yield the same type of solutions after an evolution time of t_f.
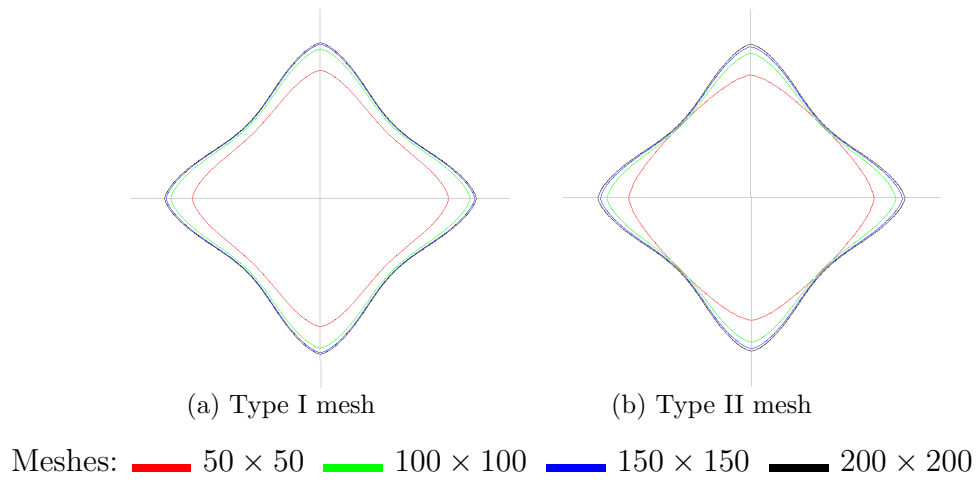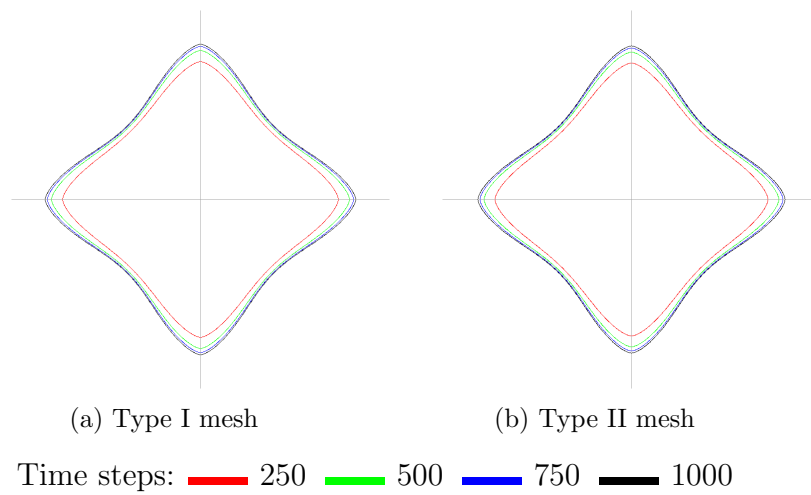
(a) Type I mesh   (b) Type II mesh

Meshes: ▬▬ 50×50 ▬▬ 100×100 ▬▬ 150×150 ▬▬ 200×200

Figure 4.4: Convergence in mesh, fixed 1000 time steps

(a) Type I mesh   (b) Type II mesh

Time steps: ▬▬ 250 ▬▬ 500 ▬▬ 750 ▬▬ 1000

Figure 4.5: Convergence in time steps, fixed 200×200 meshes

Interpretation

We have shown that computations at low anisotropy are stable with respect to initial conditions, mesh size and time step. Moreover, the orientation of mesh elements has little effect on the results when the mesh is fine and the time step small, and the scheme seems to converge to solutions regular in space (the observed curves are smooth). We are therefore inclined to believe that the results of regularity and unicity (see [RS00]) and numerical convergence (see chapter 3) for the isotropic problem might remain valid at low anisotropy. This is just a conjecture, and we must not forget that we have been working on one fourth of the total domain, thus imposing certain symmetries to the solutions. Corresponding theoretical results are being investigated.

4.3.2 Behaviour at high anisotropy

Exactly the same computations as in subsection 4.3.1 are done for a high anisotropy, chosen as $\bar{a} = 0.15$. Results are shown in figures 4.6, 4.7 and 4.8.

(a) Type I mesh   (b) Type II mesh

Radius ρ_0 of initial condition: ▬ 0.1 ▬ 0.2 ▬ 0.3
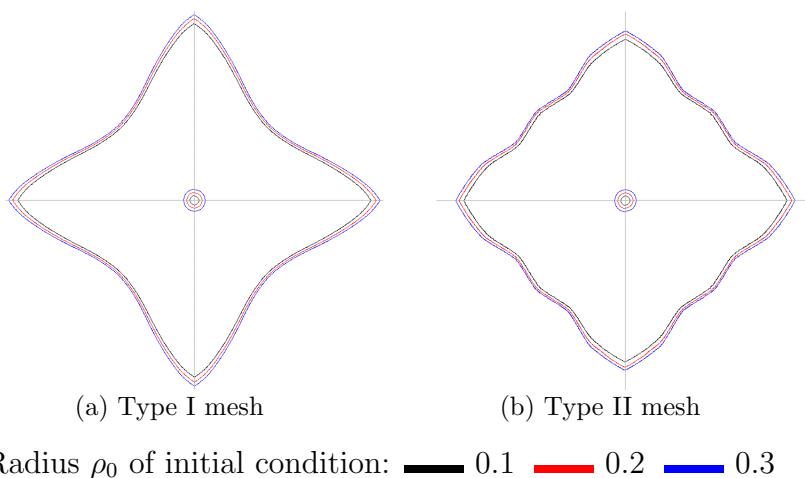
Figure 4.6: Different initial conditions in 200×200 meshes, 1000 time steps

We observe that two separate families of solutions to the discrete problem appear for the same physical parameters, depending on the type and precision of the mesh. Also, both families of solutions seem to converge to functions less regular than the corresponding ones at low anisotropy (apparition of sharp tips in the graphs of the level sets). Nevertheless, both types of solutions seem to be stable with respect to initial conditions and time steps. Therefore, we
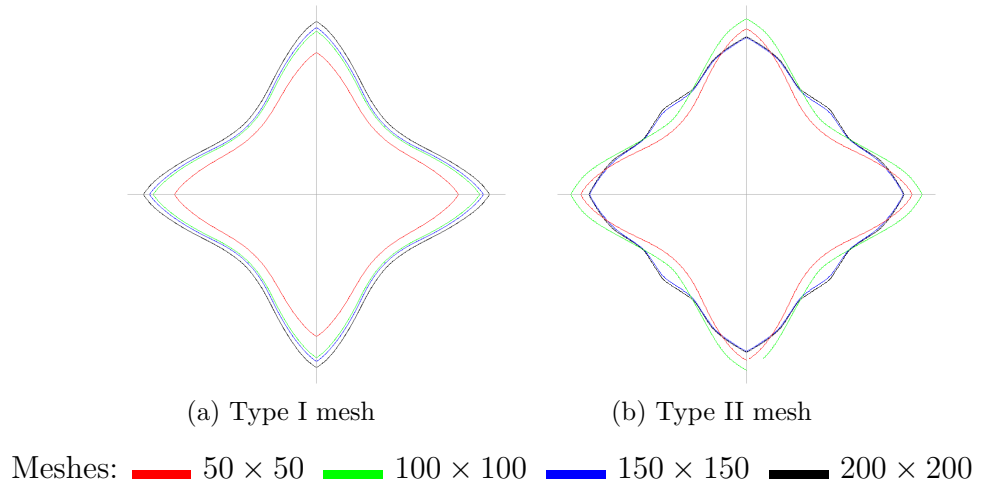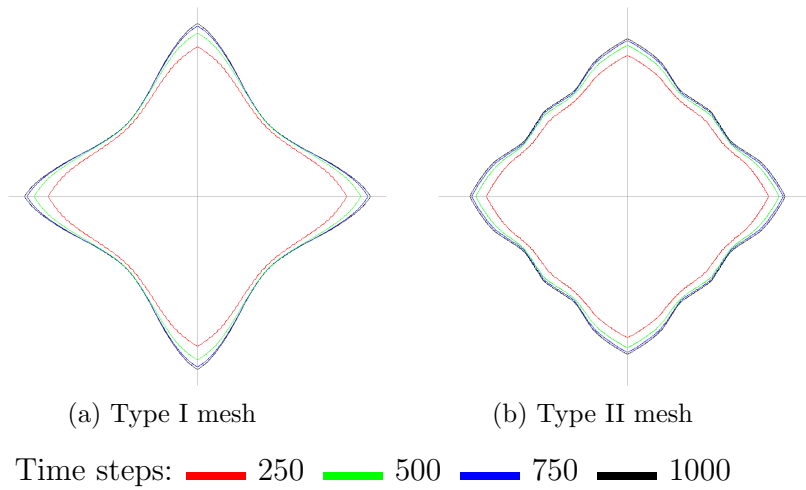
(a) Type I mesh   (b) Type II mesh

Meshes: ▬▬ 50×50 ▬▬ 100×100 ▬▬ 150×150 ▬▬ 200×200

Figure 4.7: Convergence in mesh, fixed 1000 time steps

(a) Type I mesh   (b) Type II mesh

Time steps: ▬▬ 250 ▬▬ 500 ▬▬ 750 ▬▬ 1000

Figure 4.8: Convergence in time steps, fixed 200×200 meshes

are inclined to believe that at high anisotropy, the continuous problem has multiple solutions (at least two), which are less regular than those of the low anisotropy and isotropic problems. The physical relevance of either of these solutions at high anisotropy is not straightforward.

4.4 Physical simulations

We present a physical simulation of the solidification of a Ni-Cu alloy. This is done using the numerical scheme (3.3), the initial conditions (4.8) and (4.9) with radius $\rho_0 = 0.1$, and model parameters values (4.1),(4.2) and (4.3). The domain is chosen as $\Omega = [-2, +2] \times [-2, +2]$.

As in section 4.3, computations are made only on one quarter of the domain $\tilde{\Omega} = [0, +2] \times [0, +2]$. We use an unstructured mesh, consisting of roughly $1/2 \times 600 \times 600$ evenly distributed nodes below the straight line $x_1 + x_2 = 2$, and which is much coarser above this line. The computations are made in 5000 time steps for a time of $t_f = 0.1$. The choices of anisotropy coefficient, mesh size in the relevant region and time step size ensure that the computation will be performed in the range of numerical parameters validated by section 4.3.

In section 4.3, we used an anisotropy of $\bar{a} = 0.05$ for our tests because it is near the critical anisotropy $\bar{a}_c = 1/15$. However, we now fix $\bar{a} = 0.02$, which is an approximation of the physical value for the Ni-Cu alloy. Resulting graphs of functions ϕ and c at final time are presented in figures 4.9 and 4.10, and the evolution of the level set $\phi = 1/2$ is presented in figure 4.11. The computation is very long, taking 5 `CPU` days to complete with the hardware mentioned in section 4.1. Performance could be drastically increased using adaptive meshing, which is out of the scope of this work (this is the subject of [KPS]).

It is noticeable in figure 4.11 that the tips of the dendrite advance at a constant velocity (after a transient regime near the initial condition). This is a good indication of qualitative agreement with physics. Quantitatively, far from the initial condition we have measured a tip velocity (after re-dimensionalization) of $0.73\,cm\,s^{-1}$, which is of the expected order of magnitude. Indeed, a computation using Ivantsov's model and marginal stability analysis (see [KF98, ch. 4]) yields a dendrite tip velocity of $0.35\,cm\,s^{-1}$ with our physical parameters [3], without accounting for anisotropy undercooling, which should accelerate the dendritic growth.

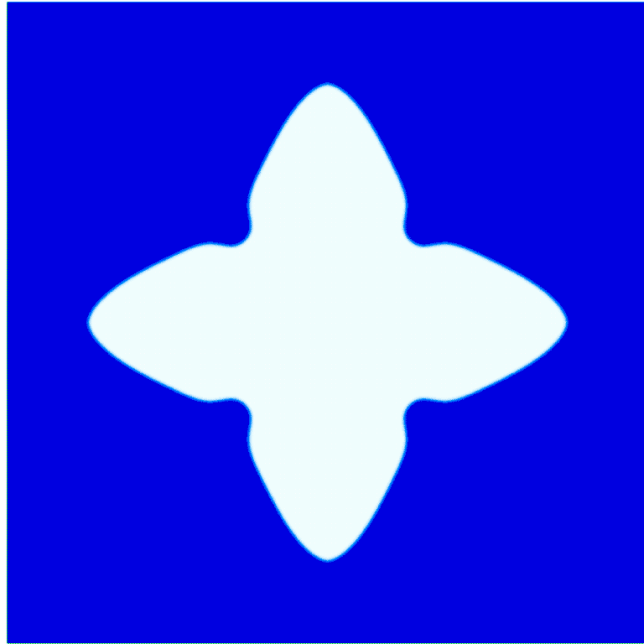[3]This value has been kindly computed by Alain Jacot from the Materials Science Department, EPFL.

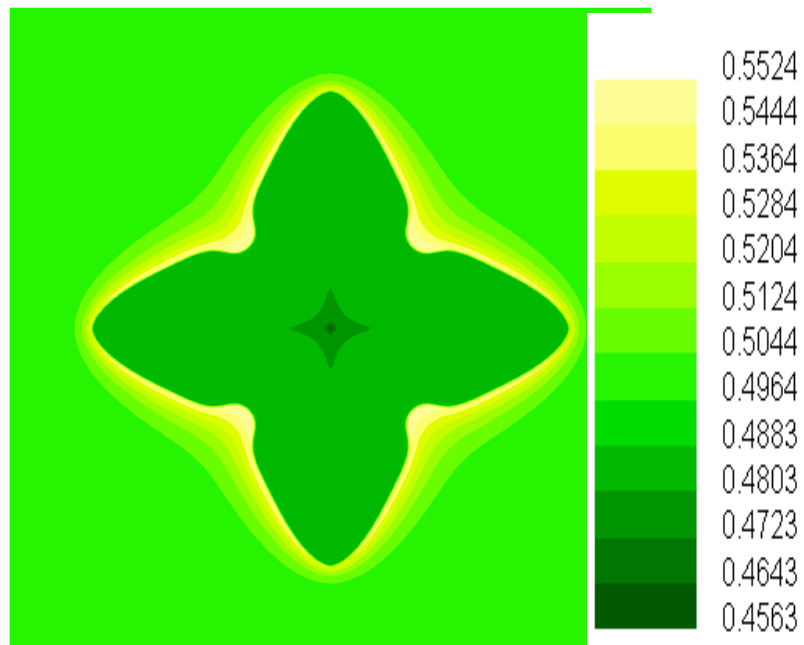Figure 4.9: Phase-Field ϕ, $\bar{a} = 0.02$, $t = 0.1$

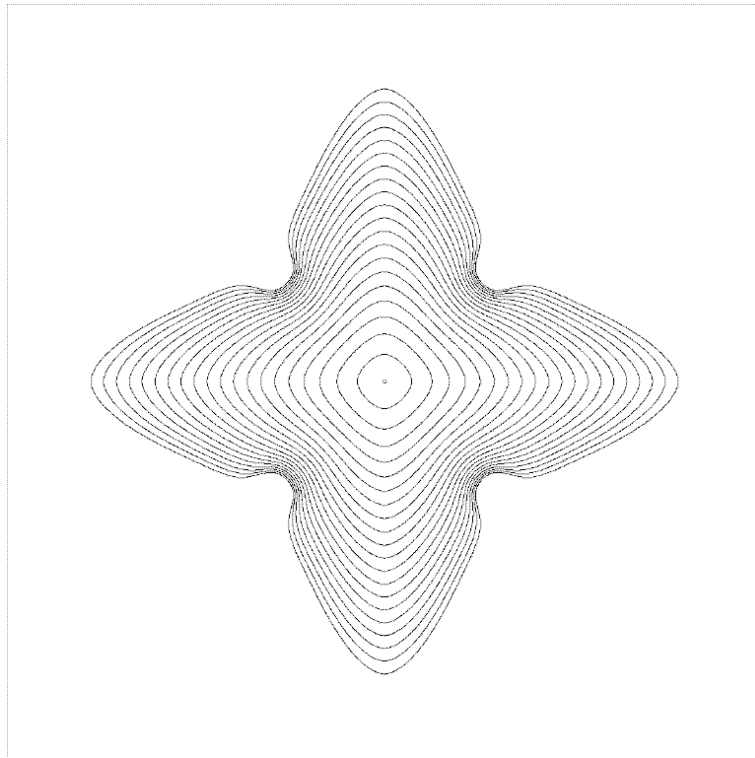Figure 4.10: Concentration c, $\bar{a} = 0.02$, $t = 0.1$

Figure 4.11: Evolution of level set $\phi = 1/2$, $\bar{a} = 0.02$, $t = 0, 0.5 \times 10^{-2}, 10^{-2}, 1.5 \times 10^{-2}, \ldots, 10 \times 10^{-2}$.

   To illustrate the physical behaviour at longer times and the apparition of
secondary branches of the dendrite, we performed a similar computation with
a final time $t_f = 0.3$. However, due to technical limitations, we kept a mesh
of approximately $1/2 \times 600 \times 600$ nodes for a domain two times larger $\Omega =
[-4, +4] \times [-4, +4]$, and computed the solution using 7500 time steps. The
resulting graphs of functions ϕ are c were presented in the Introduction. The
mesh size and time step are coarser than the values validated in section 4.3,
but the observed growth corresponds nevertheless to the expected physical
behaviour. Quantitatively, the tip velocity remains constant, as can be seen
in figure 4.12. Dendrite tip velocity is a functional of the solution which
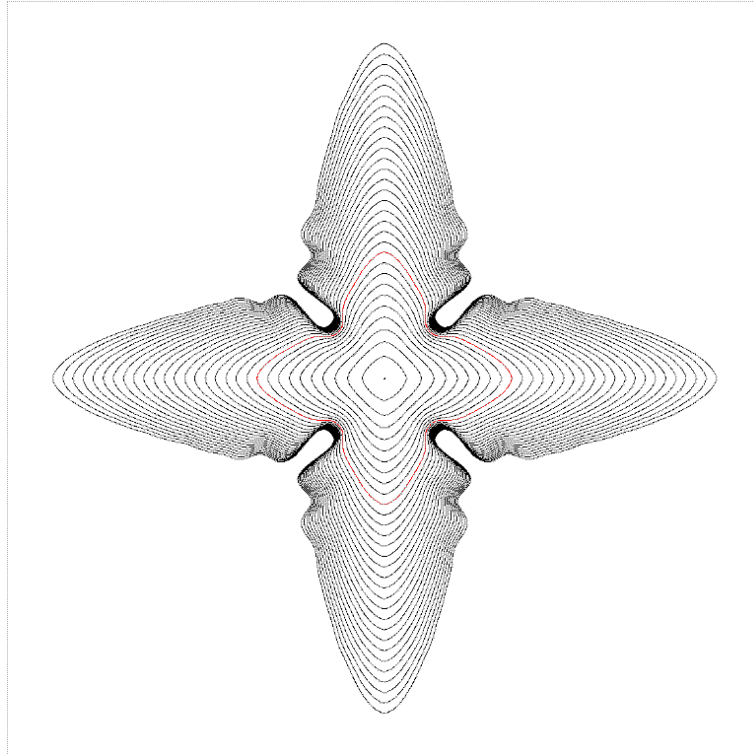seems to be very stable with respect to numerical parameters.

Figure 4.12: Evolution of level set $\phi = 1/2$, $\bar{a} = 0.02$, $t = 0, 10^{-2}, 2 \times
10^{-2}, \dots, 30 \times 10^{-2}$. The red level is at time $t = 10^{-1}$, and corresponds to
the last level set in figure 4.11.

   Finally, we want to verify that the physical simulations are stable with
respect to small changes in the interface thickness. For this purpose, com-
putations at anisotropy $\bar{a} = 0.05$ (i.e. near the critical anisotropy limit)
are done for three different values of δ, under the same conditions as be-

fore. Resulting graphs of level sets $\phi = 0.5$ have been superimposed in figure 4.13. From this figure one may conclude that small perturbations of δ do not excessively influence the computations. However, it is clear that the sharp interface asymptotic limit has not yet been reached for the chosen range of values for δ. Nevertheless, smaller values of the interface thickness would induce much stiffer problems (some terms in the evolution equations are of order $1/\delta^2$), and therefore much longer computations. They would certainly require adaptive mesh and a faster computer.
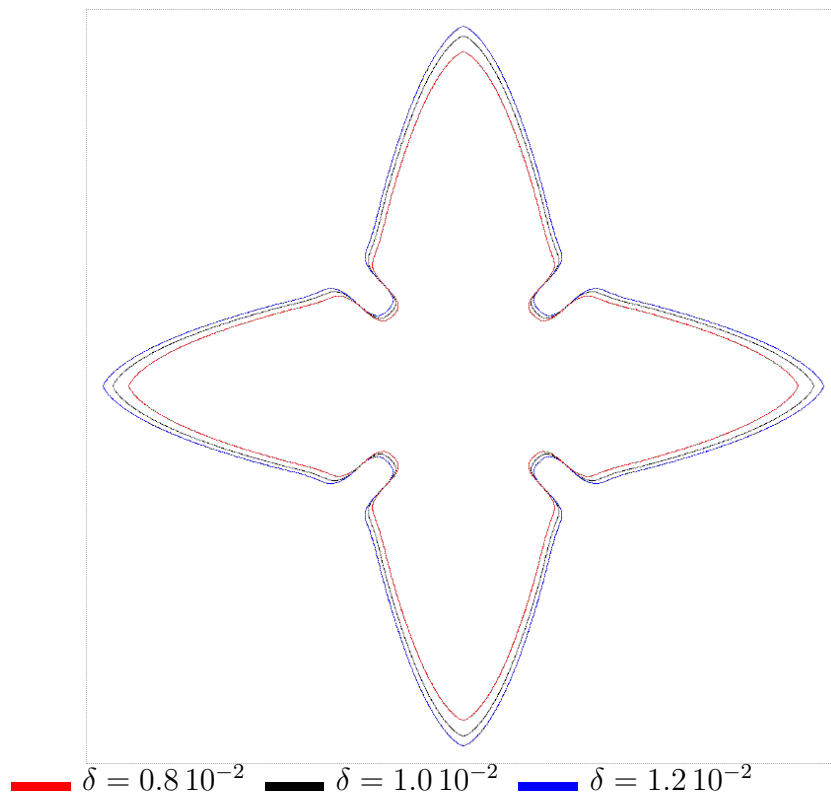

Figure 4.13: Influence of interface thickness δ on a physical computation at near critical anisotropy $\bar{a} = 0.05$.

Conclusion

We have introduced a thermodynamically consistent solutal phase-field model in two variants: isotropic and anisotropic. The simpler isotropic model has been the object of theoretical investigations. On the one hand, we derived Stefan-like limit models, with a formal asymptotic analysis. On the other hand, we investigated the convergence of a finite element in space, semi-implicit Euler in time numerical scheme.

For numerical simulations, we worked with the anisotropic problem, choosing model parameters in order to fit a realistic physical alloy. We have mainly studied the phase-field function. We investigated the stability of its level set $\phi = 1/2$ – which corresponds roughly to the solid-liquid interface – with respect to numerical parameters and to the model interface thickness. The interface is stable at low anisotropy, while at high anisotropy we observe at least two different families of discrete solutions, depending on symmetries of the mesh used in the computations. At low anisotropy, we also observe that the dendrite tips grow at a constant velocity, as is expected from physics, and the velocity observed in the simulations has the expected order of magnitude.

Several questions remain open for future investigation. One could try to extend the different theoretical results to the anisotropic problem with low anisotropy. It would also be useful to derive a posteriori error estimates for the numerical scheme, in order to justify and implement efficient algorithms for adaptive mesh refinement. Finally, many issues could be investigated about the behaviour of the concentration in numerical simulations. We have observed some instabilities which seem to result from the initial condition for c. It may be possible to correct this problem by choosing smoother initial conditions (i.e. veryfying the convergence theorem's assumptions) which should nevertheless somehow fit the physics. Also, a complete study of the behaviour of concentration profiles around the solid-liquid interface could help to validate the numerical simulations by comparison with the limit models derived.

Appendix A

Construction of the pure element free energy density

In this appendix, we want to build a thermodynamically consistent free energy density $f^\xi(T, \phi)$ for the pure elements $\xi = A$ ans $\xi = B$. This appendix is based on material originally presented in [KKS98], and is a justification for the choice of a model close to that of Warren and Boettinger [WB95]. It is in this part of the modelling that one may really get a grasp of the passage from a classical approach to a phase-field approach for phase transitions.

A.1 Internal energy density

We start by thinking in terms of internal energy. From the classical theory of phase transitions, we know that the classical internal energy density $e_{cl}^\xi(T)$ is discontinuous at the melting temperature T_m^ξ, where its value is increased by the latent heat L^ξ. Near the melting temperature, it is almost affine, the slopes of its graph at either side of the gap being equal to the specific heat C^ξ. Both the latent heat and the heat capacity are experimentally known quantities for most metals. A typical graph of the classical internal energy is given in figure A.1.

With the introduction of the phase-field ϕ as a new thermodynamic variable, the temperature T should no longer give any information about the phase state of the physical system. Therefore, both liquid ans solid states should be possible for all temperatures, and consequently two branches of internal energies - solid state and liquid state energies - should exist, defined by:
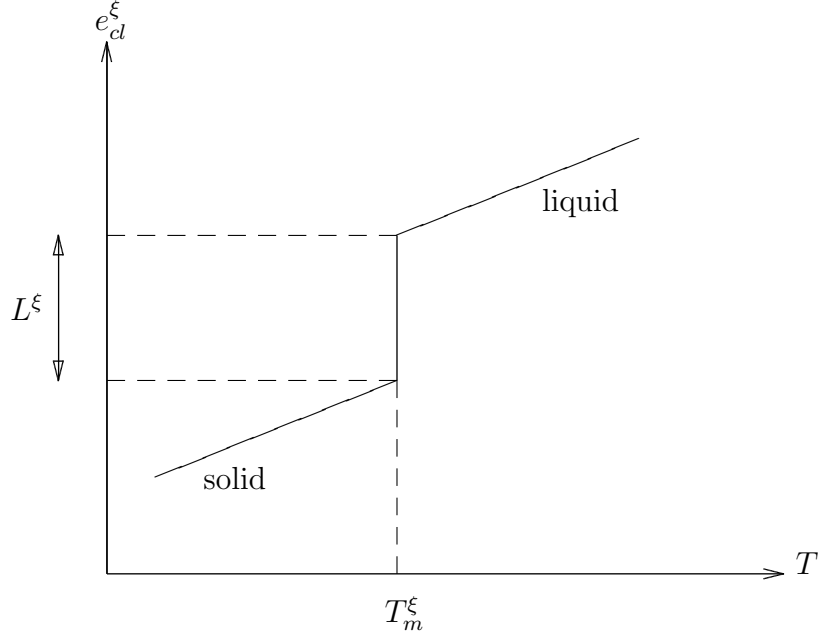
Figure A.1: Sketch of the classical internal energy

$$
\begin{cases}
e_s^\xi(T) = e_{cl}^\xi(T_m^{\xi-}) + C^\xi(T - T_m^\xi), & \text{(A.1a)} \\[2mm]
e_l^\xi(T) = e_{cl}^\xi(T_m^{\xi+}) + C^\xi(T - T_m^\xi), & \text{(A.1b)}
\end{cases}
$$

as shown in in figure A.2.

Now the phase-field ϕ is introduced to describe a smooth transition between the solid and liquid internal energies. Thus we define an internal energy depending (monotonously) on the phase-field as

$$
e^\xi(T, \phi) = e_s^\xi(T) + p(\phi)\left(e_l^\xi(T) - e_s^\xi(T)\right) = e_s^\xi(T) + L^\xi p(\phi), \qquad \text{(A.2)}
$$

where p is a C^1 function such that

$$
\begin{cases}
p(0) = 0, & \text{(A.3a)} \\[2mm]
p(1) = 1, & \text{(A.3b)} \\[2mm]
p'(\phi) > 0, \quad \forall \phi \in (0, 1). & \text{(A.3c)}
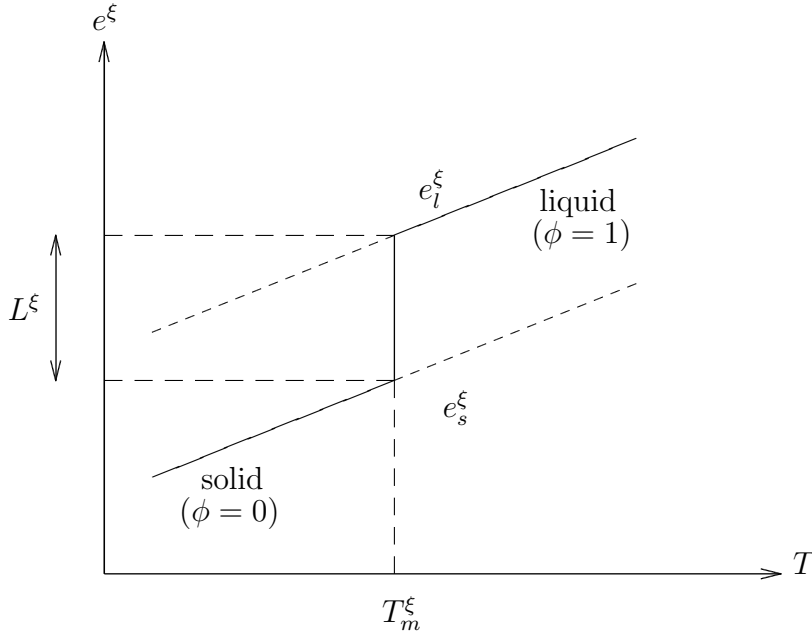\end{cases}
$$

Figure A.2: Solid and liquid internal energies

A.2 From internal to free energy

In order to link the free energy density $f^\xi(T, \phi)$ to the internal energy density $e^\xi(T, \phi)$, we use the following thermodynamic rules:

$$
\begin{cases}
f^\xi(T, \phi) = e^\xi(T, \phi) - T s^\xi \left(e^{\xi(T,\phi)}, \phi \right) & \text{(A.4a)} \\[2mm]
\dfrac{\partial s^\xi \left(e^{\xi(T,\phi)}, \phi \right)}{\partial e} = \dfrac{1}{T}, & \text{(A.4b)}
\end{cases}
$$

where s^ξ is the entropy density for pure element ξ.

Differentiating (A.4a) with respect to T and then combining it with (A.4b) we obtain that

$$
f^\xi(T, \phi) = e^\xi(T, \phi) + T \frac{\partial f^\xi(T, \phi)}{\partial T}, \tag{A.5}
$$

which can also be written as

$$
e^\xi(T, \phi) + T^2 \frac{\partial f^\xi(T, \phi)/T}{\partial T} = 0. \tag{A.6}
$$

By integrating this last equation from an arbitrary T to the melting temperature T_m^ξ, we get

$$f^\xi(T, \phi) = T \left(\int_T^{T_m^\xi} \frac{e^\xi(T, \phi)}{\tau^2} d\tau + \frac{1}{T_m^\xi} f^\xi(T_m^\xi, \phi) \right). \qquad (A.7)$$

We already derived an expression for the internal energy density $e^\xi(T, \phi)$ in section A.1. However, we also need to describe the free energy at melting temperature $f^\xi(T_m^\xi, \phi)$ before we can get an explicit expression for the free energy density at all temperatures.
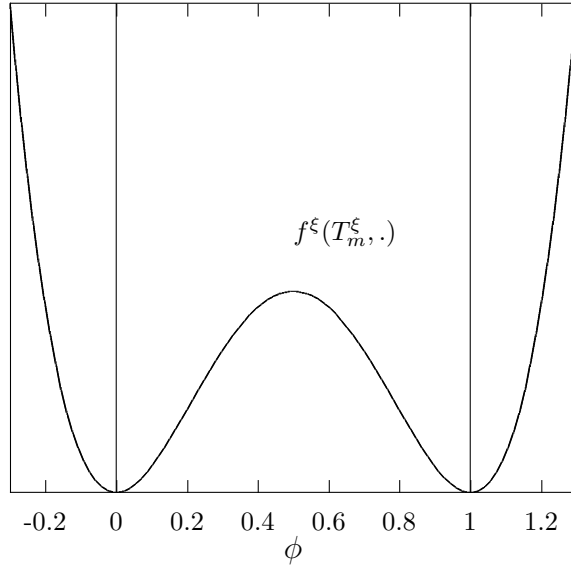
A.3   Free energy density at melting temperature

Figure A.3: Pure element free energy density at melting temperature

At melting temperature, both solid ($\phi = 0$) and liquid ($\phi = 1$) states should be equally stable, and they should be the only stable states. We decide to describe this situation by a double-well potential

$$f^\xi(T_m^\xi, \phi) = W^\xi \phi^2 (1 - \phi)^2, \qquad (A.8)$$

where the positive number $W^\xi/16$ is the height of the potential barrier's maximum value at $\phi = 1/2$. Note that this model parameter is linked to physical parameters in subsection 1.1.3. The resulting free energy at melting temperature is represented in figure A.3.

A.4 Free energy density

Combining (A.2), (A.7) and (A.8) we derive the following expression for the pure element free energy density:

$$f^\xi(T, \phi) = \frac{T_m^\xi - T}{T_m^\xi} L^\xi p(\phi) + W^\xi \frac{T}{T_m^\xi} \phi^2 (1 - \phi)^2$$
$$+ \frac{T_m^\xi - T}{T_m^\xi} e_{cl}^\xi (T_m^{\xi-}) + C^\xi \left(T \ln \frac{T_m^\xi}{T} - T_m^\xi + T \right). \quad \text{(A.9)}$$

We still need to specify one important constraint on the final form of $f^\xi(T, \phi)$, which will affect the definition of $p(\phi)$, our only remaining degree of freedom. Indeed, for all positive values of T, and not only $T = T_m^\xi$, the only stable states of the pure element should be solid ($\phi = 0$) and liquid ($\phi = 1$). In other words, we make the following assumption on $f^\xi(T, \phi)$:

(HA.1) $\phi = 0$ and $\phi = 1$ should be the two and only local minima of $f^\xi(T, \phi)$ in the range $\phi \in [0, 1]$, for any fixed value of $T > 0$.

Notice that

$$\frac{\partial f^\xi}{\partial \phi}(T, \phi) = \frac{T_m^\xi - T}{T_m^\xi} L^\xi p'(\phi) + 2W^\xi \frac{T}{T_m^\xi} \phi(1 - \phi)(1 - 2\phi) \quad \text{(A.10)}$$

and

$$\frac{\partial^2 f^\xi}{\partial \phi^2}(T, \phi) = \frac{T_m^\xi - T}{T_m^\xi} L^\xi p''(\phi) + W^\xi \frac{T}{T_m^\xi}(2 - 12(\phi^2 - \phi)). \quad \text{(A.11)}$$

Therefore, if we consider f^ξ as being still defined outside the physical interval $\phi = [0, 1]$ by the same expression (A.9) and that p is a C^2 function fulfilling constraints (A.3), assumption (HA.1) implies that

$$\begin{cases} p'(0) = p'(1) = 0, & \text{(A.12a)} \\[2mm] \dfrac{T_m^\xi - T}{T_m^\xi} L^\xi p''(0) + 2W^\xi \dfrac{T}{T_m^\xi} \geqslant 0, \quad \forall T > 0, & \text{(A.12b)} \\[2mm] \dfrac{T_m^\xi - T}{T_m^\xi} L^\xi p''(1) + 2W^\xi \dfrac{T}{T_m^\xi} \geqslant 0, \quad \forall T > 0. & \text{(A.12c)} \end{cases}$$

These constraints are necessary for a non-truncated model to be thermodynamically consistent.

To be certain that these last conditions are always fulfilled by the model, independently of the specific values of materials parameters $W^\xi > 0$ and $L^\xi > 0$, we need to impose the following extra constraints on function $p(\phi)$:

$$
\begin{cases}
p'(0) = p'(1) = 0, & \text{(A.13a)} \\
p''(0) = p''(1) = 0. & \text{(A.13b)}
\end{cases}
$$

Notice that the polynomial of lowest degree verifying constraints (A.3) and (A.13) is precisely the one chosen by Warren and Boettinger [WB95]:

$$
p(\phi) = 6\phi^5 - 15\phi^4 + 10\phi^3. \tag{A.14}
$$

This choice also ensures that there are no other minima of f^ξ in $[0, 1]$, which was also required by (HA.1).

We also remark that in the truncated model introduced in section 1.3, constraints (A.13) are no longer necessary for $\phi = 0$ and $\phi = 1$ to be local minima of f^ξ. However, it is still useful to keep (A.13a), as it ensures that all non-linearities in ϕ of the problem are still of class C^1 after truncation.

Finally, we represent the resulting pure element free energy densities with Warren and Boettinger's choice of $p(\phi)$ for temperatures above and below the melting temperature T_m^ξ in figure A.4. One can clearly see that, as expected, the solid state ($\phi = 0$) is prefered (it has a lower free energy) below the melting temperature, and the liquid state ($\phi = 1$) above.
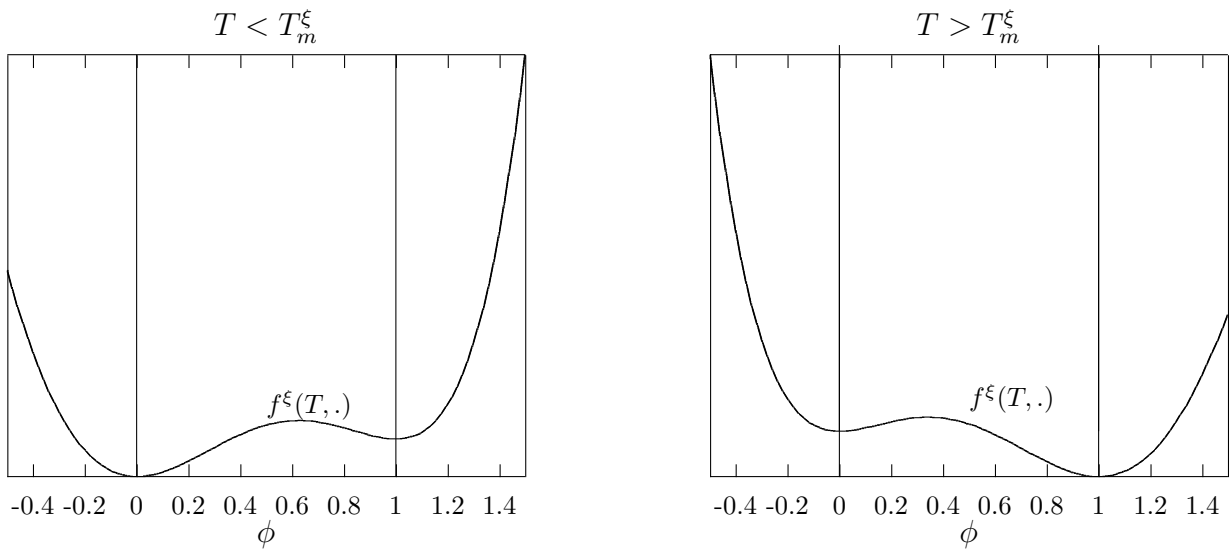
Figure A.4: Pure element free energy densities below and above melting temperature

Appendix B

List of symbols

$a(\psi)$	anisotropy factor
$\bar{a}$	anisotropy amplitude
$a_t(\vec{u}, \vec{v})$	bilinear form defining π_h
$\vec{b}$	generic vector
$c(x, t)$	concentration variable
$c_l(s, t), c_s(s, t)$	liquid and solid concentrations
e	exp(1), internal energies in appendix A
e_h	truncation error
$f(T, c, \phi), f(c, \phi)$	alloy free energy density (T is often omitted)
$f_\xi(T, \phi)$	pure element free energy density
$f^{sol}(c), f^{sol}(c)$	free energy densities at $\phi = 0$ and $\phi = 1$
$g(\phi)$	double-well potential
h	mesh size
i, j	generic indices
k	degree of anisotropy / generic index
l	characteristic domain length
n	normal direction ($\rightarrow \partial/\partial n$)
$p(\phi)$	auxiliary function in $f(T, \phi)$
$q(\phi)$	auxiliary function in $D_1(\phi)$
r, s	local curvilinear coordinate system
t	time coordinate
t_f	final time
$\vec{u}(x, y)$	vectorial variable
$\vec{v}, \vec{w}$	generic vectors
v_n	local interface normal velocity
v_m	molar volume
x	space coordinate

Table B.1: Lower-case latin

A, B	pure elements
A	generic matrix
C	generic constant
$C^j(X, Y)$	set of continuously j-differentiable functions
$D_1(\phi), D_2(c, \phi)$	non-linear factors in the evolution equation for c
$D(\vec{u})$	diffusivity matrix in the vectorial formulation
D_s, D_l	solid and liquid diffusivity coefficients
D_m	uniform coercivity constant for $D(\vec{u})$
D_M	maximum bound for elements of $D(\vec{u})$
$\vec{F}(\vec{u})$	source term in the evolution equation for ϕ
$\mathcal{F}(T, c, \phi)$	total free energy
$H^i(X, Y)$	Sobolev spaces $(= W^{i,2})$
J	rotation matrix
J_c	concentration flux
K	mesh triangle
$\mathcal{L}_D, \mathcal{L}_{\vec{F}}$	Lipschitz constants for D and $\vec{F}$
L^ξ	latent heats $(L = A, B)$
L^j	Sobolev spaces $(= W^{0,j})$
M	phase-field diffusivity
$\mathcal{M}_2$	set of 2×2 real matrices
R	Boltzmann constant
T	temperature
T_m^ξ	melting temperatures
$\mathcal{T}_h$	mesh triangulation
V	Sobolev space $H^1(\Omega)$
V_h	finite elements space
W^ξ	double-well barrier heights
$W^{i,j}(X, Y)$	Sobolev spaces
X, Y	generic Banach spaces

Table B.2: Upper-case latin

$\alpha(c), \beta(c)$	auxiliary functions in $f(c, \phi)$
α	continuity constant of a_t
α_ξ, β_ξ	adimensional constants in $\alpha(c), \beta(c)$
β	coercivity constant of a_t
γ	adimensional constant in $f(c, \phi)$
δ	interface width
ε	Ginzburg-Landau coefficient
ζ	weight for c equation in vectorial formulation
$\eta(c, \phi)$	coefficient of $\delta\mathcal{F}/\delta\phi$
θ	parameter of numerical scheme
κ	local interface curvature
λ	generic auxiliary function or constant
μ	coefficient of $\delta\mathcal{F}/\delta c$
ξ	pure element ($\xi = A$ or $\xi = B$)
$\vec{\xi}$	generic vector
π_h	generalized vectorial elliptic projector
ρ	re-scaled local coordinate r
σ^ξ	surface tensions
τ	time step
$\phi(x, t)$	phase-field
$\phi_m(x)$	stationary phase-field at melting temperature
χ	"Gibbs-Thomson" coefficient in sharp-interface limits
$\psi(\nabla\phi)$	anisotropy angle
ω	Gronwall's lemma main constant

Table B.3: Lower-case greek

Γ	liquid-solid interface
Δ	laplacian
$\Theta(\nabla\phi)$	anisotropy matrix
Λ	auxiliary linear operator during formal asymptotics
Π	product
Σ	sum
Ω	space domain
Ω_s, Ω_l	solid and liquid subdomains
$\partial\Omega$	space domain boundary

Table B.4: Upper-case greek

$\tilde{.}$	explicitly adimensional quantity
$\vec{.}$	vector with respect to $(c, \phi)^T$
$\lvert \vec{.} \rvert$	euclidian norm
$\lVert \vec{.} \rVert_X$	norm in space X
$\lvert \vec{.} \rvert_X$	seminorm in space X
$\lVert \vec{.} \rVert_0$	norm in $L^2(\Omega)$
$[\,.\,]_l^s$	jump of quantity across solid-liquid interface
$\hat{.}/\check{.}$	δ-independent quantities in limits 1,2 / 3,4.
$\overline{.}^{\,n}$	average of an integrable function on $[t^{n-1}, t^n]$

Table B.5: Others

Bibliography

[BCG+00]   W. J. Boettinger, S. R. Coriell, A. L. Greer, A. Karma, W. Kurz,
           M. Rappaz, and R. Trivedi. Solidification microstructures: Re-
           cent developments, future directions. *Acta mater.*, 48:43–70,
           2000.

[BK97]   E. Boillat and O. Krüger. Entropie d'un alliage binaire. *DMA-
           EPFL Internal Report*, 1997.

[BR]   Erik Burman and Jacques Rappaz. Existence of solutions to an
           anisotropic phase-field model. *in preparation*.

[Cag86]   G. Caginalp. An analysis of a phase-field model for free bound-
           ary. *Arch. Rational Mech. Anal. 92*, pages 205–245, 1986.

[Cag89]   G. Caginalp. Stefan and Hele-Shaw type models as asymptotic
           limits of the phase-field equations. *Phys. Rev. A*, 39(11):5887,
           1989.

[CH58]   J. W. Cahn and J. E. Hilliard. Free energy of a nonuniform
           system. i. interfacial free energy. *J. Chem. Phys.*, 28(2):258–267,
           1958.

[Cia78]   P. G. Ciarlet. *The finite element method for elliptic problems.*
           North-Holland, 1978.

[CLS99]   Pierluigi Colli, Philippe Laurençot, and Jürgen Sprekels. Global
           solution to the Penrose-Fife phase field model with special heat
           flux laws. In *Variations of domain and free-boundary problems
           in solid mechanics (Paris, 1997)*, pages 181–188. Kluwer Acad.
           Publ., Dordrecht, 1999.

[CNS00]   Z. M. Chen, R. H. Nochetto, and A. Schmidt. Error control and
           adaptivity for a phase relaxation model. *ESAIM Math. Model.
           and Num. Anal.*, 34:775–797, 2000.

[DD95]   Klaus Deckelnick and Gerhard Dziuk. Convergence of a finite element method for non-parametric mean curvature flow. *Numer. Math.*, 72(2):197–222, 1995.

[DHL98]   C. Dupaix, D. Hilhorst, and Ph. Laurençot. Upper-semicontinuity of the attractor for a singularly perturbed phase field model. *Adv. Math. Sci. Appl.*, 8(1):115–143, 1998.

[Ell97]   C. M. Elliott. Approximation of curvature dependent interface motion. In *State of the Art in Numerical Analysis*, pages 407–440. Clarendon Press, 1997.

[Gri85]   P. Grisvard. *Elliptic problems in nonsmooth domains*. Pitman, 1985.

[Kes01]   D. Kessler. Sharp interface limits of a thermodynamically consistent solutal phase-field model. *J. Crystal Growth*, 224:175–186, 2001.

[KF98]   W. Kurz and D. J. Fisher. *Fundamentals of solidification*. Trans Tech Publications, fourth revised edition edition, 1998.

[KKS98]   D. Kessler, O. Krüger, and J.-F. Scheid. Construction d'un modèle de champ de phase à température homogène pour la solidification d'un alliage binaire. *DMA-EPFL internal report*, 1998.

[KPGD98] Y.-T. Kim, N. Provatas, N. Goldenfeld, and J. Dantzig. Universal dynamics of phase-field models for dendritic growth. *Cond. Mat.*, 1998.

[KPS]   O. Krüger, M. Picasso, and J.-F. Scheid. A posteriori error estimates and adaptive finite elements for a nonlinear parabolic problem related to solidification. *in preparation*.

[Krü99]   O. Krüger. *Modélisation et analyse numérique de problèmes de réaction-diffusion provenant de la solidification d'alliages binaires*. PhD thesis, EPFL, 1999.

[PF90]   O. Penrose and P. C. Fife. Thermodynamically consistent models of phase-field type for the kinetics of phase transitions. *Physica D*, 43:44–62, 1990.

[QV91]   A. Quarteroni and A. Valli. *Numerical approximation of partial differential equations*. Springer-Verlag, 1991.

[RS00]   J. Rappaz and J.-F. Scheid. Existence of solutions to a phase-field model for the solidification process of a binary alloy. *Math. Methods Appl. Sci.*, 23:491–513, 2000.

[Set96]   J. A. Sethian. *Level set methods : evolving interfaces in geometry, fluid mechanics, computer vision and materials science.* Cambridge University Press, 1996.

[Tho91]   V. Thomée. *Galerkin Finite Element Methods for Parabolic Problems.* Springer, 2$^{\text{nd}}$ edition, 1991.

[Vis98]   A. Visintin. Introduction to the models of phase transitions. *Boll. Unione Mat. Ital. Sez. B Artic. Ric. Mat. (8)*, 1(1):1–47, 1998.

[War95]   J. A. Warren. How does a metal freeze? a phase-field model of alloy solidification. *IEEE Comp. Sci. & Eng.*, pages 38–49, Summer 1995.

[WB95]   J. A. Warren and W. J. Boettinger. Prediction of dendritic growth and microsegregation patterns in a binary alloy using the phase-field model. *Acta metall. mater.*, 43(2):689–703, 1995.

[WBM92]   A. A. Wheeler, W. J. Boettinger, and G. B. McFadden. Phase-field model for isothermal phase transitions in binary alloys. *Phys. Rev. A*, 45(10):7424–7439, 1992.

[WSW$^+$93] S. L. Wang, R. F. Sekerka, A. A. Wheeler, B. T. Murray, S. R. Coriell, R. J. Braun, and G. B. McFadden. Thermodynamically-consistent phase-field models for solidification. *Physica D*, 1993.

Index

Curriculum Vitae

I was born in May 29, 1975 in Lausanne, from a swiss father and an argentinian mother. I went to elementary school at the Lycée Pasteur in São Paulo, Brazil, and to secondary school at the Lycée Franco-Mexicain in Mexico City. After obtaining the french baccalauréat of type C (math-physics) with honors, I was admitted in EPFL in 1992. I got the degree of physics engineer in 1997, after having done my diploma work in the theoretical physics institute under the supervision of professor Hervé Kunz. I received the *Prix de la Jeunesse* distinction, given each year to EPFL's youngest graduate. Since 1998, I have been working as an assistant for professor Jacques Rappaz in the department of mathematics, EPFL, where I fulfill teaching and research tasks in the field of numerical analysis.